Genetic and functional characterization of RUNX2

Alexandre Stephens
B.Biomed Sc (Hons), School of Medical Sciences, Griffith University. Submitted in fulfilment of the requirements of the degree of Doctor of Philosophy

September 2006

Statement of Originality

This work has not previously been submitted for a degree or diploma in any university. To the best of my knowledge and belief, the thesis contains no material previously published or written by another person except where due reference is made in the thesis itself.

Alexandre Stephens

September 2006

Acknowledgments

I would like to thank Dr Nigel Morrison for giving me the opportunity to carry out a PhD. As my principle supervisor he has taught me countless techniques and research methodologies and has given me the opportunity to acquire the necessary skills required for a successful career as a research scientist. I would like to thank the members of the Morrison laboratory, Chris, James, Michael, Rouha, Seb, Tanya and Tina for their help, insight and support. Many thanks to members of the Beecham/Peak, Korolik and Ralph labs which have been kind neighbours over the years. I would like to acknowledge our collaborators in Geelong, Professor Geoff Nicholson and Dr Julie Pascoe for the Geelong Osteoporosis Study. I thank my family, Mum, Dad, Seb and Anthony for their support, advice and helping me out during my PhD candidature. I would like to give a special thanks to my girlfriend Isabelle, for always been there for me and giving me support and encouragement during the tough times.

Abstract

RUNX2 belongs to the RUNT domain family of transcription factors of which three have been identified in humans (RUNX1, RUNX2 and RUNX3). RUNX proteins are vital for metazoan development and participate in the regulation of cellular differentiation and cell cycle progression (Coffman, 2003). RUNX2 is required for proper bone formation by driving the differentiation of osteoblasts from mesenchymal progenitors during development (Ducy *et al*, 1997; Komori *et al*, 1997; Otto *et al*, 1997). RUNX2 is also vital for chondrocyte maturation by promoting the differentiation of chondrocytes to the hypertrophic phenotype (Enomoto *et al*, 2000). The consequences of completely disrupting the RUNX2 locus in mice provided compelling and conclusive evidence for the biological importance of RUNX2 where knockout mice died shortly after birth with a complete lack of bone formation (Komori *et al*, 1997; Otto *et al*, 1997). A further indication of the requisite role of RUNX2 in skeletal development was the discovery that RUNX2 haploinsufficiency in humans and mice caused the skeletal syndrome Cleidocranial Dysplasia (CCD) (Mundlos *et al*, 1997; Lee *et al*, 1997).

A unique feature of RUNX2 is the consecutive polyglutamine and polyalanine tracts (Q/A domain). Mutations causing CCD have been observed in the Q/A domain of RUNX2 (Mundlos *et al*, 1997). The Q/A domain is an essential part of RUNX2 and participates in transactivation function (Thirunavukkarasu *et al*, 1998). Previous genotyping studies conducted in our laboratory identified several rare RUNX2 Q/A variants in addition to a frequently occurring 18 base pair deletion of the polyalanine tract termed the 11Ala allele. Analysis of serum parameters in 78 Osteoarthritis

patients revealed the 11Ala allele was associated with significantly decreased osteocalcin. Furthermore, analysis of 11Ala allele frequencies within a Geelong Osteoporosis Study (GOS) fracture cohort and an appropriate age matched control group revealed the 11Ala allele was significantly overrepresented in fracture cases indicating an association with increased fracture risk.

To further investigate the 11Ala allele and rare Q/A variants, 747 DNA samples from the Southeast Queensland bone study were genotyped using PCR and PAGE. The experiment served two purposes: 1) to detect additional rare Q/A variants to enrich the population of already identified mutants and 2) have an independent assessment of the effect of the 11Ala allele on fracture to either support or refute our previous observation which indicated the 11Ala allele was associated with an increased risk of fracture in the GOS. From the 747 samples genotyped, 665 were WT, 76 were heterozygous for the 11Ala allele, 5 were homozygous for the 11Ala allele and 1 was heterozygous for a rare 21 bp deletion of the polyglutamine tract.

Chi-square analysis of RUNX2 genotype distributions within fracture and non-fracture groups in the Southeast Queensland bone study revealed that individuals that carried at least one copy of the 11Ala allele were enriched in the fracture group ($p = 0.16$, OR = 1.712). The OR of 1.712 was of similar magnitude to the OR observed in the GOS case-control investigation (OR = 1.9) providing support for the original study. Monte-Carlo simulations were used to combine the results from the GOS and the Southeast Queensland bone study. The simulations were conducted with 10000 iterations and demonstrated that the maximum probability of obtaining both study

results by chance was less than 5 times in two hundred ($p < 0.025$) suggesting that the 11Ala allele of RUNX2 was associated with an increased fracture risk.

The second element of the research involved the analysis of rare RUNX2 Q/A variants identified from multiple epidemiological studies of bone. Q/A repeat variants were derived from four populations: the GOS, an Aberdeen cohort, CAIFOS and a Sydney twin study. Collectively, a total of 20 rare glutamine and one alanine variants were identified from 4361 subjects. All RUNX2 Q/A variants were heterozygous for a mutant allele and a wild type allele. Analysis of incident fracture during a five year follow up period in the CAIFOS revealed that Q-variants ($n = 8$) were significantly more likely to have fractured compared to non-carriers ($p = 0.026$, OR 4.932 95% CI 1.2 to 20.1). Bone density data as measured by quantitative ultrasound was available for CAIFOS. Analysis of BUA and SOS Z-scores revealed that Q-repeat variants had significantly lower BUA ($p = 0.031$, mean Z-score of -0.79) and a trend for lower SOS ($p = 0.190$, mean Z-score of -0.69). BMD data was available for all four populations. To normalize the data across the four studies, FN BMD data was converted into Z-scores and the effect of the Q/A variants on BMD was analysed using a one sample approach. The analysis revealed Q/A variants had significantly lower FN BMD ($p = 0.0003$) presenting with a 0.65 SD decrease.

Quantitative transactivation analysis was conducted on RUNX2 proteins harbouring rare glutamine mutations and the 11Ala allele. RUNX2 proteins containing a glutamine deletion (16Q), a glutamine insertion (30Q) and the 11Ala allele were overexpressed in NIH3T3 and HEK293 cells and their ability to transactivate a known target promoter was assessed. The 16Q and 30Q had significantly decreased reporter

activity compared to WT in NIH3T3 cells ($p = 0.002$ and 0.016, for 16Q and 30Q, respectively). In contrast 11Ala RUNX2 did not show significantly different promoter activation potential ($p = 0.54$). Similar results were obtained in HEK293 cells where both the 16Q and 30Q RUNX2 displayed decreased reporter activity ($p=0.007$ and 0.066 for 16Q and 30Q respectively) whereas the 11Ala allele had no material effect on RUNX2 function ($p = 0.20$). The RUNX2 gene target reporter assay provided evidence to suggest that variation within the glutamine tract of RUNX2 was capable of altering the ability of RUNX2 to activate a known target promoter. In contrast, the 11Ala allele showed no variation in RUNX2 activity.

The third feature of the research served the purpose of identifying potential RUNX2 gene targets with particular emphasis on discovering genes cooperatively regulated by RUNX2 and the powerful bone promoting agent BMP2. The experiment was conducted by creating stably transfected NIH3T3 cells lines overexpressing RUNX2 or BMP2 or both RUNX2 and BMP2. Microarray analysis revealed very few genes were differentially regulated between standard NIH3T3 cells and cells overexpressing RUNX2. The results were confirmed via RT-PCR analysis which demonstrated that the known RUNX2 gene targets Osteocalcin and Matrix Metalloproteinase-13 were modestly induced 2.5 fold ($p = 0.00017$) and 2.1 fold ($p = 0.002$) respectively in addition to identifying only two genes (IGF-II and SCYA11) that were differentially regulated greater than 10 fold. IGF-II and SYCA11 were significantly down-regulated 27.6 fold ($p = 1.95 \times 10^{-6}$) and 10.1 fold ($p = 0.0002$) respectively. The results provided support for the notion that RUNX2 on its own was not sufficient for optimal gene expression and required the presence of additional factors.

To discover genes cooperatively regulated by RUNX2 and BMP2, microarray gene expression analysis was performed on standard NIH3T3 cells and NIH3T3 cells stably transfected with both RUNX2 and BMP2. Comparison of the gene expression profiles revealed the presence of a large number of differentially regulated genes. Four genes EHOX, CCL9, CSF2 and OSF-1 were chosen to be further characterized via RT-PCR. Sequential RT-PCR analysis on cDNA derived from control cells and cells stably transfected with either RUNX2, BMP2 or both RUNX2/BMP2 revealed that EHOX and CSF2 were cooperatively induced by RUNX2 and BMP2 whereas CCL9 and OSF-1 were suppressed by BMP2. The overexpression of both RUNX2 and BMP2 in NIH3T3 fibroblasts provided a powerful model upon which to discover potential RUNX2 gene targets and also identify genes synergistically regulated by BMP2 and RUNX2.

The fourth element of the research investigated the role of RUNX2 in the ascorbic acid mediated induction of MMP-13 mRNA. The study was carried out using NIH3T3 cell lines stably transfected with BMP2, RUNX2 and both BMP2 and RUNX2. The cell lines were grown to confluence and subsequently cultured for a further 12 days in standard media or in media supplemented with AA. RT-PCR analysis was used to assess MMP-13 mRNA expression. The RT-PCR results demonstrated that AA was not sufficient for inducing MMP-13 mRNA in NIH3T3 cells. In contrast RUNX2 significantly induced MMP-13 levels 85 fold in the absence of AA ($p = 0.0055$) and upregulated MMP-13 mRNA levels 254 fold in the presence of AA ($p = 0.0017$). The results demonstrated that RUNX2 was essential for the AA mediated induction of MMP-13 mRNA in NIH3T3 cells. The effect of BMP2 on MMP-13 expression was also investigated. BMP2 induced MMP-13 mRNA

transcripts a modest 3.8 fold in the presence of AA ($p = 0.0027$). When both RUNX2 and BMP2 were overexpressed in the presence of AA, MMP-13 mRNA levels were induced a massive 4026 fold ($p = 8.7 \times 10^{-4}$) compared to control cells. The investigation revealed that RUNX2 was an essential factor for the AA mediated induction of MMP-13 and that RUNX2 and BMP2 functionally cooperated to regulate MMP-13 mRNA levels.

Table of contents

Chapter 2

Chapter 3

Chapter 4

Chapter 6

List of figures

Chapter 5

Chapter 6

List of tables

Pg

Chapter 3

Chapter 4

Chapter 5

Chapter 6

Abbreviations

A-	alanine
AA-	ascorbic acid
ABDN-	Aberdeen
AD-	activation domain
AGRF-	Australian genome research facility
APS-	ammonium persulfate
BMD-	bone mineral density
BMI-	body mass index
BMP-	bone morphogenic protein
BMU-	basic multicellular unit
Bp-	base pairs
BUA-	broadband ultrasound attenuation
CAIFOS-	calcium intake fracture outcome study

CCD- cleidocranial dysplasia

CCL9- chemokine (C-C motif) ligand 9

cDNA- complementary deoxyribonucleic acid

CE1- Cbfa1 element 1

CI- confidence interval

CsCl- cesium chloride

CSF2- colony stimulating factor 2

CSIRO- commonwealth scientific and industrial research organisation

DEPC- diethylpyrocarbonate

DEXA- dual-energy X-ray absorptiometry

dHPLC- denaturing high-performance liquid chromatography

DNA- deoxyribonucleic acid

dNTPs- deoxyribonucleotide triphosphates

DZ- dizygotic

ECM- extracellular matrix

EDTA- ethylenediaminetetraacetic acid

EHOX- ES cell derived homeobox containing gene

FBAT- family based association test

FN- femoral neck

GOS- Geelong osteoporosis study

HDAC- histone deacetylase

IGF-II- insulin like growth factor-II

Int- intertrochanteric

Kbp- Kilobase pairs

LOD- logarithm of odds

LS-	lumbar spine
M-	molar
M-CSF-	macrophage colony stimulating factor
mL-	millilitre
mM-	milimolar
MMP-	matrix metalloproteinase
MMP-13-	matrix metalloproteinase-13
mRNA-	messenger RNA
MZ-	monozygotic
NF-KB-	nuclear factor of kappa light polypeptide gene enhancer in B-cells
ng-	nanogram
NLS-	nuclear localisation signal
nM-	nanomolar
NMTS-	nuclear matrix targeting signal
N-MYC-	v-myc myelocytomatosis viral related oncogene, neuroblastoma derived (avian)
OA-	osteoarthritis
OC-	osteocalcin
OPG-	osteoprotegerin
OR-	odds ratio
OSE-	osteocalcin specific element
OSF-1-	osteoblast specific factor-1
OSF2-	osteoblast specific factor 2
OSX-	osterix
PAGE-	polyacrylamide gel electrophoresis

PBS- phosphate buffered saline

PCR- polymerase chain reaction

PST- proline/serine/threonine rich region

PTH- parathyroid hormone

PTHrP- parathyroid hormone related peptide

Q- glutamine

Q/A domain- polyglutamine/polyalanine domain

QTL- quantitative trait loci

RANK- receptor activator of NF-KB

RANKL- receptor activator of NF-KB ligand

RD- RUNT domain

RHD- RUNT homology domain

RLU- relative light units

RNA- ribonucleic acid

RT-PCR- reverse transcription polymerase chain reaction

RUNX2- RUNT related transcription factor 2

SCYA11- small inducible cytokine A11

SD- standard deviation

SDS- sodium dodecyl sulphate

SE- standard error

SFRP2- secreted frizzled-related protein 2

SLS- lauryl sarcosine

SMID- SMAD interacting domain

SNP- single nucleotide polymorphism

SOS- speed of sound

Stiff-	bone stiffness
SYD-	Sydney
TAE-	tris-acetate-EDTA
TB-	terrific broth
TBE-	tris-borate-EDTA
TE-	tris-EDTA buffer
TEMED-	tetramethylethylenediamine
TGF-	transforming growth factor
TNF-	tumour necrosis factor
Troch-	trochanter
UV-	ultraviolet
VDR-	vitamin D receptor
VDRE-	vitamin D response element
VEGF-	vascular endothelial growth factor
WrT-	Wards triangle
WT-	wild type
μCT-	micro-computed tomography
μg-	microgram
μl-	microlitre
μM-	micromolar

Journal publications arising from this work

Doecke JD, Day CJ, Stephens AS, Carter SL, van Daal A, Kotowicz MA, Nicholson GC and Morrison NA. (2006). Association of Functionally Different RUNX2 P2 Promoter Alleles With BMD. *J Bone Miner Res.* **21:**265-73.

Stephens AS, Doecke JD, Ralston SH, Prince RL, Nicholson GC and Morrison NA. (2006). Glutamine repeat mutations define a new Cbfa1/RUNX2 related syndrome with decreased femoral neck BMD, decreased calcaneal broadband ultrasound and increased risk of osteoporotic fracture. Manuscript in preparation.

Stephens AS, Vaughan T, Cheras P, Pasco JA, Kotowizc MA, Nicholson GC and Morrison NA. (2006). Clinical correlates of a polyalanine deletion polymorphism in RUNX2. Manuscript in preparation.

Stephens AS and Morrison NA. (2006). Identification of genes cooperatively regulated by RUNX2 and BMP2. Manuscript in preparation.

Conference presentations arising from this work

Alexandre Stephens and Nigel Morrison. Identification of genes cooperatively regulated by RUNX2 and BMP2. 3rd IOF Asia-Pacific Regional Conference on Osteoporosis and 16th annual Meeting of the Australian & New Zealand Bone & Mineral Society, Port Douglas, Australia, October 2006.

Alexandre Stephens, James Doecke, Stuart Ralston, Richard Prince, Geoff Nicholson and Nigel Morrison. Glutamine repeat mutations define a new Cbfa1/RUNX2 related syndrome with decreased femoral neck BMD, decreased calcaneal broadband ultrasound and increased risk of osteoporotic fracture. 27th annual meeting of the American Society for Bone and Mineral Research, Nashville, Tennessee, USA, September 2005.

Alexandre Stephens, James Doecke, Stuart Ralston, Richard Prince, Geoff Nicholson and Nigel Morrison. Glutamine repeat mutations define a new Cbfa1/RUNX2 related syndrome with decreased femoral neck BMD, decreased calcaneal broadband ultrasound and increased risk of osteoporotic fracture. 15th annual Meeting of the Australian & New Zealand Bone & Mineral Society, Perth, Australia, September 2005.

Alexandre Stephens, Tanya Vaughan, Phillip Cheras, Mark Kotowizc, Geoff C Nicholson and Nigel A Morrison. Polyalanine deletion polymorphism in RUNX2 is associated with an increased risk of fracture and decreased serum osteocalcin levels. 13th annual Meeting of the Australian & New Zealand Bone & Mineral Society, Coolum, Australia, July 2003.

Chapter 1

Introduction

1.1 Functions of the skeleton

The skeleton is primarily composed of osseous tissue and cartilage and performs several vitally important functions. The skeleton provides support for the entire body by forming a structural framework upon which soft tissues and organs attach. The combined strength and resilience of bones creates a protective barrier for organs; the rib cage serves to protect the lungs and the heart, the spinal cord is sheltered by the vertebral column, the skull encapsulates the brain and the delicate digestive and reproductive organs are shielded by the pelvis. The skeleton is essential for locomotion and provides leverage for attached skeletal muscle to change the direction and magnitude of forces created by contracting and relaxing muscles to ultimately enable movement. Bones serve as reservoirs for lipids and minerals and have essential roles in maintaining homeostasis. The internal cavities of many bones contain red marrow which is responsible for the production of blood cells and blood elements (Martini, 1998; Sherwood, 1997).

1.2 Types of bones

Bones fall into six broad categories in relation to their shapes. Long bones such as the humerus and the femur are long and slender. Short bones acquire box like shapes and carpal bones and tarsal bones are examples of such bones. Flat bones such as the sternum, ribs and scapula have thin, parallel surfaces that provide protection for underlying soft tissues. The surface of flat bones also provides sites for attachment of skeletal muscles. Irregular bones adopt complex shapes and form short, flat, notched

or ridged surfaces. Examples of irregular bones are vertebrae and some bones of the skull. Sesamoid bones have a small, flat appearance and are located at the joints of the knees, hands and feet. The patella is an example of a sesamoid bone. Sutural bones are small, flat, irregular shaped and found in the skull (Martini, 1998).

1.3 Skeletal development

Skeletal development is a multistep process involving the migration and differentiation of a number of cells (Ducy and Karsenty, 1998). Skeletal formation requires stem cells which originate from three distinct embryonic lineages. Craniofacial bones are formed by cells from the cranial neural crest, the axial skeleton develops from cells originating from the paraxial mesoderm and the appendicular skeleton is derived from lateral plate mesodermal cells (Olsen *et al,* 2000).

Skeletal formation occurs via two different mechanisms: endochondral ossification and intramembranous ossification. Endochondral ossification is the process of bone formation via a cartilage template and is the course by which the entire skeleton with the exception of the clavicles, mandibles and certain bones of the cranium form (Ducy and Karsenty, 1998). The first step is characterized by the migration of undifferentiated mesenchymal cells into areas destined to become bone. (Ducy and Karsenty, 1998). Mesenchymal cells organize into condensations that acquire the general shape of future bones to provide a template upon which future bone is built. Cells within these condensations begin to express both type I and type IIa collagen and start to differentiate along the chondrocytic pathway (Ducy and Karsenty, 1998).

A change in collagen expression patterns and the expression of other matrix genes accompany the differentiation of the mesenchymal cells into chondrocytes. The chondrocytes secrete a collagenous extracellular matrix that forms a cartilage template. The chondrocytes mature and eventually undergo hypertrophy where they secrete type X collagen and mineralize the surrounding matrix (Ducy and Karsenty, 1998; Provot and Schipani, 2005). Vascular invasion from the perichondrium accompanies the death of hypertrophic chondrocytes through apoptosis and brings in mesenchymal cells that differentiate into osteoblasts. Osteoblasts form bone by secreting proteins and structural elements that form a collagen rich, mineralized extracellular matrix (Karsenty, 2001; Provot and Schipani, 2005).

Endochondral bone formation occurs centripetally and consumes most of the anlagen cartilage in the process (Ducy and Karsenty, 1998). A thin layer of cartilage known as the articular cartilage remains from the original model and functions to prevent damage occurring from bone to bone contact in joints (Martini, 1998). Growing bones also contain another narrow section of cartilage termed the epiphyseal plate or growth plate. This cartilage separates the epiphyses from the diaphyses and contains chondrocytes that are responsible for longitudinal bone growth (Martini, 1998). Intramembranous ossification, the second method of bone formation does not use a cartilage template. Rather mesenchymal condensations vascularize and precursor cells brought in the by the vasculature differentiate directly into osteoblasts to form mineralized bone (Ducy & Karsenty, 1998).

1.4 Bone remodeling

Once established, the skeleton undergoes continuous remodeling which is characterized by the replacement of old bone with new bone (Manolagas, 2000). Bone remodeling serves the purpose of maintaining bone mass, skeletal integrity and skeletal function (Pogoda *et al,* 2005). Remodeling requires both osteoclasts and osteoblasts and together they assemble temporary anatomical structures termed basic multicellular units (BMUs). BMUs are comprised of a team of osteoclasts to degrade bone via acidification and proteolytic digestion leading a squad of osteoblasts which are responsible for laying down new mineralized bone. In addition, the BMU also contains a vascular capillary, a nerve and surrounding connective tissue (Manolagas, 2000; Jilka, 2003). The BMU originates at a specific time and place and progresses towards the region of bone destined to be degraded and then subsequently replaced. The process occurs in both cortical and trabecular bone and at any one time there can be up to 1 million BMUs operating in a healthy human body (Manolagas, 2000). The duration of BMUs range from 6-9 months; this is considerably greater than the life spans of the individual cells which form the unit and indicates that a fresh supply of both osteoblast and osteoclast progenitors are required for the maintenance of the BMUs (Manolagas, 2000; Jilka, 2003). BMU formation is thought to be regulated by osteocytes which are uniquely position within bone to sense any changes in bone quality and integrity and thus the need for repair. The use of the extensive canaliculi system creating the functional syncytium allows osteocytes to sense and respond to any changes in bone, allowing them to initiate appropriate responses such as recruiting osteoblasts and osteoclasts from bone marrow progenitors to form BMUs and initiate bone remodeling (Jilka, 2003).

1.5 Cells in bone

The primary tissues of the skeleton, cartilage and bone are associated with four main cell types; chondrocytes in cartilage and osteoblasts, osteocytes and osteoclasts in bone.

1.5.1 Chondrocytes

Chondrocytes are the primary residents of cartilage, a unique tissue which performs many essential functions during vertebrate development and in adulthood (Archer and Francis-West, 2003; Lefebvre and Smits, 2005). Cartilage serves as a template for future bones in the developing embryo and forms the growth plate in long bones which facilitates body growth. Cartilage also provides structural support for the airways, joints and ears and thus is essential for breathing, hearing, movement and articulation (Archer and Francis-West, 2003; Lefebvre and Smits, 2005). Chondrocytes in cartilage are unique in that they are isolated from neighboring cells and are embedded in a tissue that is non-innervated and has no ready access to the vasculature (Archer and Francis-West, 2003).

Chondrogenesis in the developing embryo is initiated by the condensation of mesenchymal precursors that migrate into presumptive skeletogenic sites. The cell mass condensation expresses cell adhesion molecules such as N-cadherin, N-CAM and tenascin C and secrete extracellular matrix. Pre-chondrocytes emerge from the centre of the condensations and begin to express several chondrocyte specific genes

such as SOX-9, collagen IIa1 and aggrecan. SOX-9 is a transcription factor that plays an essential, non-redundant role in directing the commitment and differentiation of chondrocytes from mesenchymal stem cells (Archer and Francis-West, 2003; Stanton *et al,* 2003; Lefebvre and Smits, 2005). In the centre of the cartilage elements, cells further differentiate into hypertrophic chondrocytes which is accompanied by the expression of type X collagen and mineralization of the extracellular matrix. Cells directly adjacent to the hypertrophic zones form the epiphyseal growth plates which undergo a programmed cycle of proliferation in a unilateral manner facilitating longitudinal bone growth. Chondrocytes that form the articular cartilage persist and survive (Archer and Francis-West, 2003; Stanton *et al,* 2003). Once differentiated, chondrocytes function to synthesize and maintain the ECM of tracheal, nasal and articular cartilage as well as undergoing proliferation and hypertrophy and secreting matrix in growth plates to promote longitudinal bone growth (Archer and Francis-West, 2003).

1.5.2 Osteoblasts

Osteoblasts are responsible for bone formation and deposit bone by secreting a complex mixture of bone matrix proteins termed the osteoid. Osteoblasts subsequently mineralize the osteoid by depositing hydroxyapatite (Manolagas, 2000; Mackie, 2003). Osteoblasts are derived from multipotent mesenchymal stem cells and their differentiation is controlled by several growth factors, hormones and transcription factors (Ducy & Karsenty, 1998; Mackie, 2003; Kobayashi & Kronenberg, 2005). Two transcription factors, RUNT related transcription factor 2 (RUNX2) and osterix (OSX) are absolutely essential for osteoblast differentiation. RUNX2 belongs to the

family of RUNT domain transcription factors and binds directly to osteoblast specific elements (OSEs) present in many genes expressed by osteoblasts (Ducy & Karsenty, 1998; Kobayashi & Kronenberg, 2005). RUNX2 is initially expressed in mesenchymal condensations during development and promotes the differentiation of these cells towards the osteoblast lineage (Ducy & Karsenty, 1998). RUNX2 is also positive regulator of chondrocyte maturation by promoting hypertrophy (Enomoto *et al,* 2000). Later in development, RUNX2 expression is restricted to the osteoblast lineage and is not expressed to any considerable level in other cells of mesenchymal origin such as chondrocytes and fibroblasts (Ducy & Karsenty, 1998). The essential role of osterix in osteoblast differentiation was demonstrated via mouse knockouts. Osterix knockout models presented with no bone formation and examination of endochondral skeletal elements revealed the presence of vascular invasion in mineralized cartilage however mesenchymal cells brought in by blood vessels failed to deposit bone and were unable to adopt an osteoblastic phenotype. Expression analysis revealed RUNX2 was expressed in these cells. However, OSX is not expressed in RUNX2 null mice indicating that OSX acts downstream of RUNX2 (Nakashima *et al*, 2002).

The function of mature osteoblasts is to produce and secrete the mineralized bone matrix (Manolagas, 2000; Mackie, 2003). Osteoblasts are also responsible for regulating the differentiation and activity of bone resorbing osteoclasts; thus osteoblasts play an important role in regulating calcium homeostasis and bone remodeling (Mackie, 2003). The major protein secreted by osteoblasts is type 1 collagen which is released in the form of a precursor (Manolagas, 2000; Mackie, 2003). Collagen type 1 propeptides undergo proteolytic cleavage and further

extracellular processing to ultimately form mature three-chained type 1 molecules that assemble into fibrils (Manolagas, 2000). Osteoblasts also secrete non-collagenous proteins that incorporate into the bone matrix. Such proteins include osteocalcin and osteonectin which constitute 40% to 50% of non-collagenous proteins of bone and function to limit bone formation and regulate the numbers of osteoblasts and osteoclasts respectively (Manolagas, 2000). Proteoglycans are also secreted by osteoblasts and function to regulate fibrillogenesis (Manolagas, 2000; Mackie, 2003). In addition to osteoid production, osteoblasts are also responsible for directing the mineralization of bone matrix by altering the local concentrations of calcium and phosphate ions as to promote hydroxyapatite deposition. The release of enzymes by osteoblasts that regulate phosphoprotein phosphorylation such as alkaline phosphatase also contributes to the mineralization process (Manolagas, 2000; Mackie, 2003).

1.5.3 Osteocytes

Osteocytes are the most abundant cell type in bone and constitute 95% of all bone cells (Manolagas, 2000; Franz-Odendaal *et al,* 2005). Osteocytes function to maintain bone matrix and are thought to act as mechanosensors. Osteocytes are derived from osteoblasts which become embedded in newly synthesized bone matrix. These cells occupy a space termed lacunae and remain in contact with bone lining cells, osteoblasts and other osteocytes via cell processes. The formation of these processes gives osteocytes a stellate morphology. The plasma membrane extensions of osteocytes occupy channels termed canaliculi and serve as conduits for the exchange of metabolites and interstitial fluid. These interconnected cells create an osteocytic network that is linked by multiple cell processes and gap junctions forming a

functional syncytium. The syncytium forms a network for the communication and transmission of mechanosensory signals via changes in interstitial fluid flow produced by mechanical forces. Osteocytes are uniformly distributed throughout the bone matrix and are ideally located to receive and respond to mechanosensory stimuli by belonging to such an extensive functional syncytium. This arrangement permits osteocytes to act upon any mechanical, chemical or electrical signal and elicit appropriate cellular responses such as secreting secondary messengers, activating transcription factors and altering gene expression of cells (Manolagas, 2000; Knothe Tate *et al*, 2004).

1.5.4 Osteoclasts

Osteoclasts are multinucleated giant cells that are only present in bone and mediate the resorption of mineralized bone matrix (Suda *et al,* 1999; Manolagas, 2000). Osteoclasts originate from hemopoietic stem cells of the monocyte/macrophage lineage and their differentiation is directed by cell-cell contact with either bone marrow stromal cells or osteoblasts (Suda *et al,* 1999; Miyamoto & Suda, 2003). In vitro co-culture models of hemopoietic stem cells or osteoclast precursor cells derived from spleen or bone marrow mononuclear cells and stromal/osteoblastic cells demonstrated that cell-cell contact was indispensable for osteoclast formation (Suda *et al,* 1999). Further analysis revealed stromal/osteoblasts expressed receptor activator of NF-kB ligand (RANKL), a type 2 transmembrane protein belonging to the TNFα superfamily (Yasuda *et al,* 1998). RANKL binds to its receptor, receptor activator of NF-kB (RANK) on osteoclast precursor cells and promotes their differentiation into mature osteoclasts (Suda *et al,* 1999). Binding of RANKL to RANK elicits a signal

transduction cascade involving TRAFs, NF-kB, and JNK and ultimately leads to osteoclast maturation and function (Karsenty, 1999). RANKL is capable of binding to a decoy receptor, OPG which is also secreted by stromal cells and osteoblasts. Binding of RANKL to OPG decreases available RANKL and acts to inhibit osteoclast differentiation. Collectively, the balance between RANKL and OPG expression is critical for osteoclast formation (Miyamoto & Suda, 2003). Another factor necessary for osteoclast differentiation is macrophage colony stimulating factor (M-CSF) which is also secreted by marrow stromal cells and osteoblasts. Transgenic mice encoding a non-function M-CSF protein presented with impaired bone resorption and an osteopetrotic phenotype. Calvarial osteoblasts from the transgenic mice were unable to support osteoclast differentiation in co-culture models. Administration of functional M-CSF protein restored osteoclast differentiation demonstrating the essential role of M-CSF in osteoclast differentiation (Suda *et al,* 1999).

Osteoclasts function to resorb calcified matrix and have an essential role in skeletogenesis by creating bone marrow cavities which house the blood cell and blood element production facilities. The absence of osteoclasts during development results in defective bone marrow cavities forcing hematopoiesis to take place in extramedullary regions such as the spleen, liver and kidneys (Miyamoto & Suda, 2003). During adulthood, osteoclasts maintain important functions by participating in the continuous regeneration of bone. This periodic replacement of old bone with new bone is facilitated by both osteoblasts and osteoclasts and results in the complete regeneration of the skeleton approximately every 10 years (Manolagas, 2000). Osteoclasts have distinct morphological features that assist in the resorption process. The ruffled border of osteoclasts, which is characterized by finger-like projections of

the plasma membrane, facilitates calcified matrix degradation. The region of cytoplasm surrounding the ruffled border, the clear zone, functions to seal off other bone surfaces from the region of bone to be resorbed. The seal allows the osteoclast to generate a microenvironment suitable for bone resorption (Manolagas, 2000). Osteoclasts degrade bone mineral by creating an acidic environment facilitated by ATP-driven proton pumps situated in the ruffled border. Matrix metalloproteinases (MMPs) and cathepsins K, B and L are secreted by osteoclasts to degrade the protein components of bone (Manolagas, 2000).

1.6 RUNX2

RUNX2/PEBP2αA/AML-3/CBFA1/OSF2 is a transcriptional activator of osteoblast differentiation and is essential for bone formation (Ducy *et al,* 1997; Komori *et al,* 1997; Otto *et al,* 1997). RUNX2 belongs to the family of runt domain transcription factors and contains a highly conserved RUNT DNA binding domain and a C-terminal proline-serine-threonine rich (PST) region both of which participate in transcriptional activation (Thirunavukkarasu, *et al* 1998). A notable feature of human and mouse RUNX2 are the consecutive polyglutamine and polyalanine tracts (Q/A domain) which also contribute to transactivation function (Thirunavukkarasu, *et al* 1998). RUNT domain proteins have essential roles in organogenesis and mutations in the genes can lead to disease. Three RUNX proteins exist in humans and all three associate with a common beta subunit which enhances DNA binding (Ogawa *et al*, 1993; Wang *et al*, 1996).

The identification of RUNX2 as an osteoblast specific transcription factor was achieved through the extensive analysis of the mouse osteocalcin promoter. Ducy and Karsenty (1995) identified two distinct cis-acting elements which controlled the expression of the mouse osteocalcin promoter. One of these elements, osteocalcin-specific element 2 (OSE2) was highly active in differentiated osteoblasts and its sequence was identical to the DNA-binding site of PEBP2 alpha/AML-1 transcription factors (Ducy and Karsenty, 1995; Geoffroy *et al,* 1995). The ability of AML transcription factors to bind OSE2 was evaluated using AML-1B. Through gel retardation assays, recombinant protein and DNA co-transfection experiments, it was found that AML-1B could bind to OSE2 oligonucleotides and was able to transactivate a short mouse osteocalcin promoter through binding to OSE2. It was also determined that AML-1B was immunologically related to a factor specifically expressed in osteoblasts termed osteoblast specific factor 2 (OSF2) (Geoffroy *et al,* 1995). Subsequent research revealed that OSF2 protein derived from the nuclear extract of osteoblasts was able to specifically bind to OSE2 in gel shift assays and belonged to the family of PEBP2 alpha transcription factors (Ducy *et al*, 1996). Further characterization of the factor binding to OES2 was enabled when the cDNA encoding OSF2 (referred to as RUNX2 from here) was cloned from a mouse osteoblast cDNA library (Ducy *et al,* 1997). Histidine-tag purified RUNX2 protein was able to bind to OSE2 in gel shift studies and in DNA co-transfection experiments RUNX2 was able to strongly induce the promoter activity of a synthetic reporter construct consisting of multimers of OSE2 driving luciferase. The expression of RUNX2 during development was evaluated using mouse embryos. RUNX2 was initially expressed in mesenchymal condensations and its expression was subsequently restricted to cells of the osteoblast lineage. The presence of OSE2-like

elements in the promoters of several osteoblast specific genes indicated that RUNX2 could possibly directly regulate their expression. This hypothesis was tested by over expressing RUNX2 in osteoblast and non-osteoblast cells lines. The presence of increased levels of RUNX2 was able to significantly induce the expression of several osteoblast specific genes in both types of cell lines (Ducy *et al*, 1997). Cloning and characterization of RUNX2 firmly established its role as an osteoblast specific factor. The importance of RUNX2 during embryonic development was demonstrated via knockout mouse models. RUNX2 deficient mice presented with a complete lack of bone mineralization and died shortly after birth due to respiratory failure. Examination of their skeletal systems revealed the presence of very few immature osteoblasts and osteoclasts in the perichondrial region. Vascular and mesenchymal cell invasion in the cartilaginous templates was absent demonstrating the essential role of RUNX2 in bone formation (Komori *et al,* 1997; Otto *et al*, 1997).

1.6.1 RUNX2 and Cleidocranial Dysplasia

Analysis of the RUNX2 locus in patients presenting with the rare skeletal disorder, cleidocranial dysplasia (CCD) revealed that at least one copy of the gene was mutated in each case. These findings were supported by data generated from heterozygous knockout mice which presented with a skeletal phenotype similar to that of CCD patients (Otto *et al*, 1997). The disorder is dominantly inherited and is characterized by gross dysgenesis of the skeleton. Common features of the disorder include short stature, supernumerary and late erupting teeth, wide pubic symphisis, delayed closure of cranial fontanels and sutures and hypoplasia or aplasia of the clavicles (Mundlos, 1999).

Investigation of the RUNX2 locus in CCD families revealed that the disease phenotype segregated with deletion, insertion and nonsense mutations that lead to premature stop codons in the RUNT domain or in the C-terminal transactivation domain (Mundlos *et al,* 1997). Other causative alterations include missense mutations that abolish the DNA binding activity of RUNX2, mutations in the SMAD interacting domain, frameshift mutations, disruption of splice donor sites and mutations within the promoter (Lee *et al*, 1997; Quack *et al,* 1999; Zhang *et al,* 2000a; Zhang *et al,* 2000b; Kim *et al,* 2005 Napierala *et al*, 2005). Careful analysis of genotypes and corresponding phenotypes failed to indicate any correlation between the types of mutations and the clinical severity of the disorder. The absence of obvious differences in phenotype between patients with insertions, deletions and other intragenic mutations suggested that the disease is generally caused by RUNX2 haploinsufficiency rather than specific changes in function (Quack *et al*, 1999).

However, functional analysis of RUNX2 mutants through the use of DNA binding experiments and reporter gene assays revealed that alleles with intact RUNT domains retained residual DNA binding and transactivation functions (Zhang *et al,* 2000b; Yoshida *et al,* 2003). Surprisingly the extent of RUNX2 function was positively correlated with height in such that those with intact runt domains were significantly taller than patients with impaired RUNT domains. In addition, a significant correlation between the height and the numbers of supernumerary teeth in patients was observed indicating that partial changes in RUNX2 activity have an effect on both tooth development and skeletal bone growth in a proportional manner (Yoshida *et al,* 2003). Interestingly, a T200A missense mutation in the RUNT domain of one family with CCD exhibited normal DNA binding and transactivation function. The

effect of the mutation in vivo is not known. Two of the four children in the family exhibited a classic CCD phenotype however the father who also carried the mutation only displayed dental abnormalities with no evidence of CCD on skeletal radiographs. In addition, an insertion mutation positioned between two translational start sites displayed transactivation function (20% that of wild type) and was associated with a milder CCD phenotype. The mutation caused one of the two possible protein products to be nonfunctional via premature translational termination in the RUNT domain. The second, less favoured start site (as predicted by kozak consensus sequence) is predicted to be intact and is still capable of providing some RUNX2 function (Zhou *et al,* 1999). Collectively, these results indicated that a milder CCD phenotype was associated with mutant RUNX2 alleles which retained some transactivation function.

The classical features of CCD do not generally include osteoporosis or reduced bone mass. However a patient presenting with severe CCD also suffered from osteoporosis and sustained recurrent fractures. Examination of the skeletal system by x-ray revealed the patient had very thin and undermineralized cortical bone as well as dramatically reduced levels of trabecular bone. The patient also presented with spinal deformity which was caused by the severe loss of bone. These data introduced the notion that RUNX2 could regulate adult bone mass. In support of these findings, a mother and daughter suffering from CCD presented with decreased bone density and lower plasma alkaline phosphatase levels further indicating that RUNX2 may have a role in maintaining adult bone in addition to its essential role during development (Quack *et al*, 1999; Morava *et al*, 2002).

There is also evidence to suggest that chondrogenesis is altered in patients with CCD. Zheng *et al* (2005) reported the presence of growth-plate abnormalities in a patient presenting with CCD caused by a single C insertion in the coding region of RUNX2 leading to a premature stop codon. Histological examination of rib and long bone cartilages revealed the presence of diminished hypertrophic zones in addition to reduced mRNA levels of the hypertrophic chondrocyte markers VEGF, MMP-13 and COLL10A1 as measured by quantitative real-time PCR (Zheng *et al*, 2005).

1.6.2 RUNX2 isoforms and expression

Human RUNX2 spans approximately 220 Kbp and is composed of a least 8 exons. It is expressed as two major isoforms (Figure 1.1) driven from two different promoters (Stock and Otto, 2005). The isoform expressed from the P1 promoter is termed RUNX2 type-II and starts with the sequence MASNSL. The isoform driven from the P2 promoter is termed RUNX2 type-I and begins with the amino acid sequence MRIPVD (Stock and Otto, 2005). A third isoform (type-III) identified by Ducy *et al* (1997) is present in mice and is derived from an alternative splice donor site which results in an additional 68 amino acids at the N-terminal compared to the type-II protein. However, this isoform is not conserved in humans due to the presence of a 2-nucleotide insertion shifting the reading frame (Xiao *et al*, 1998). Functional analysis of type-I, type-II and type-III mouse isoforms revealed that only type-I and type-II were able to significantly increase alkaline phosphatase activity when transiently transfected in C3H10T1/2 fibroblasts. In addition, type-I and type-II isoforms were able to significantly increase alkaline phosphatase activity whereas type-III had no effect in stable transfection experiments. In the stably transfected cell lines, all three

isoforms were able to induce osteocalcin, osteopontin and collagen 1 mRNA expression (Harada *et al*, 1999). The ability of the three isoforms to transactivate a synthetic reporter plasmid consisting of 6xOSE2 driving luciferase was investigated. All three types were able to induce luciferase activity with RUNX2 type-II having the greatest effect. Similar results were obtained when a short mouse osteocalcin promoter driving luciferase was used as a reporter plasmid. The results indicated that RUNX2 type-II was more efficient in transactivating OSE2 and the osteocalcin promoter (Harada *et al*, 1999). In support for these results, Xiao *et al* (1999) demonstrated that all three RUNX2 isoforms were able to transactivate 1.3kbp of the mouse osteocalcin promoter in NIH3T3 fibroblasts, C3H10T1/2 pluripotent cells and MC3T3-E1 pre-osteoblasts. However, type-II had the greatest transactivation potential in all three cell lines when higher amounts of expression plasmid were used (Xiao *et al*, 1999).

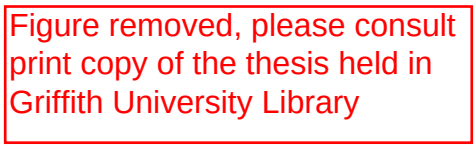

Figure 1.1: Genomic organization of human RUNX2. The gene spans 220 kbp and has two major protein isoforms. RUNX2 is composed of eight exons termed 1, 2, 3, 4, 5, 6, 6.1, and 7. The larger RUNX2-II is expressed from the P1 promoter with the N-terminal pentapeptide MASNS. The slightly smaller RUNX2-I isoform is driven from the P2 promoter and contains the N-terminal pentapeptide MRIPV. QA, QA domain; RHD, RUNT homology domain; NLS, nuclear localization signal; PST, proline/serine/threonine rich domain; NMTS, nuclear matrix targeting signal; VWRPY, TLE interacting domain (Stock and Otto, 2005).

In addition to the major type-I and type-II human isoforms, an alternative variant was cloned from SAOS-2 osteosarcoma RNA. Sequencing of the isoform revealed that 66 bp from the PST region was deleted in comparison to the type-II RUNX2. Functional analysis demonstrated that the variant could transactivate a synthetic target promoter however at levels that were significantly lower than the RUNX2-II (Geoffroy *et al*, 1998).

The osteoblast specificity of the major isoforms has been investigated by numerous studies. Ducy *et al* (1997) demonstrated that RUNX2 type-II was able to induce osteoblast specific gene expression in both osteoblast and non-osteoblast cells providing support for type-II RUNX2 as being the bone specific isoform. However, the investigation of RUNX2 type-I and type-II expression in embryonic tissues revealed that both RUNX2-I and RUNX2-II were expressed in terminal hypertrophic chondrocytes as well as osteoblasts. Type-1 isotype expression was also detected in prehypertrophic and hypertrophic chondrocytes (Enomoto *et al*, 2000). The analysis of RUNX2 type-I and type-II protein expression in osteoblasts revealed that both isotypes were expressed in mature osteoblasts but only type-I was detected in partially differentiated osteoblasts (Sudhakar *et al*, 2001). The study of cranial suture morphogenesis showed differential expression of type-I and type-II isoforms. The study demonstrated that RUNX2-I and RUNX2-II were highly expressed in osteogenic fronts and developing parietal bones. However, RUNX2 type-I was also intensely expressed in the sutural mesenchyme whereas the type-II isoform was not detected. In addition, RUNX2-I was prominently expressed in primordial cartilage located under the sutural mesenchyme. These data suggested that type-II RUNX2 was more specific for terminal osteoblast differentiation whereas the type-I isoform participated in a variety of cellular activities such as early, middle and late stages of osteoblast differentiation and in cartilage formation (Park *et al*, 2001). Banerjee *et al* (2001) demonstrated that the type-I isoform was constitutively expressed in non-osseous mesenchymal cells in addition to osteoprogenitor cells. The levels of RUNX2-I did not change during osteoblast differentiation which is in contrast to type-II where transcript levels were dramatically elevated during the differentiation of primary osteoblasts. In addition, type-II RUNX2 levels were induced in

osteoprogenitors and premyoblasts in response to bone morphogenic protein-2. The results suggested that type-I RUNX2 is involved in early stages of mesenchymal cell development and that the type-II isotype is required for osteogenesis and maintenance of the osteoblast phenotype (Banerjee *et al*, 2001). In summary, the results indicated that RUNX2-II primarily acted in mature osteoblasts whereas the type-I isoform was more widely expressed and was present in precursor cells and in chondrocytes.

In order to determine the exact role of RUNX2 type-II in bone development, transgenic mice selectively deficient for the type-II locus were generated. Homozygous RUNX2 type-II knockout mouse were unexpectedly able to form axial, appendicular and craniofacial bones, all of which are derived from intramembranous ossification. However, the mice presented with severe abnormalities in endochondral bone formation and failed to form some bones of the face and skull as well as other bones derived through cartilage templates (figure 1.2).

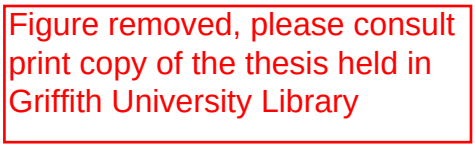

Figure 1.2: μCT analysis of whole skeleton and metaphyseal and cortical regions of tibial bones from new born RUNX2-II wild type and mutant mice. A) Whole skeleton scans revealed defective skeletal development in RUNX2-II mutant mice. B) The metaphyseal bone content was slightly diminished in RUNX2-II$^{+/-}$ mice whereas a much larger reduction in trabecular bone was observed in complete RUNX2-II knockouts. C) The levels of cortical bone are largely normal in RUNX2-II$^{+/-}$ mice but are significantly reduced in RUNX2-II$^{-/-}$ mutant mice (Xiao *et al*, 2004).

Micro-computed tomography (μCT) analysis revealed diminished cortical bone and a reduction in the primary trabeculae of the metaphyseal region in RUNX2-II$^{-/-}$ mice. Heterozygous RUNX2-II$^{+/-}$ deficient mice had grossly normal skeletal phenotypes but were osteopenic presenting with reduced trabecular volume and thickness. The study provided support for distinct functions of the two isoforms in regulating skeletal development. The study concluded that RUNX2-I could support early stages of osteoblastogenesis and intramembranous ossification and that RUNX2-II was

required for osteoblast maturation and endochondral bone formation to successfully complete the developmental process (Xiao *et al*, 2004).

1.6.3 RUNX2 structure and function

The two major RUNX2 isoforms share the same functional domains which include the glutamine/alanine rich (Q/A) tract, the RUNT DNA binding domain, the nuclear localization signal (NLS), the PST domain, the nuclear matrix targeting signal (NMTS) and the carboxy terminal pentapeptide VWRPY (figure 1.1, Stock and Otto, 2005). Structure-function analysis revealed the NLS was closely related to the c-Myc NLS and was narrowed down to a 9-amino acid sequence. The same amino acid sequence is present in other RUNX proteins at the same location providing support for its functional role. Removal of the 9-amino acid stretch via in-frame deletion created a RUNX2 protein that was localized to the cytoplasm. In contrast, full length RUNX2 was situated in the nucleus. Mutant RUNX2 lacking the NLS was unable to transactivate the 6xOSE2-luc target promoter indicating that an intact NLS was essential for transactivation function (Thirunavukkarasu *et al*, 1998). Deletion analysis revealed that two domains unique to RUNX2 participated in transactivation function. The first of these domains, termed activation domain 1 (AD1) consists of the first 19 amino acids of RUNX2-II. Removal of the 19 amino acids from the protein resulted in a 4 fold decrease in transactivation function (Thirunavukkarasu *et al*, 1998). The second transactivation domain (AD2) was determined to be the Q/A tract and its complete removal caused a 75% decrease in transcriptional activity. Further deletion analysis revealed the glutamine tract in AD2 was responsible for the majority of the transactivation function. A 3rd activation domain (AD3) was found in the PST

region and removal of the entire PST region resulted in a four to five decrease in transactivation function. This region has also been identified to contain a nonsense mutation that causes CCD providing strong support for the essential role of AD3 in RUNX2 function (Thirunavukkarasu *et al*, 1998).

In addition to contributing to transactivation function, the PST region also contains a large repression domain (Thirunavukkarasu *et al*, 1998). The c-terminus of RUNX2 contains the pentapeptide sequence, VWRPY which is present in all RUNX proteins and facilitates the physical interaction between RUNX proteins and members of the Groucho family of co-repressors (Aronson *et al*, 1997). Removal of VWRPY from RUNX2 reproducibly increased transactivation function indicating the short motif alone had repressor function. In addition, further c-terminal deletion extending to 154 amino acids progressively resulted in increased transactivation capacity indicating the repression domain (RD) was 154 amino acids long (Thirunavukkarasu *et al*, 1998).

RUNX2 is directed into the nucleus via the NLS. Once in the nucleus, RUNX2 protein is further localized to specific areas of nuclear matrix which is facilitated by the nuclear matrix targeting signal (NMTS). The NMTS of RUNX2 consists of a 38 amino acid segment located in the c-terminus and is distinct from the NLS (Zeng *et al,* 1997; Zaidi *et al*, 2001). Similar NMTS sequences are present in RUNX1 and RUNX3 and the association of RUNX1 with nuclear matrix was required for effective transactivation function indicating that the interaction between RUNX proteins and nuclear matrix is required for efficient function (Zeng *et al,* 1997; Zeng *et al,* 1998). In support for these findings it was demonstrated that the NMTS of RUNX2 directed

the protein to specific subnuclear domains and contributed to the effective transactivation of the osteocalcin promoter (Zaidi *et al*, 2001).

In addition to containing the NMTS and the PST domain, the c-terminus of RUNX2 interacts with proteins which function to modulate its activity by either enhancing transactivation capacity or by promoting repression of target genes at specific nuclear matrix sites. The conserved VWRPY motif facilitated the interaction between RUNX2 and members of the Groucho family and it was shown that overexpression of the Groucho family members TLE1 and TLE2 significantly repressed RUNX2 induced osteocalcin promoter activity. In situ localization analysis revealed that TLE1 and TLE2 were associated with the nuclear matrix at sites which contained RUNX2 proteins (Javed *et al*, 2000). HES-1, a helix-loop-helix protein also physically binds to RUNX2. The interaction is not dependent on the presence of an intact VWRPY motif but requires the c-terminus and binding of HES-1 to RUNX2 potentiates transactivation function by preventing the binding of Groucho transcriptional co-repressors (McLarren *et al*, 2000).

1.6.4 RUNX2 regulation: the role of promoters

RUNX2 is driven from two distinct promoters which generate two major isoforms. The mouse P1 (distal) promoter, which gives rise to RUNX2-II is highly active in differentiated osteoblasts but less active in immature osteoblasts and in cells originating from other organs (Fujiwara *et al*, 1999; Zambotti *et al*, 2002). In addition, 1.4 kbp of the murine P1 promoter was found to highly active in CH3T101/2, C2C12, and L929 cells which are of mesenchymal origin (Xiao *et al*, 2001). Deletion analysis

revealed that the first 600 bp of the rat RUNX2 P1 promoter was sufficient to confer transcriptional activity and contained multiple domains which positively and negatively regulated transcription. (Drissi *et al*, 2000). In support for these results, Zambotti *et al* (2002) showed that 976-bp of the murine RUNX2 P1 promoter was able to confer osteoblast specific activity demonstrating that the majority of promoter activity resided within 1-kbp from the transcriptional start site. Further progressive deletion analysis revealed that removal of rat promoter segments between -392 to -96 bp caused a massive 30-100 fold reduction in promoter activity. The 5' UTR was found to contain repressor function and decreased promoter activity 2-3 fold (Drissi *et al*, 2000).

Several factors have been implicated in regulating RUNX2 expression. Both RUNX2 P1 and P2 promoters contain multiple RUNX consensus binding sites suggesting the possibility of RUNX2 auto-regulation. The ability of RUNX2 to regulate its own expression was investigated by Drissi *et* al (2000). The study demonstrated via the use of gel shift assays that the major protein binding to the 5' region of the RUNX2-II gene in osseous cells was RUNX2. Overexpression analysis revealed that RUNX2 was able to repress P1 promoter activity and that a single RUNX binding site was sufficient for facilitating autosuppression (Drissi *et al*, 2000). There is evidence to suggest that the P2 promoter is also a target of RUNX2 auto-regulation. RUNX2-II null mice demonstrated an incremental compensation of RUNX2 levels via the increased expression of RUNX2-I (Xiao *et al*, 2004). The increased expression of RUNX2-I in response to complete RUNX2-II knock down provided support for RUNX2 negative auto-regulation via the P2 promoter.

A 40-bp region of the mouse P1 promoter was determined to contain a functional enhancer element (CE1) via promoter deletion analysis and DNase I footprinting assays (Zambotti *et al*, 2002). When multimerized, CE1 was capable of conferring osteoblast specific activity in a heterologous promoter and the enhancing ability was conserved in the CE1 elements of rat, mouse and humans present in their respective RUNX2 promoters. Site-specific mutagenesis of CE1 revealed it bound NF1 and AP-1 like proteins (Zambotti *et al*, 2002). The highly conserved –92 to –78 bp region of the P1 promoter contains a VDR response element (VDRE) which interacts with VDR/RXR heterodimers. The binding of the VDR/RXR complex to the P1 promoter suppresses RUNX2 gene promoter activity in response to treatment with 1, 25-(OH) 2-vitamin D3 (Drissi *et al*, 2002). TGF-β has also been implicated in the regulation of RUNX2. Treatment of C2C12 cells with TGF-β enhanced RUNX2 expression whereas TGF-β repressed RUNX2 expression in primary calvarial cells and the rat osteosarcoma cell line ROS17/2.8 (Lee *et* al, 1999; Alliston *et al*, 2001). BMP2, a member of the TGF-β super-family was able to induce RUNX2 levels in C2C12 cells and specifically stimulated RUNX2-II expression in C3H10T1/2 cells (Lee *et al*, 1999; Banerjee *et al*, 2001). BMP4/BMP7 heterodimers were shown to induce RUNX2 expression in C2C12 and MC3T3-E1 cells (Tsuji *et al*, 1998).

The P2 promoter of RUNX2 is thought to be largely constitutively active with a constant basal rate of transcription (Stock and Otto, 2005). However, there is some data to suggest that it is also regulated. Gilbert *et al*, (2002) demonstrated that treatment of fetal calvaria precursor cells or MC3T3-E1 pre-osteoblastic cells with TNFα dose dependently inhibited RUNX2 expression. Analysis of RUNX2 isoforms revealed that the inhibition of RUNX2 levels via TNFα treatment was more profound

on RUNX2-I (Gilbert *et al*, 2002). The P2 promoter is situated within a large CpG island which extends to the 5'-untranslated region of exon 2. The feature is conserved between the mammalian RUNX paralogues. The exact role of the CpG island in RUNX2 regulation is unknown (Stock and Otto, 2005). Possibly, the CpG island could regulate RUNX2 expression via DNA methylation which would serve to modulate promoter activity by changing the binding of histone complexes (Fuks, 2005).

1.6.5 RUNX2-protein interactions

RUNX2 is essential for osteoblast differentiation and proper skeletal development (Komori *et al*, 1997; Otto *et al*, 1997). Although necessary for the expression of genes required for skeletal development, RUNX2 is not sufficient for optimal gene expression or bone formation. RUNX2 requires several other factors in order to direct bone development (Schroeder *et al*, 2005). RUNX2 acts as a master organizer of skeletal formation by associating with numerous factors such as co-activators, co-repressors and transcription factors at specific nuclear matrix sites to regulate the complex machinery required for skeletal gene expression. Numerous proteins have been implicated in regulating RUNX2 function by directly interacting with the transcription factor at specific structural domains (figure 1.3).

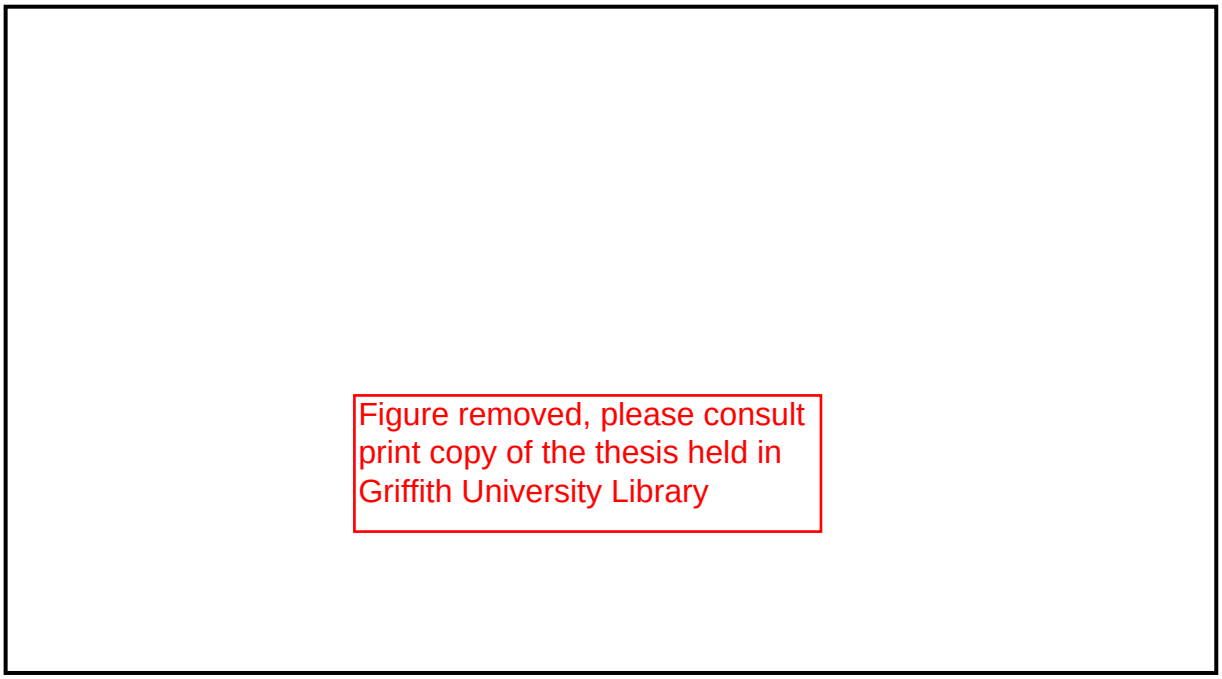

Figure 1.3: Structural and functional domains of RUNX2 type-I and type-II isofroms. The positions of co-factors and transcription factors binding to RUNX2 are indicated by the lines beneath RUNX2. The interaction domains of the proteins listed below the dashed line have not yet been identified (Schroeder *et al*, 2005).

Various proteins have been demonstrated to enhance the transcriptional activity of RUNX2. The VDR has been shown to directly interact with RUNX2 to cooperatively regulate the osteocalcin promoter (Paredes *et al*, 2005). Furthermore, the coordinated activity RUNX2 and VDR was demonstrated to participate in the transcriptional regulation of the osteopontin gene (Shen and Christakos, 2005). BMP2 has the ability to modulate RUNX2 expression and also able to regulate RUNX2 activity via SMAD activation. SMADs are downstream signal transducers of the TGF-β superfamily and have been shown to physically interact with RUNX2 (Zhang *et al*, 2000a). The interaction between SMAD5 and RUNX2 was shown to synergistically regulate alkaline phosphatase gene expression in C2C12 cells (Lee *et al*, 2000). RUNX2 also interacts with co-activators such as p300, CBP, MOZ and MORF (Schroeder *et al*, 2005, Sierra *et al*, 2003).

RUNX2 has also been demonstrated to interact with proteins which repress its activity. The c-terminus of RUNX2 contains the conserved VWRPY motif which was demonstrated to be essential for the interaction between RUNX2 and TLE transcriptional co-repressors (Thirunavukkarasu *et al*, 1998; Javed *et al*, 2000). Co-expression assays revealed that TLE proteins were capable of repressing RUNX2-mediated activation of the osteocalcin promoter and the p6OSE reporter construct (Thirunavukkarasu *et al*, 1998; Javed *et al*, 2000). In contrast, Grg5, also a member of the TLE/groucho family enhanced RUNX2 activation of the p6OSE reporter construct (Wang *et al*, 2004). HDACs have also been implicated in regulating RUNX2 activity. HDAC 6 was demonstrated to bind to a region of RUNX2 overlapping the NMTS in the c-terminus. The ability of RUNX2 to repress the p21 (CIP/WAF1) promoter was attributable to the c-terminus and the repression could be alleviated via the addition of the HDAC inhibitor trichostatin A (Westendorf *et al*, 2002). HDAC 3 was shown to interact with the amino terminus of RUNX2 and co-expression assays revealed that HDAC 3 suppressed RUNX2-dependent activation of the osteocalcin promoter (Schroeder *et al*, 2004).

1.7 BMP2

BMP2 belongs to the family of bone morphogenic proteins (BMPs) and are small secreted molecules which act as multifunctional growth factors. BMPs belong to the TGF-β superfamily and were originally characterized for their ability to induce ectopic bone formation when implanted under the skin of rodents (Ducy and Karsenty, 2000; Chen *et al*, 2004). Studies have revealed BMPs are involved with numerous developmental processes including playing critical roles in heart, neural and

cartilage development and postnatal bone formation (Chen *et al*, 2004). BMP2 is a powerful osteogenic factor and is capable of driving the differentiation of C2C12 pre-myoblasts and stromal cells towards the osteoblast lineage. In addition, BMP2 directs the synthesis of several osteoblast specific genes such as alkaline phosphatase and type I collagen (Katagiri *et al*, 1994; Takuwa *et al*, 1991; Thies *et al*, 1992). Pre-clinical and clinical studies have demonstrated BMP2 could potentially be used as an effect therapeutic agent for bone related diseases and injuries (Chen *et al,* 2004). The use of recombinant human bone morphogenic protein 2 (rhBMP2) in orthopedic applications was proven to safe, successful and cost-effective. Application rhBMP2 for spinal regeneration procedures revealed it was more effective than autogenous iliac crest bone grafts by reducing blood loss, decreasing operating times and costs, having better fusion outcomes and increasing patient satisfaction (Khan and Lane, 2004).

BMP2 acts by binding to a heterodimeric complex of two transmembrane receptors, termed type I and type II. The receptors possess serine-threonine kinase activity, which upon ligand stimulation phosphorylate members of the SMAD family of transcription factors. Once phosphorylated, the SMADs are activated and translocated to the nucleus to transduce their signals (Ducy and Karsenty, 2000). SMADs 1, 5 and 8 are activated in response to BMP signaling and associate with a common co-SMAD (SMAD4) before being translocated to the nucleus (Massagué *et al*, 2005). When the activated SMADs enter the nucleus, they associate with numerous proteins and co-factors to regulate the expression of target genes (Massagué *et al*, 2005). SMADs have been shown to physically interact with RUNX proteins and the interaction between RUNX2 and SMAD3 stimulated the transcription of the germline Ig Cα

promoter in a cooperative manner (Hanai *et al*, 1999). The region of RUNX2 responsible for facilitating the interaction with either BMP2 or TGF-β responsive SMADs is the SMAD interacting domain (SMID) and is located in the well defined NMTS (Afzal *et al*, 2005). The coordinated activities of BMP2 and RUNX2 are essential for proper skeletal development. Lee *et al* (2000) demonstrated that RUNX2 was a common target of both BMP2 and TGF- β signaling and that the cooperation between SMAD5 and RUNX2 was sufficient to induce alkaline phosphatase mRNA expression in C2C12 cells (Lee *et al*, 2000). Furthermore, inhibition of autocrine BMP2 signaling disrupted RUNX2 induced osteoblastic differentiation and decreased the ability of RUNX2 to transactivate the osteocalcin promoter in mesenchymal cells (Phimphilai *et al*, 2006).

1.8 Genetics of BMD and fracture

BMD is a quantitative measure of bone strength and is commonly used to assess bone quality (Ammann and Rizzoli, 2003; Ralston, 2005). The genetic contribution to BMD has been established by twin studies. The influence of genetics on a particular trait is commonly determined by comparing the correlation in the trait value in monozygotic (MZ) twins to the correlation in the trait value in dizygotic (DZ) twins. If the difference in correlation coefficients between MZ and DZ twins is statistically significant, then genetics significantly contributes to the trait. In the case of BMD, twin and family studies have estimated that 60-85 % of the variation in BMD can be explained by genetics (Ralston, 2005). Pocock *et al* (1987) was the first study to demonstrate the significant contribution of genetics in determining bone mass at multiple skeletal sites. The results showed that heritability of BMD ranged from site

to site and heritability estimates for the lumbar spine, femoral neck, Wards triangle and the trochanter were 0.92, 0.73, 0.85 and 0.57 respectively. Subsequent studies have confirmed the initial observations of Pocock *et al* (1987) in addition to revealing that other indicators of bone strength and bone quality such as femoral neck geometry, quantitative ultrasound properties of bone and bone turnover markers also have large genetic components with heritability estimates ranging from 50-80 % (Ralston, 2005).

BMD has an important application in terms of its use in defining the existence of the metabolic bone disease osteoporosis. Osteoporosis is characterized by the microarchitectural deterioration of bone tissue subsequently leading to reduced bone mass, bone strength and an increased risk of fracture (Kanis *et al*, 1994). Fractures are a leading health problem as they cause significant pain, loss of movement and increase healthcare costs (Reginster and Burlet, 2005). An individual is defined to suffer from osteoporosis when the BMD measured at the spine or femoral neck is equal to or less than 2.5 SD below the normal population mean of young adults (Kanis, 2002).

Osteoporosis is a polygenic disorder dependent on multiple genes in addition to environmental risk factors (Andrew and Macgregor, 2005). The clinical outcome of osteoporosis, fracture is also dependent on genetics factors and has a heritability estimate ranging from 25-35 % (Ralston, 2005). BMD is a major determinant of osteoporotic fractures and for every one SD decrease in BMD, the risk of fracture increases 1.5 to 3.0 fold (Kanis, 2002). Since BMD, osteoporosis and fracture are invariably linked; genetic risk factors for BMD and osteoporosis are also risk factors for fracture. Searching for genetic factors related to BMD, osteoporosis and ultimately

fracture would be beneficial in understanding the genetic basis of susceptibility to osteoporosis and possibly aid in the development of potential therapeutic agents to treat the disease. Procedures implemented for the search of genetic factors regulating BMD, osteoporosis and the risk of osteoporotic fractures involve the identification of Quantitative trait loci (QTL) through linkage analysis, use of animal models and analysis of candidate genes via association analyses (Ralston, 2005).

Numerous genome-wide linkage scans have been conducted in an attempt to identify chromosomal regions and genes (via fine mapping) linked to BMD. A logarithm of odds (LOD) score of 3.0 or greater is generally accepted as indicating the presence of linkage. Deng *et al* (2002) showed that chromosome 4q31-32 was linked to LS-BMD with a LOD score of 3.08. LS-BMD was also linked to 1q21-23 with a LOD score of 3.11 (Koller *et al*, 2000). A LOD score of 3.14 indicated that total hip BMD was linked to 21qter (Karasik *et al*, 2002), FN-BMD was linked to 20p12 (LOD 3.18, Styrkarsdottir *et al*, 2003) and Kammerer *et al* (2003) demonstrated that FN-BMD and trochanter BMD were linked to 2pter (LOD 3.98) and 13q14 (LOD 3.46) respectively. Despite the fact that significant linkage has been observed in several studies, very few results have been replicated between studies and there is evidence to suggest that linkage to specific chromosomal regions is dependent on skeletal site (Ralston, 2005). The limited replication in results between studies reflects the polygenic nature of BMD and suggested that the effect of individual genes on BMD was modest. Animal models are used much in the same way as human family studies to assess linkage of BMD to chromosomal regions. QTL influencing other phenotypes linked to the pathogenesis of osteoporosis have also been identified in mice (Ralston, 2005).

Gene association studies have identified several genes associated with the pathogenesis of osteoporosis and BMD. The Vitamin D receptor was the first candidate gene studied and has undergone extensive analysis since the initial discovery that common allelic variants accounted for up to 75 % of the genetic effect on BMD (Morrison *et al*, 1994). The magnitude of the genetic effect of VDR polymorphisms on BMD has subsequently been revised in a multitude of other studies which combined in a meta-analysis indicated that the BB genotype was associated with significantly decreased BMD with a net effect of a 0.15 Z-score decrease at the spine (Thakkinstain *et al*, 2004).

Collagen type 1α1 is another gene that has been the focus of numerous studies. Type 1 collagen is the major protein constituent of bone and several polymorphisms within the promoter and 1st intron have been reported to be associated with BMD (Grant *et al*, 1996; Utterlinden *et al*, 1998; Garcia-Giralt *et al*, 2002) . The polymorphism in intron 1 caused by a G-T transition occurs on a Sp1 binding site and has attracted the most attention. A multicentre analysis of 20,786 individuals from several European countries revealed that the Sp1 polymorphism was associated with a modest but significant decrease in BMD and showed a trend for an increased risk of vertebral fracture in women independent of BMD (Ralston *et al*, 2006). Other genes which have shown associations with BMD include lipoprotein receptor-related protein-5, transforming growth factor beta 1, PTH/PTHrP receptor type 1, oestrogen receptor and sclerostin (Yamada *et al*, 1998; Koay *et al*, 2004; Zhang *et al*, 2006; Utterlinden *et al*, 2004).

RUNX2 is absolutely vital for skeletogenesis and also participates in maintaining skeletal integrity in adults (Ducy *et al*, 2000). Based on these facts, RUNX2 is also a strong candidate gene for regulating BMD. Our laboratory has published a study which investigated the effect of a synonymous G to A SNP in the polyalanine tract of RUNX2. The A allele was significantly associated with increased BMD and was protective against Colles fracture (Vaughan *et al*, 2002). The effect of the A allele on increased BMD persisted when re-tested in a Scottish population (Vaughan *et al*, 2004). Furthermore, analysis of RUNX2 P2 promoter polymorphisms revealed a haplotype block was associated with increased BMD (Doecke *et al*, 2006). Collectively, the investigations of RUNX2 allelic variants suggested RUNX2 significantly contributed to BMD and indicated it was a legitimate candidate gene for influencing BMD and possibly fracture.

1.9 Aims and objectives

The project consisted of four main elements of research focused towards characterizing the bone specific transcription factor RUNX2. The first element consisted of genotyping the Southeast Queensland bone study for gross variations of the RUNX2 Q/A domain. Genotyping was carried out by PCR amplifying RUNX2 exon 2 fragments from genomic DNA templates. PCR amplified DNA samples were subsequently resolved through polyacrylamide matrices and RUNX2 genotypes were called according to the banding patterns observed. Statistical analyses were employed to determine if any associations existed between the common 18 bp deletion allele of the alanine tract (11Ala allele) and fracture.

The second facet of the research focused on the analysis of rare polyQ/A mutations in RUNX2. Rare RUNX2 Q/A variants were identified through the genotyping of multiple epidemiological studies of bone. Bone density and fracture data available from the studies was assessed to determine if rare Q/A variants presented with altered bone phenotypes. In addition, the transactivation function of the rare Q/A variants was analysed. The analysis was carried out by creating RUNX2 expression vectors harbouring variant Q/A domains. The ability of wild type and mutant RUNX2 proteins to transactivate two target promoters was assessed in two different cell lines. The results were statistically analysed to determine if the RUNX2 Q/A mutants significantly altered protein transactivation function.

The third element of the research consisted of identifying RUNX2 transcriptional gene targets. The functional cooperation between RUNX2 and BMP2 in regulating

target genes was also addressed. The investigation was conducted by stably transfecting NIH3T3 mouse embryonic fibroblasts with either RUNX2, BMP2 or both RUNX2 and BMP2 simultaneously. A fibroblastic cell line was determined to be the most appropriate cell line to conduct the experiment as fibroblasts are derived from the same mesenchymal precursor cells as osteoblasts and all genes expressed in osteoblasts are expressed in fibroblasts with the exception of osteocalcin and RUNX2 (Ducy *et al*, 2000). The expression profiles of the cell lines were analysed via microarrays to identify potential gene targets. Differentially regulated genes identified via the microarray analyses were subjected to quantitative RT-PCR to confirm the microarray results and to further characterize the genes by determining if gene expression was dependent on RUNX2, BMP2 or both RUNX2 and BMP2.

The fourth component of the research was based on investigating the role of RUNX2 in the ascorbic acid mediated induction of MMP-13 mRNA in NIH3T3 cells. AA regulates MMP-13 expression in osteoblasts which express high levels of RUNX2. NIH3T3 mouse embryonic fibroblasts express low levels of RUNX2. The aims of the project were to determine if RUNX2 was required for the AA mediated induction of MMP-13 mRNA in NIH3T3 cells and to determine the effect of combined BMP2 and RUNX2 overexpression in regulating MMP-13 mRNA levels in the presence of AA.

1.10 Significance

RUNX2 is a key regulator of osteoblast differentiation and chondrocyte maturation and plays an essential role in skeletal development (Komori *et al*, 1997; Otto *et al*, 1997; Kim *et al*, 1999). Haploinsufficiency of RUNX2 leads to the skeletal syndrome cleidocranial dysplasia. RUNX2 has been implicated in the regulation of BMD (Vaughan *et al*, 2002; Vaughan *et al*, 2004; Doecke *et al*, 2006) and is a candidate gene for osteoporosis. Osteoporosis is a highly prevalent metabolic bone disease characterized by the microarchitectural deterioration of bone tissue leading to an increased risk of fracture (Ralston, 2005). The incidence of osteoporosis is progressively increasing with aging populations and the reduction in bone strength associated with osteoporosis markedly increases the risk of fracture. The pain and loss of function arising from fractures impacts negatively on the quality of life and is a burden on health systems via increasing healthcare costs (Reginster and Burlet, 2006).

Identifying genes implicated in the pathogenesis of the disease would be beneficial in elucidating the pathways and mechanisms which lead to osteoporosis and perhaps lead to the development of effective and cost efficient treatments. We had previously identified several gross variations of the repeat sequence encoding the Q/A domain of RUNX2. The variants were associated with altered bone parameters and identifying additional variants would provide a means to further characterize the effects of Q/A mutants on bone. Investigating the transactivation function of Q/A variants would provide an insight into how the mutations influence bone parameters. Identifying downstream RUNX2 gene targets would give an insight into how RUNX2 directs osteoblast differentiation and contributes to the maintenance of the osteoblast

phenotype. In addition, identifying genes cooperatively regulated by RUNX2 and BMP2 would aid in elucidating the complex functions carried out by RUNX2 within the context of regulating cell differentiation and cell cycle progression.

Collectively, the research conducted served the purpose of characterizing the bone specific transcription factor RUNX2 to further increase the understanding of bone biology. A greater knowledge of bone biology would assist in better understanding bone disorders such as osteoporosis and aid in the development of effective treatment strategies.

Chapter 2

Materials and methods

2.1 Overview of research approach

The research was conducted to genetically and functionally investigate the bone specific transcription factor RUNX2 using genetic and molecular biological approaches. The research was conducted in 4 parts, each of which is presented as a chapter in this thesis (chapters 3-6).

The first component of the research focused on genotyping a DNA cohort in relation to variations within the poly Q/A tract of RUNX2. The procedures implemented for the search of RUNX2 sequence variants consisted of:

1) Gathering the DNA samples from the cohort.
2) Using PCR to amplify the RUNX2 DNA segment that contains the Q/A domain.
3) Resolving the PCR amplified DNA fragments via polyacrylamide gel electrophoresis (PAGE) which enabled the identification of WT genotypes and deletion/insertion mutants by observing the banding patterns of the resolved DNA.

Subsequent to identifying mutants via PCR and PAGE, statistical analyses were conducted to determine if any associations existed between RUNX2 variants and anthropomorphic measurements and measures of bone quality.

The second part of the research was conducted to genetically and functionally analyse RUNX2 Q/A mutants. An overview of the methods used to conduct the research is as follows:

1) DNA samples from multiple epidemiological studies of bone were obtained.
2) PCR was used to amplify RUNX2 DNA fragments containing the poly Q/A domain.
3) Genotyping of the DNA fragments was carried out using a combination of gel electrophoresis and HPLC.
4) Statistical analyses were conducted to assess the effect of rare glutamine and alanine mutations on measures of bone density and fracture.
5) The function of mutant RUNX2 proteins was analysed using a RUNX2 gene target reporter assay where mutant forms of RUNX2 proteins were overexpressed in tissue culture cells and their ability to transactivate known target promoters was assessed.

The third element of the research endeavoured to elucidate the functional role of RUNX2 in contributing to the transcriptional regulation of genes using tissue culture models. A major component of the research focused on identifying synergism between RUNX2 and the powerful bone promoting agent BMP2 in regulating target genes. The research was achieved by creating a series of stably transfected cell lines. NIH3T3 embryonic fibroblasts were used as model cell line and stable transfectants overexpressing RUNX2, BMP2 and both RUNX2 and BMP2 were created. The expression profiles of the cell lines were assessed using microarray analysis and quantitative RT-PCR. The quantitative methods of gene expression permitted the identification of genes regulated by RUNX2 and BMP2.

The fourth part of the research analysed the role of RUNX2 in the ascorbic acid mediated induction of MMP-13 mRNA. To achieve this, the stably transfected cell lines created in the third element of the research (chapter 5) were cultured in standard media or in media supplemented with ascorbic acid. Quantitative RT-PCR was used to assess the expression of MMP-13 mRNA levels in the various cell lines treated with and without ascorbic acid. The MMP-13 expression patterns provided an insight into the role of RUNX2 in the ascorbic mediated induction of MMP-13 mRNA.

Methodologies were in common for the four major chapters of research conducted. These methods are outlined in the following section (section 2.2). Experimental procedures related to specific phases of the research are outlined within chapters 3, 4, 5 and 6.

2.2 Methods in common between the four research chapters

2.2.1 Polymerase chain reaction (PCR)

PCR was used for multiple purposes including screening of a DNA cohort for RUNX2 Q/A variants, creation of mutant RUNX2 cDNAs, construction of reporter and target promoter vectors and the amplification of full length cDNA. All PCRs were conducted using the same general protocol. The precise nature of the primers and thermal cycler conditions relating to specific experimental procedures are detailed in

the methods sections of chapters 3, 4, 5 and 6. PCRs were carried out in 20 µl reactions and consisted of 2.5 x 10^{-7} M of each primer, 20ng-100ng of DNA template, 1 x Qiagen Q-solution, 1 x Qiagen PCR buffer, 1.25 x 10^{-5} M dNTPs (equiconcentration of dATP, dCTP, dGTP and dTTP, promega corp.), 0.5 units Qiagen hotstar Taq DNA polymerase and pure H_2O up 20 µl. The general thermal cycler conditions were: cycle 1: 15 minutes @ 95˚C (1x), cycle 2: 30 seconds @ 95˚C, 30 seconds @ 59˚C and 30 seconds @ 72˚C (35x), cycle 3: 1 minute @ 4˚C (1x). All PCR reactions were carried out in Bio-Rad thermal iCycler PCR machines.

2.2.2 Agarose gel electrophoresis

Agarose gel electrophoresis was used to resolve and visualise PCR amplified DNA, observe native and restriction enzyme cleaved plasmid DNA and to purify DNA fragments for subsequent cloning experiments. The percentage of agarose in the gels used for the aforementioned purposes ranged from 1-2%, contained 0.2 mg/ml ethidium bromide and were TAE based. Once set with wells created by specific combs which governed the size of the wells and ultimately the amount of DNA solution that could be loaded, the agarose gels were fully submerged in TAE buffer. The DNA samples to be electrophoresed were loaded into the wells and the gels were exposed to an electrical potential ranging from 80 to 120 volts to resolve the loaded DNA. Once the DNA migrated the desired distance, the gels were carefully removed from the tanks and exposed to UV light in a transilluminator to visualize the DNA.

2.2.3 Polyacrylamide gel electrophoresis (PAGE)

PAGE was used to separate PCR amplified DNA fragments with greater precision than agarose gels. The greater resolution of polyacrylamide gels in relation to its agarose counterpart permitted the identification of small variations in size between DNA fragments facilitating the correct genotyping of RUNX2 Q/A domains. Resolution of DNA via polyacrylamide matrices was also used as a means to purify DNA products for subsequent use in re-amp PCRs. All polyacrylamide gels were used at a concentration of 7.5% and the ratio of acrylamide to bis-acrylamide was 29:1. A typical polyacrylamide gel was prepared using 12.5 ml 30% acrylamide solution, 37.5 ml 0.5x TBE buffer, 75 µl TEMED and 350 µl 10% APS. The resulting solution was mixed and poured between two glass plates and a well forming comb was put in place. Once set, the gel was positioned in a polyacrylamide gel tank, the combs were removed and enough 0.5x TBE running buffer was added to submerge the wells. DNA was loaded into the wells and the gels were run at 200-220 volts to resolve the DNA fragments. Once the DNA had migrated the desired distance, the gels were removed from the tanks and stained in an ethidium bromide bath (distilled H_2O with 0.5 mg/ml ethidium bromide) for 10 minutes. After the staining period, the gels were de-stained in distilled H_2O for 10 minutes and visualized under UV light in a transilluminator.

2.2.4 Restriction enzyme digestion

Restriction endonucleases were routinely used for cloning purposes. All restriction enzymes used in the research were produced by New England Biolabs (NEB) and were purchased via the local distributor Genesearch. The enzymes were used to digest both plasmid and PCR amplified DNA. Reactions were generally carried out in 20-100 µl volumes depending on the amount of DNA to be digested. A typical reaction contained the appropriate 1x reaction buffer, 5 units of enzyme per microgram of DNA, PCR amplified or plasmid DNA and pure H_2O up to the desired volume. The reaction mixture was vortex briefly and incubated at 37˚C for two-three hours. The reaction was then heat inactivated according to enzyme specifications ready for subsequent use.

2.2.5 DNA ligation

DNA ligations were used for the generation of expression, reporter and promoter constructs. All DNA ligations were performed using T4 DNA ligase (NEB) and were generally carried out in a total volume of 10 µl. The molar ratio of vector to insert was 3:1 and the reactions contained between 50-100 ng of vector DNA with the corresponding amounts of insert. The reactions consisted of vector/insert DNA, 1x reaction buffer, 80 units of T4 DNA ligase and pure H_2O up to 10 µl. The reactions were incubated at room temperature for at least 2 hours before use in transformation procedures.

2.2.6 DNA purification

Purification of DNA from agarose and polyacrylamide gels was implemented to yield pure DNA fragments for subsequent use in cloning experiments, DNA sequencing and re-amplification PCRs. Purified DNA was extracted from agarose gels via the use of the Wizard® PCR preps DNA purification system (Promega corp.) according to the manufactures protocol. Briefly, DNA fragments destined to be purified were resolved through agarose gels and the DNA bands were excised using sterile scalpels. The excised agarose/DNA samples were placed in microcentrifuge tubes and incubated at 70˚C until fully melted. Once melted, 1 ml of DNA purification resin was added to each sample and mixed thoroughly for 20 seconds without vortexing. For each sample, the plunger from a disposable syringe was removed and the barrel attached to the Lure-Lok® extension of a minicolumn. The resin/DNA mix from the microcentrifuge tube was placed into the syringe barrel using a pipette and the slurry was gently pushed through using the plunger. The barrel was detached from the minicolumn and the plunger removed. The barrel was re-attached to the minicolumn and 2 ml of 80% isopropanol added. The solution was pushed through the column using the plunger. The syringe was removed and the minicolumn was transferred to a microcentrifuge tube for centrifugation. The minicolumn was centrifuged at 10,000 x g for 2 minutes to dry the resin. The minicolumn was transferred to a fresh microcentrifuge tube and 50 µl of TE buffer was added to the column and incubated at room temperature for 1 minute. To elute the purified DNA, the minicolumn was centrifuged at 10,000 x g for 20 seconds.

The purification of DNA from polyacrylamide gels was used to yield pure DNA fragments to serve as templates for PCR. DNA was extracted from the gels by excising resolved DNA bands using sterile scalpels and placing the samples in microcentrifuge tubes. For each sample, the polyacrylamide containing the DNA was crushed using a pipette tip and 200 µl of pure H_2O was added. The samples were incubated at room temperature overnight to elute the DNA. The samples were centrifuged at 10,000 x g for 2 minutes to pellet the polyacrylamide and the supernatant containing the purified DNA was removed and placed in a fresh microcentrifuge tube ready for subsequent use.

2.2.7 DNA Sequencing

DNA sequencing was employed to verify the exact sequence of RUNX2 Q/A repeat variants identified in the Southeast Queensland bone study and to confirm the identity of plasmid constructs. DNA sequencing was carried out using the dideoxy method and the reactions were conducted using the Big Dye® terminator V1.1 reagent (Applied Biosystems). DNA sequencing reactions were performed in total volumes of 20 µl and each reaction comprised of 3.2 pmoles of primer, 50-100 ng of pure DNA template, 4 µl of Big Dye® terminator V1.1 reagent and pure H_2O up to 20 µl. The mixture was vortexed briefly and placed in a PCR machine. The thermal cycler conditions were: cycle 1: 2 minutes @ 96˚C (1x), cycle 2: 20 seconds @ 96˚C, 15 seconds @ 55˚C and 1 minute @ 60˚C (26x) and cycle 3: 2 minutes @ 4˚C (1x). The DNA was precipitated via the addition of 2 µl of 3M Na acetate and 50 µl of 95% ethanol. The mixture was vortexed for 20 seconds and was incubated at room temperature for 15 minutes. The samples were centrifuged at 14,000 rpm for 20

minutes in a bench-top centrifuge. The supernatant was discarded and the DNA pellet was washed with 250 µl of 70% ethanol followed by centrifugation at 14,000 rpm for 15 minutes. The supernatant was discarded and the DNA pellets dried under vacuum. Once dry, the samples were sent to the DNA sequencing facility in Nathan where they were reconstituted via the addition of pure H_2O and analysed by gel electrophoresis and fluorescence detection.

2.2.8 Electrotransformation of *E.coli*

Electroporation was used to transform *E.coli* cells by facilitating the uptake of plasmid DNA. The process required pre-treating *E.coli* DH5α cells with 10% glycerol and centrifugation steps to prepare them for electroporation. The protocol for preparing electrocompetent cells was as follows: 200 ml of Luria broth was inoculated with 1/100 volume of fresh overnight culture of DH5α cells. The cells were grown @ 37˚C shaking at 100 rpm until the OD_{600} reached approximately 0.5. The cells were chilled on ice for 20 minutes and then transferred to four 50 ml corning centrifuge tubes. The cells were harvested via centrifugation at 4000 rpm for 15 minutes at 4˚C. The supernatant was carefully removed and discarded and the cell pellets were gently resuspended in 50 ml of ice-cold 10% glycerol per tube. Once resuspended, the cells were spun at 4000 rpm for 15 minutes at 4˚C. The supernatant was carefully removed and discarded and the cells were resuspended in 25 ml of ice-cold 10% glycerol per tube. The cells were centrifuged at 4000 rpm for 15 minutes at 4˚C. The supernatant was carefully removed and the cells were resuspended in 2 ml of ice-cold 10% glycerol per tube. Once fully resuspended, the cell suspensions from each of the four tubes were combined into one 10 ml centrifuge tube creating a final volume of

approximately 8 ml. The cells were centrifuged at 4000 rpm for 15 minutes at 4˚C. The supernatant was carefully discarded and the cells were resuspended in a final volume of 600 µl via the addition of 10% glycerol. The cells were transferred into microcentrifuge tubes in 50 µl aliquots ready for direct use or storage for up to 6 months at -80˚C.

Electroporation of *E.coli* cells was carried out using the Bio-Rad Micropulsar^{TM}. For electroporation, the desired quantity (1-2 µl) of plasmid DNA or DNA ligation mix was added to fresh or thawed electrocompetent cells and vortexed briefly. The cell/DNA mixture was transferred to a sterile, ice-cold 0.2 cm electroporation cuvette and placed in the chamber slide of the micropulsar. The cuvette was pushed into position and pulsed once. Following the pulse, the cuvette was quickly removed from the micropulsar and the cells were gently resuspended in 1 ml of terrific broth (TB). The cell suspension was transferred to a 10 ml polypropylene tube and incubated at 37˚C shaking @ 220 rpm for an hour to allow the cells to recover from the electric pulse. The cells were then spread at the appropriate dilution on LB agar plates containing selective medium and incubated overnight at 37˚C.

2.2.9 Small scale preparation of plasmid DNA: DNA minipreps

Extraction of plasmid DNA from *E.coli* cells was carried out during cloning experiments. DNA minipreps were performed to extract plasmid DNA from single bacterial colonies. The method used for the extraction of DNA was a modified version

of the protocol outlined in Maniatis *et al* (1982) and was as follows: 1 ml of TB was placed into a 10 ml polypropylene tube and the broth was inoculated with bacteria from a single colony and incubated at 37˚C shaking at 200-220 rpm overnight. The grown cells were transferred to a 1.5 ml microcentrifuge tube and harvested via centrifugation at 8000 rpm for 20 seconds. The supernatant was removed using a pipette and discarded. The cells were resuspended in 100 µl of TE buffer and placed on ice. 200 µl of freshly made lysis solution (0.2 N NaOH, 1% SDS) was added to each sample and the contents were mixed by inverting five times. The samples were then placed on ice for 10 minutes allowing the cells to lyse completely. To precipitate the protein, 150 µl of KAc buffer (5 M potassium acetate, pH 5.5) was added to each sample and mixed via inversion. The samples were placed on ice for five minutes before being centrifuged at 14,000 rpm for 5 minutes in a bench top centrifuge to pellet the proteins. The resulting supernatant was carefully removed and placed into a fresh tube. The double stranded DNA was precipitated via the addition of 2 volumes of 100 % ethanol at room temperature. The DNA was harvested via centrifugation at 14,000 rpm for 5 minutes. The supernatant was removed and the DNA pellet was washed with 70 % ethanol followed by another centrifugation step at 14,000 rpm for 5 minutes. The supernatant was removed and the DNA pellet was dried under vacuum. The DNA pellet was re-dissolved via the addition of 50 µl of TE buffer containing RNAase (20 µg/ml).

2.2.10 Large scale preparation of plasmid DNA and purification via equilibrium centrifugation in CsCl-Ethidium Bromide gradients

Large scale purification of plasmid DNA was carried out to yield large amounts of ultra pure plasmid DNA for subsequent use in DNA transfection experiments. The protocol used for harvesting the plasmid DNA was an up-scaled version of the DNA miniprep method and is outlined as follows: 100 ml of fresh TB was placed into an autoclaved 2-litre beaker and inoculated with a single bacterial colony. The cells were grown overnight at 37˚C shaking at 110 rpm. The cultured cells were divided into two 50 ml corning centrifuge tubes and harvested via centrifugation at 5,000 rpm for 10 minutes. The supernatant was discarded and the cells were resuspended in 5 ml of TE buffer per tube. 10 ml of fresh alkaline lysis buffer (0.2 N NaOH, 1% SDS) was added to each tube and the contents were mixed by inverting five times. The tubes were placed on ice for 10 minutes allowing lysis to occur. To precipitate the proteins, 7.5 ml of KAc buffer (5 M potassium acetate, pH 5.5) was added to each tube and mixed via inversion. The tubes were placed on ice for a further 5 minutes prior to centrifugation at 5,000 rpm for 10 minutes to pellet the precipitated proteins. The supernatant was transferred to fresh 50 ml centrifuge tubes (usually divided equally into four tubes per 100 ml of starting culture) and the DNA was precipitated via the addition of two volumes of 100 % ethanol at room temperature. The contents were mixed gently and the DNA was pelleted via centrifugation at 5,000 rpm for 10 minutes. The supernatants were removed and discarded and the nucleic acid pellets were rinsed with 70 % ethanol. The DNA pellets were allowed to dry at room temperature and re-dissolved in 2.4 ml of TE. The DNA solution was transferred to a

10 ml polypropylene tube and 4.4 g of ultra pure CsCl was added to the DNA solution. Once the CsCl was fully dissolved, 40 µl of 10 mg/ml ethidium bromide solution was added and the plasmid solution was layered under 5 ml of CsCl/TE ρ1.47 in a polyallomer ultracentrifuge tube. The tube was filled up to the desired level with CsCl/TE ρ1.47 solution and the cap was placed on top of the tube. The plasmid/CsCl solution was placed in an ultracentrifuge and spun at 50,000 rpm for 18-20 hours. After centrifugation, the tubes were removed from the rotor and the plasmid band (seen as a band of ethidium bromide solution) was removed using an 18-gauge needle and placed into a fresh 10 ml tube. The plasmid solution was extracted three times with butanol saturated TE to remove the ethidium bromide. 1 ml of pure H_2O was added to the tube and the plasmid DNA was precipitated via the addition of 2.5 volumes of 100 % ethanol. The DNA was pelleted via centrifugation at 5,000 rpm for 10 minutes. The supernatant was removed and the plasmid pellet was rinsed with 70 % ethanol. The pellet was dried under vacuum and re-dissolved in 500 µl of TE buffer ready for use.

Chapter 3

Association of the RUNX2 11Ala allele with fracture

3.1 Introduction

3.1.1 Background

Osteoporosis is a systemic skeletal disease characterized by the microarchitectural deterioration of bone tissue which ultimately leads to compromised bone strength (Ralston, 2003). The reduction in bone strength markedly increases the risk of fracture (Reginster and Burlet, 2005). The consequent pain and disability resulting from osteoporotic fractures creates a large burden on society by impinging adversely on the quality of life and increasing health care costs (Atik *et al*, 2006; Reginster and Burlet, 2005). Bone mineral density (BMD) is used to define the existence of osteoporosis and is a quantitative measure of bone mass (Ralston, 2005). BMD is a multifactorial trait dependent on both genetic and environmental factors. Twin studies have revealed that 60-85 % of the variance in BMD can be explained by genetics (Ralston, 2005). BMD is a primary predictor of osteoporotic fractures and the risk of fracture increases by 1.5 to 3.0 fold for every 1 standard deviation (SD) reduction in BMD (Kanis, 2002). Although BMD is a very strong predictor of fracture, it does not explain all of the variance in fracture and as such is not a perfect predictor. The disconnection between BMD and fracture could potentially be explained by other determinants of fractures such as bone geometry, ultrasound properties of bone and biochemical markers of bone turnover. Such determinants of fracture also have strong genetic components with heritability estimates ranging from 50-80% (Ralston, 2005).

The search for genetic loci and genes involved in the regulation of BMD is commonly achieved via genome-wide linkage scans and quantitative trait loci (QTL) analysis.

An alternative approach is to study genes which are strong candidates for influencing BMD and/or the risk of fracture via gene association studies. Candidate genes for BMD include the vitamin D receptor (VDR), type 1 collagen, oestrogen receptor α, transforming growth factor-β 1 and interleukin-6 (Ralston, 2003). The RUNX2 transcription factor is also a suitable candidate gene and it has been demonstrated that RUNX2 alleles and polymorphisms within the RUNX2 P2 promoter were associated with changes in BMD and the risk of fracture (Vaughan *et al*, 2002; Vaughan *et al*, 2004; Doecke *et al*, 2006). RUNX2 is fundamental for osteoblast differentiation and is essential for skeletal development (Ducy *et al*, 1997; Komori *et al*, 1997; Otto *et al*, 1997). Mutations within the RUNX2 gene of humans and mice cause the skeletal disorder cleidocranial dysplasia which is characterized by critical defects in bone formation (Mundlos *et al*, 1997; Lee *et al*, 1997). RUNX2 is involved in a myriad of regulatory activities pertaining to cellular differentiation and cell cycle progression and functions by interacting with a variety of co-regulatory molecules to form multimeric complexes to regulate target genes (Schroeder *et al*, 2005).

A unique feature of RUNX2 is the consecutive polyglutamine and polyalanine tracts (Q/A domain). We hypothesized that the repeat sequence encoding the Q/A domain could potentially vary via strand slippage during DNA replication and cause alterations in bone phenotypes such as biochemical markers of bone turnover, bone density and fracture. We undertook genotypic analysis of several DNA cohorts where we screened the RUNX2 Q/A tract for deletions and insertions. The studies identified several rare, in-frame glutamine repeat mutations as well as a commonly occurring deletion mutation (18 base pair deletion) of the polyalanine tract. The polyalanine deletion allele was observed at a frequency of approximately 6 %. The deletion

mutation results in the removal of 6 alanine residues from the polyalanine tract of RUNX2 changing the normal alanine repeat from 17 alanine residues to 11 alanine residues (17Ala-11Ala). We hypothesized the deletion of the 6 alanine residues would cause a functional alteration in RUNX2 activity subsequently affecting bone parameters.

3.1.2 Prior knowledge associating the 11Ala allele with altered bone phenotypes

Upon the discovery of the 11Ala allele and considering the proposed hypothesis that it was a good candidate for causing a functional alteration in RUNX2, several experiments were conducted to determine if the 11Ala allele was associated with altered bone phenotypes. The first investigation was conducted in 78 osteoarthritis (OA) patients who had multiple determinations of serum parameters. Analysis of serum parameters revealed that only serum osteocalcin was significantly different between 11Ala carriers (subjects which carried at least one copy of the 11Ala allele) and non-carriers (no copies of the 11Ala allele). The analysis determined that carriers of the 11Ala allele were associated with significantly reduced serum osteocalcin levels ($p = 0.01$, figure 3.1). Information on environmental factors was not available and thus was not adjusted for in the analysis. This was perhaps a limitation of the analysis, however it was unlikely that the environmental factors would have accumulated in such a way as to confound the analysis assuming the 78 OA subjects were a random sample drawn from a larger population.

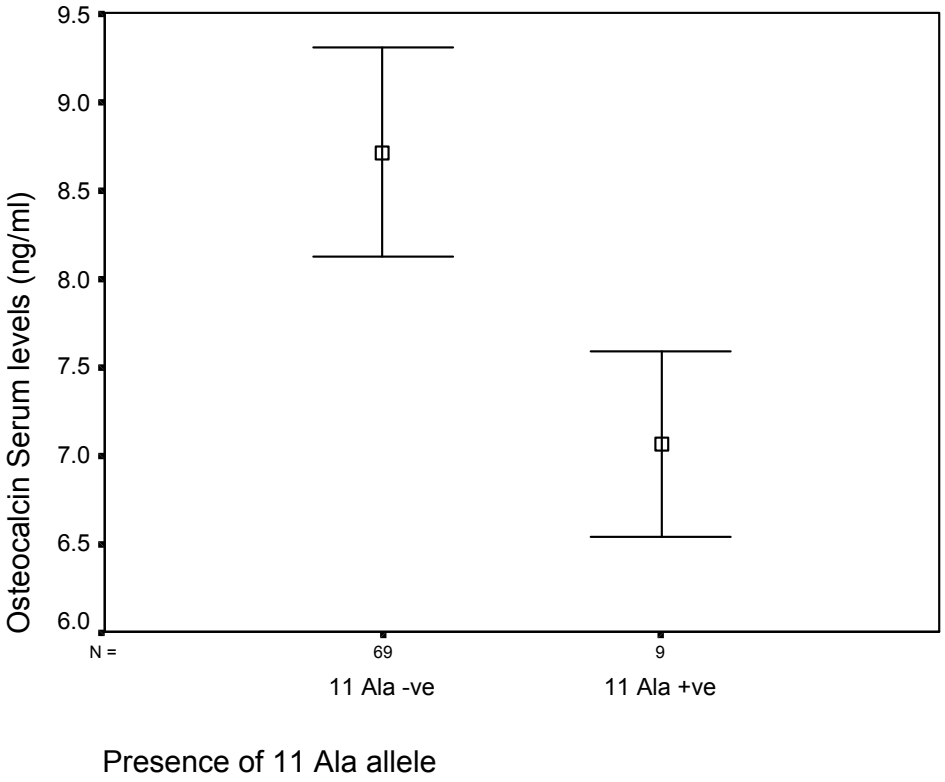

Figure 3.1: Serum Osteocalcin levels (mean ± 2SD) in 11Ala -ve and 11Ala +ve genotype groups. Presence of the 11Ala allele was significantly related to decreased serum osteocalcin levels (P = 0.01).

Osteocalcin (OC) is small secreted extracellular matrix protein involved in regulating bone mass and its expression is known to be regulated by RUNX2 (Ducy and Karsenty, 1995; Ducy *et al*, 1996). The significantly decreased serum OC in 11Ala carriers reflected a possible functional change in RUNX2 activity providing support for the hypothesis and suggesting that 11Ala allele carriers were associated with a lower bone turnover phenotype. Note: The results of the OA study have not published in a peer reviewed journal; however the results have been published in the form of a PhD thesis written by Dr Tanya Vaughan. An electronic version of the published document is available at www4.gu.edu.au:8080/adt-root/public/adt-QGU20040430.161453/index.html.

To further characterize the 11Ala allele, its effect on BMD was investigated in the Geelong Osteoporosis Study (GOS). The GOS is based in the Barwon Statistical Division of Victoria, Australia and subjects recruited for participation in the GOS are comparable to the Australian population with respect to age and socioeconomic background (Henry *et al*, 2002). 495 random population subjects from the GOS were genotyped for the presence or absence of the 11Ala allele. BMD data as measured by DEXA was available for multiple skeletal sites and the BMD of 11Ala allele carriers was compared to non-carriers. The analysis revealed there were no significant differences in BMD between 11Ala allele carriers and non-carriers at any skeletal site (Vaughan *et al*, 2002). As a follow up to the GOS, an investigation of the 11Ala allele and BMD was conducted in a Scottish cohort from Aberdeen. Analysis of BMD data from 991 genotyped random population subjects revealed there were no significant differences in BMD between 11Ala allele carriers and non-carriers (Vaughan *et al*, 2004). Collectively, the analyses revealed the 11Ala allele did not significantly influence BMD as measured by DEXA. However, a recessive effect of the 11Ala allele on BMD could not be ruled due to the low numbers of homozygous 11Ala genotypes.

Despite the lack of an association between the 11Ala allele and BMD, an investigation was conducted to test any possible effects of the 11Ala allele on fracture keeping in mind that even though BMD is a powerful predictor of fracture it does not explain all of the variance in fracture. To analyse the 11Ala allele and fracture, a case-control study was implemented using cohorts derived from the GOS. A fracture cohort and an appropriate age-matched control group from the same population catchment and who did not sustain incident fracture during the study period were

genotyped for the 11Ala allele. A total of 591 fracture samples and 224 age-matched controls was genotyped (table 3.1). Analysis of allele frequencies using chi-square revealed the 11Ala allele was significantly enriched in the fracture group (table 3.2). The over-representation of 11Ala alleles in the fracture cohort provided evidence to suggest the 11Ala allele conferred an increased fracture risk.

Table 3.1: RUNX2 genotypes in fracture and control groups.

Group	WT/WT	11Ala/WT	11Ala/11Ala
Fracture	511	78	2
Control	207	17	

Table 3.2: Chi-Square analysis of 11Ala genotypes within fracture and non-fracture groups.

Fracture * 11Ala Crosstabulation

			11Ala		
			yes	no	Total
Fracture	yes	Count	80	511	591
		Expected Count	70.3	520.7	591.0
	no	Count	17	207	224
		Expected Count	26.7	197.3	224.0
Total		Count	97	718	815
		Expected Count	97.0	718.0	815.0

Chi-Square Tests

	Value	df	Asymp. Sig. (2-sided)	Exact Sig. (2-sided)	Exact Sig. (1-sided)
Pearson Chi-Square	5.479[b]	1	.019		
Continuity Correction[a]	4.927	1	.026		
Likelihood Ratio	5.937	1	.015		
Fisher's Exact Test				.021	.011
Linear-by-Linear Association	5.472	1	.019		
N of Valid Cases	815				

Risk Estimate

	Value	95% Confidence Interval	
		Lower	Upper
Odds Ratio for Fracture (yes / no)	1.906	1.102	3.297
For cohort 11Ala = yes	1.784	1.081	2.942
For cohort 11Ala = no	.936	.891	.983
N of Valid Cases	815		

Note: The case-control study of the 11Ala allele and fracture has not been published in a peer reviewed journal; however the results have been published in an honours thesis written by Alexandre Stephens.

Collectively, the prior analyses revealed the 11Ala allele was significantly associated with decreased serum osteocalcin and an increased risk of fracture independent of BMD.

3.2 Methods

3.2.1 Southeast Queensland bone study

The Southeast Queensland bone study was the source of 980 subjects from which 747 were genotyped. The study was based at the Genomics Research Centre, Griffith University on the Gold Coast, Queensland, Australia. Study participants were recruited via notices in the local newspaper and from a hypertension database. DNA extraction and serum parameters were obtained via standard procedures. The study was comprised of singletons and families and the number of individuals within families ranged from 2 to 16.

Multiple serum parameters were available for analysis and included sodium, potassium, chloride, bicarbonate, glucose, urea, creatinine, uric acid, total bilirubin, alkaline phosphatase, gamma-glutaminase, calcium, phosphate, total protein, albumin, globins, magnesium, iron, cholesterol and triglycerides. RUNX2 genotype was determined according to the protocol below (Genotyping via PCR and PAGE). Self reported fracture data was available and included information on the site of fracture, the force of impact which caused the fracture (traumatic or non-traumatic) and the age at which the fracture was sustained. Anthropomorphic measurements weight (kg), height (cm) and body mass index (BMI) were accessible. Age, gender and information of family structures were available.

3.2.2 Genotyping via PCR and PAGE

PCR was used to amplify RUNX2 DNA fragments containing the Q/A domain from genomic DNA samples. The oligonucleotide primers were 5'-AGCCTGCAGCCCGGCAAAATGAGC-3' for the forward and 5'-GGGTGGTCGGCGATGATCTCCACCATG-3' for the reverse. The reaction conditions are described in section 2.2.1. The size of PCR amplified DNA derived from wild type genomic templates was 233 bp. Amplified DNA samples were resolved through 7.5% polyacrylamide gels and stained with ethidium bromide. The gels were placed in a transilluminator and the DNA bands were visualized under UV light. Insertion and deletion mutations were identified via their altered and unique migration rates through the polyacrylamide matrix. The presence of heteroduplex structures generated via the annealing of mutant to wild type DNA fragments was also indicative of mutations.

3.2.3 Statistical analysis

Student's t-tests were used to compare anthropomorphic measurements between the RUNX2 genotype groups. Logistic regression analysis was used to test the effect of age, gender, height, weight and RUNX2 genotype on fracture status. The logistic regression analysis was performed on the entire genotyped dataset. The relationship between the 11Ala allele and non-traumatic fracture was assessed using chi-square analysis. Generally in family based populations, linkage and association analyses are conducted using family based association tests (FBATs) such as the transmission

disequilibrium test (TDT) and the sib-transmission disequilibrium test (S-TDT). A FBAT approach could have been implemented to analyse the genotyped data from the Southeast Queensland bone study. However, FBATs do not incorporate singleton data and thus there was no way of unifying the singleton and family data collected from the Southeast Queensland bone study. In addition, only a small number of the genotyped families were informative greatly reducing the ability of FBATs to detect significant effects on polygenic traits. The alternative to the FBAT was to conduct an association analysis using chi-square. The genotyped data consisted of 322 singletons and 425 individuals from 152 families. To account for the correlation between biologically related individuals, one representative member from each family was chosen at random to contribute towards the analysis. The random selection of representative family members was carried out using the re-sampling function in PopTools (http://www.cse.csiro.au/poptools/). The process of randomly selecting one representative family member was repeated twenty times generating 20 samples of randomly selected representative family members. Each sample of randomly selected representative family members was combined with the 322 singletons to create 20 unified datasets. The 20 unified datasets were analysed via chi-square to determine the effect of the 11Ala allele on fracture. Repeating the random selection of representative family members twenty times and using each unified dataset for analysis enabled the determination of the average effect of the 11Ala allele on fracture rather than basing the entire results on only one random selection of representative family members.

As mentioned above in the section titled "Prior knowledge associating the 11Ala allele with altered bone phenotypes", a case-control study from the GOS revealed that 11Ala allele carriers were significantly overrepresented in fracture cases. To combine

the results from the GOS and the Southeast Queensland bone study in order to calculate the overall effect of the 11Ala allele on fracture, Monte-Carlo simulations were performed to determine the empirical p-value (probability) of obtaining the study results by chance. Simulations were carried out using PopTools in Microsoft excel with 10, 000 iterations and the number of observed replicates which presented with results equal to or more extreme than the actual experimental results in terms of the overrepresentation of the 11Ala allele in fracture cases was recorded. The number of observed replicates divided by the number of iterations is equivalent to the one-tailed p-value.

3.3 Results

3.3.1 Genotyping of the Southeast Queensland bone study

A total of 747 DNA samples were genotyped for the RUNX2 poly Q/A tract. Examination of PCR amplified DNA resolved via PAGE permitted the identification of deletion or insertion mutations. Figure 3.3 shows a typical polyacrylamide gel of resolved PCR amplified DNA from which genotypes were determined. From the 747 genotyped, 665 were wild type (WT), 76 were heterozygous for the 11Ala allele, 5 were homozygous for the 11Ala allele and one was a rare 7 Q deletion of the polyglutamine tract.

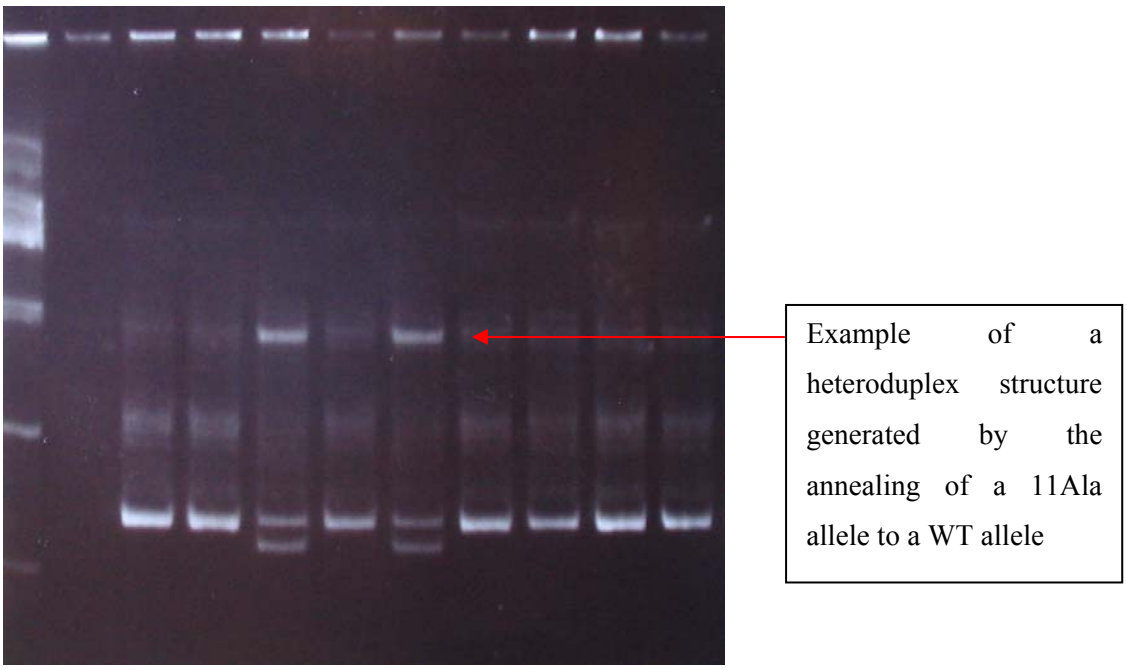

Figure 3.2: A typical polyacrylamide gel of PCR amplified RUNX2 exon 2 fragments containing the Q/A domain. Lane 1: DNA ladder, lane 2: -ve control, lanes 5 and 7 are examples of heterozygous genotypes for the common 18 bp deletion of the poly-alanine tract,

lanes 2, 3, 6 and 8-11 are examples of PCR amplified DNA generated from WT genomic templates.

3.3.2 Relationship of the 11Ala allele to fracture

Fracture data available for the Southeast Queensland bone study was used to test the relationship between RUNX2 genotypes and fracture status via chi-square analysis. Only non-traumatic fractures were considered for the analysis (fractures sustained from traumatic events such as car accidents were excluded). We had previously demonstrated that the 11Ala allele was associated with a significantly increased risk of non-traumatic fractures in the GOS. The purpose of conducting this genotyping study was to re-test the effect of the deletion allele on fracture to either confirm or refute the previously obtained results. For the analysis, the genotyped samples were divided into 11Ala -ve and 11Ala +ve genotype groups. Table 3.3 lists anthropomorphic measurements, samples sizes and fracture data for the two genotype groups.

Table 3.3: Anthropomorphic measurements ± SD, samples sizes and percentage of individuals which had sustained fracture (fracture %) for 11Ala -ve and 11Ala +ve genotypes.

Genotype	N	Age	Height	Weight	BMI	Fracture (%)
11Ala -ve	665	57.9 ± 13.4	167.0 ± 9.5	78.1 ± 17.7	28.1 ± 7.0	16.9
11Ala +ve	81	55.3 ± 13.7	165.8 ± 8.8	78.0 ± 21.4	30.0 ± 18.3	26.3

T-tests were conducted to determine if there were any significant differences in age, height, weight or BMI between the two groups (table 3.4).

Table 3.4: T-test results for the comparison of age, height, weight and BMI between 11Ala –ve and 11Ala +ve genotype groups.

	11Ala	Mean	SD	t-score	Sig. 2-tailed
Age	-ve	57.9	13.4	1.6	0.10
	+ve	55.3	13.7		
Height	-ve	167.0	9.5	1.0	0.30
	+ve	165.8	8.8		
Weight	-ve	78.1	17.7	0.08	0.94
	+ve	78.0	21.4		
BMI	-ve	28.1	7.0	1.8	0.07
	+ve	30.1	18.3		

The mean values of age, height, weight and BMI of the two RUNX2 genotype groups were very similar. The t-tests revealed there were no significant differences in age, height, weight or BMI between the RUNX2 genotype groups.

The effect of the 11Ala allele on fracture was analysed using a case-control approach via chi-square. Subjects which had sustained at least one non-traumatic fracture were considered as cases and subjects which had not sustained fracture were classed as controls. Chi-square analyses were conducted on all 20 unified datasets. 20 randomized selections of representative family members provided the opportunity to quantitate the average effect of the 11Ala allele on fracture rather than using only one combination (of the many possible combinations of data that could be generated via the random selection of only one family member from each family). The results of the chi-square analyses are summarised in table 3.5. The 2 x 2 contingency tables containing the observed and expected counts for each of the unified datasets and associated chi-square tests can be seen in appendix A1.

Table 3.5: Results from the chi-square analysis of RUNX2 genotype distributions within fracture and non-fracture groups (n = 474).

Dataset	Chi-Square	p-value	OR	Lower 95%CI	Upper 95%CI
1	2.641	0.104	1.775	0.882	3.575
2	1.802	0.179	1.606	0.800	3.225
3	0.952	0.329	1.426	0.697	2.920
4	2.985	0.084	1.844	0.913	3.723
5	2.359	0.125	1.725	0.854	3.481
6	2.408	0.121	1.733	0.859	3.495
7	1.191	0.275	1.488	0.726	3.047
8	2.105	0.147	1.702	0.824	3.514
9	0.628	0.428	1.334	0.653	2.726
10	3.082	0.079	1.864	0.922	3.768
11	4.611	0.032	2.101	1.054	4.188
12	3.022	0.082	1.818	0.919	3.594
13	1.673	0.196	1.579	0.787	3.168
14	5.164	0.023	2.200	1.099	4.404
15	1.734	0.188	1.589	0.794	3.183
16	2.920	0.087	1.798	0.910	3.551
17	1.622	0.203	1.593	0.774	3.279
18	1.363	0.243	1.509	0.753	3.020
19	4.323	0.038	2.054	1.030	4.097
20	1.363	0.243	1.509	0.753	3.020
Ave.		**0.160**	**1.712**		

The resulting chi-squares ranged from 0.628-5.164 and the corresponding p-values ranged from a non-significant 0.428 to a significant 0.023 with an average of 0.16. Seven of the 20 datasets demonstrated that 11Ala allele carriers were significantly overrepresented in the fracture group at an α of 0.10 and 3 of those were significant at an α of 0.05. Without exception, the frequency of 11Ala carriers was increased in the

fracture group for each of the unified datasets and the odds ratio ranged from a minimum of 1.334 to a maximum of 2.2 with an average effect of 1.712. In summary, the analyses suggested the 11Ala allele was enriched in individuals which had sustained fracture.

The overall effect of the 11Ala allele on fracture was assessed by combining the results of the GOS case-control investigation with the results from the Southeast Queensland bone study. Monte-Carlo simulations with 10, 000 iterations were used to determine a single empirical p-value of obtaining the results from both studies by chance. Simulations were performed for each of the 20 unified datasets from the Southeast Queensland bone study (table 3.6).

Table 3.6: Monte-Carlo simulations and associated p-values combining the results from the GOS and from the Southeast Queensland bone study with respect to the 11Ala allele and fracture.

Dataset	Iterations	Observed	p-value
1	10000	61	0.0061
2	10000	118	0.0118
3	10000	157	0.0157
4	10000	43	0.0043
5	10000	59	0.0059
6	10000	71	0.0071
7	10000	154	0.0154
8	10000	80	0.0080
9	10000	235	0.0235
10	10000	35	0.0035
11	10000	14	0.0014
12	10000	63	0.0063
13	10000	117	0.0117
14	10000	8	0.0008
15	10000	108	0.0108
16	10000	43	0.0043
17	10000	96	0.0096
18	10000	127	0.0127
19	10000	24	0.0024
20	10000	133	0.0133

Monte-Carlo analysis provided a suitable means to combine the results of both studies by calculating the probability of obtaining the results by chance. Each dataset produced a p-value less than 0.05 (α level) and ranged from a maximum p-value of 0.0235 to a minimum of 0.0008. The results indicated that the probability of obtaining

both study results by chance was small providing powerful evidence to link the 11Ala allele with an increased risk of fracture.

3.4 Discussion

RUNX2 is an important regulatory factor in bone development and cartilage formation (Komori *et al*, 1997; Otto *et al*, 1997; Enomoto *et al*, 2000). It performs many functions and these functions depend heavily on distinct structural domains of the protein (Stock and Otto, 2005). The structural integrity of RUNX2 is fundamental for proper activity (Thirunavukkarasu, *et al* 1998). One of the unique structural domains of RUNX2 is the poly Q/A region. The Q/A domain participates in transactivation function and is an essential component of the protein. Complete removal of the Q/A domain renders RUNX2 to have a capacity to transactivate a target promoter at a level 25% that of wild type (Thirunavukkarasu, *et al* 1998). The sequence encoding the Q/A region is unique in that it is composed of consecutive tri-nucleotide repeat tracts which have the ability to vary due to strand slippage during DNA replication. We tested the hypothesis that the repeat sequence encoding the Q/A domain could vary by conducted genotyping studies. The studies identified several rare in-frame insertion/deletion mutations of the glutamine tract as well as a common 18 bp deletion within the alanine tract (11Ala allele) and thus confirmed the hypothesis. Association analyses revealed the 11Ala allele was associated with significantly decreased serum osteocalcin and was associated with an increased risk of fracture in the GOS (Stephens *et al*, manuscript in preparation).

To ensure the effect on fracture was not a false positive, the Southeast Queensland bone cohort was used as an independent study to assess the effect of the 11Ala allele on fracture. The GOS population and the Southeast Queensland bone study differed in a number of ways. The patients were obtained from different geographical locations

within Australia (The Barwon statistical division, Vic for the GOS and the Gold Coast, QLD for the Southeast Queensland bone study). The GOS fracture cohort was composed entirely of females whereas both males and females were present within the Southeast Queensland cohort. The Southeast Queensland bone study also contained families in addition to singletons. The fracture data was confirmed radiologically in the GOS whereas self reported fracture data was recorded in the Southeast Queensland bone study. To perform the analysis, the genotyped data was divided into 11Ala –ve and 11Ala +ve groups. T-tests revealed there were no significant differences in age, height, weight or BMI between the two RUNX2 genotype groups. Logistic regression analysis of the entire genotyped cohort revealed that age, gender, height and weight were not significant predictors of fracture. In contrast, RUNX2 genotype was significantly related to fracture with 11Ala carriers being enriched in fracture cases. However, the logistic regression analysis was performed on the entire genotyped dataset and could have been influenced by the presence of family relationships.

To test the effect of the 11Ala allele on fracture while adjusting for family relationships, a case-control approach using chi-square was implemented. The correlation in biologically related individuals was controlled for by randomly selecting one representative member from each family to be included in the chi-square analysis. The random selection of one family member from each family was repeated 20 times generating 20 possible unified datasets when the data from the randomly selected individuals was combined with the data from singletons. The distribution of RUNX2 genotypes in fracture and non-fracture groups was assessed using chi-square for each unified dataset.

The chi-square analyses showed differing results. Some of the results reached statistical significance in demonstrating that 11Ala allele carriers were significantly overrepresented in fracture cases while the majority of the other results showed trends in the same direction. In all chi-square analyses conducted, the frequency of 11Ala allele carriers was greater in fracture cases compared to controls putting forward the notion that the 11Ala allele was associated with fracture. The average effect across the 20 chi-square analyses was an odds ratio of 1.712 which is similar to the odds ratio obtained from the GOS (OR = 1.9) and provided good replication between studies. Overall, the results from the Southeast Queensland bone study provided support for the original case-control study conducted in the Geelong cohort suggesting the 11Ala allele was associated with fracture.

Monte-Carlo simulations provided a suitable method of combining the results from the GOS and the Southeast Queensland bone study with respect to the 11Ala allele and fracture. Simulations were used to combine the GOS results with each of the unified datasets derived from the Southeast Queensland bone study. Each of the simulations presented the empirical probability of obtaining both study results by chance. For each dataset the p-values were less than 0.025 with a maximum of 0.0235 and a minimum of 0.0008 (mean = 0.00873). The results demonstrated that individuals which carried at least one copy of the 11Ala allele were significantly enriched in fracture cohorts.

Collectively, the heightened risk of fracture in carriers of the 11Ala allele suggested that the deletion mutation compromised an aspect of bone quality that ultimately

increased an individual's susceptibility to fracture. An interesting aspect of the association between the 11Ala allele and the increased fracture risk lies with the fact that there were no significant differences in BMD between 11Ala carriers and non-carriers as demonstrated by Vaughan *et al* (2002) and Vaughan *et al* (2004). The lack of an effect on BMD indicated that the 11Ala allele conferred its detrimental effects on fracture via a pathway independent of BMD as measured by DEXA. This scenario is possible considering BMD does not explain all of the variance in fracture and that fracture is also dependent on other factors such as bone geometry, ultrasound properties of bone and biochemical markers of bone turnover (Ralston, 2005). Similar effects have been observed in other studies where increases in the risk of fracture associated with polymorphisms could not be fully explained by changes in BMD. For example, a study conducted by Langdahl *et al* (2002) showed that polymorphisms within the osteoprotegerin (OPG) promoter were related to vertebral fracture within a Denmark population with no significant effects on BMD. Similarly an investigation of polymorphisms within the gene encoding Sp1 Collagen type Iα1 revealed the relative risk of fracture was two to three times greater than that predicted by BMD suggesting that the polymorphism may act as a marker for bone structure or matrix composition (Uitterlinden *et al*, 1998). A 2005 study demonstrated that vitamin D receptor gene polymorphisms were associated with an increased risk of fracture in post-menopausal women independent of BMD (Garnero *et al*, 2005).

In an attempt to elucidate that mechanism via which the deletion allele conferred an increased risk of fracture, quantitative transactivation analysis was performed (chapter 4) to determine if the deletion of 6 alanine residues from the polyalanine tract influenced RUNX2 function. The analysis revealed that the deletion mutation did not

significantly alter the ability of RUNX2 to transactivate a known target promoter. The results were consistent with data obtained from Thirunavukkarasu *et al* (1998) which demonstrated that complete removal of the alanine tract from the Q/A domain of RUNX2 did not significantly change the transcriptional activity of RUNX2. However, the analysis (chapter 4) was conducted using only one reporter plasmid and thus the effect of the 11Ala allele in the context of other target genes is not known. In addition, the expression plasmids were based on the RUNX2-I isoform and thus the effect of the deletion mutation on the activity of RUNX2-II is yet to be determined.

Collectively, analysis of the 11Ala deletion allele in relation to bone parameters revealed that carriers of the mutation presented with a significantly increased risk of fracture independent of BMD. The mechanism via which the deletion imposes its negative effects on fracture is yet to be discovered and more experimental research would be required to further characterize the exact effects of the deletion mutation on the function of RUNX2 and subsequently its consequences on bone.

Chapter 4

Analysis of RUNX2 poly Q/A variants

4.1 Introduction

RUNX2 is a member of the RUNT-domain family of transcription factors that regulate the expression of genes involved in cellular differentiation and cell cycle progression (Durst and Hiebert, 2004). RUNX2 directs the differentiation of osteoblasts from mesenchymal precursor cells in the developing embryo and is required for proper bone formation (Komori *et al*, 1997; Otto *et al*, 1997). Heterozygous mutations in coding and promoter sequences of RUNX2 cause the dominantly inherited skeletal syndrome Cleidocranial Dysplasia (CCD). The disorder is characterised by persistently open or delayed closure of sutures, hypoplasia/aplasia of clavicles, Wormian bones, supernumerary teeth, short stature and other skeletal abnormalities (Mundlos *et al*, 1997; Lee *et al*, 1997; Napierala *et al*, 2005). In addition a decrease in bone mineral density and reduced plasma alkaline phosphatase were observed in a mother and daughter presenting with features of CCD (Morava *et al*, 2002). To understand the underlying mechanism of CCD, mutant RUNX2 proteins were analysed for their transactivation ability. The mutations either completely abolished or severely reduced the transactivation function of RUNX2 (Zhou *et al*, 1999; Zhang *et al*, 2000a; Yoshida *et al*, 2003).

RUNX2 acts as a transcriptional modulator by interacting with numerous cofactors and transcription factors. RUNX2 and its partner proteins form macromolecular regulatory complexes that control the activity of target promoters by binding to specific DNA sequences within the promoters (Schroeder *et al*, 2005). The factors which interact with RUNX2 dictate which genes are destined to be regulated by RUNX2 and whether RUNX2 will have repressor function or transactivator function

(Schroeder *et al*, 2005). The interaction between RUNX2 and accessory molecules is dependent on distinct structural domains of RUNX2. For example, the PST domain is responsible for the interaction between RUNX2 and the co-activator proteins p300, MOZ and MORF. The SMID located within the NMTS facilitates SMAD interaction and the last five amino acids of RUNX2 (VWRPY motif) mediate the interaction between RUNX2 and members of the TLE/Groucho family of transcriptional co-repressors (Afzal *et al*, 2005; Westendorf *et al*, 2005).

One of the distinct structural domains of RUNX2 is the consecutive polyglutamine and polyalanine tracts (Q/A domain). The Q/A domain is a unique structural region of RUNX2 that participates in transactivation function and has been implicated in limiting the interaction between RUNX2 and its partner protein Cbfβ (Thirunavukkarasu *et al*, 1998). The Q/A domain also acts as the site for the interaction between RUNX2 and HDAC3. The binding of HDAC3 to RUNX2 repressed RUNX2 mediated activation of the osteocalcin promoter indicating HDAC3 had a repressive effect on RUNX2 activity (Schroeder *et al*, 2004). The Q/A domain of RUNX2 is encoded by a repeat sequence that has the capacity to mutate via strand slippage. Repeat expansion has been the cause of some diseases that show genetic anticipation, where severity increases in subsequent generations as repeat length increases due to errors in replication (Cummings & Zoghbi, 2000). Trinucleotide repeat expansions that occur in both non-coding and coding regions of DNA are responsible for more than 20 disorders (Di Prospero & Fischbeck, 2005). Non-coding expansions exert their detrimental effects by causing loss of gene function or by creating toxic mRNA whereas coding region mutations generate toxic proteins with or without altered function (Gatchel *et al*, 2005)

Expansions of the Q/A region in RUNX2 have been identified in humans. A 16 nucleotide expansion of the CAG repeat and a 10 Alanine residue insertion of the polyalanine tract were observed in patients with CCD (Mundlos *et al*, 1997). We hypothesised that RUNX2 Q/A repeat variants would exist in normal populations and would influence adult bone density and/or risk of fracture, since RUNX2 acts in mature osteoblasts as well as differentiating osteoblasts.

We had previously identified several gross variations (insertions and deletions) of the RUNX2 Q/A domain via genotyping studies (Vaughan *et al*, 2002; Vaughan *et al*, 2004, Stephens *et al*, manuscript in preparation). A total of six independent DNA cohorts were screened for Q/A repeat mutations. The cohorts genotyped included the GOS, an Aberdeen cohort, a Western Australian study (Calcium Intake Fracture Outcome Study (CAIFOS)), an osteoarthritis population (OA), a Gold Coast population (Southeast Queensland bone study) and a Sydney twin study. The gross variations consisted of rare Q/A repeat mutations as well as a common 18 base pair deletion of the polyalanine tract (11Ala allele). The 11Ala allele (refer to chapter 3 for detailed information) was associated with significantly reduced serum osteocalcin levels in an OA study (Stephens *et al*, manuscript in preparation). Analysis of BMD data in the GOS and the Aberdeen population showed there were no significant differences in BMD between 11Ala carriers and non-carriers (Vaughan *et al*, 2002; Vaughan *et al*, 2004). Although the 11Ala allele had no affect on BMD, we still investigated the distribution of 11Ala alleles within fracture and non-fracture control groups. The analyses revealed the 11Ala allele was significantly overrepresented in fracture cases in the GOS and showed a trend in the same direction in the Southeast Queensland bone study (Stephens *et al*, manuscript in preparation). Collectively the

association analyses revealed the 11Ala allele was a functionally relevant polymorphism associated with altered bone parameters.

In this chapter, the effect of rare Q/A repeat variants derived from four epidemiological studies on bone was assessed. The analyses revealed that collectively, Q-mutants presented with significantly lower bone density as measured by quantitative ultrasound at the calcaneus and by DEXA at the femoral neck. Analysis of incident fracture revealed Q-mutants had a significantly heightened fracture risk compared to non-carriers. To elucidate the possible mechanism via which variations within the RUNX2 polyQ/A domain were significantly lowering bone density, increasing the risk of fracture and altering serum osteocalcin levels, we analysed the ability of mutant RUNX2 proteins to activate 0.6 kbp of the human osteocalcin promoter (pOSLUC) and a synthetic construct composed of 6OSEs cloned prior to the 0.6 kbp of the human osteocalcin promoter.

4.2 Methods

4.2.1 Study Subjects

The study subjects were obtained from four different epidemiological studies of bone (table 4.1). The Geelong Osteoporosis study (GOS), Australia, based in the Barwon Statistical division of Victoria was the source of 1531 subjects and has been described previously (Sanders *et al*, 1998). Voting in elections in Australia is compulsory and each region maintains an electoral roll. Subjects from the Geelong study and from the Western Australian study were recruited in a similar fashion, using random ascertainment from the electoral roll and approach by letter. The West Australian study (CAIFOS) consisted of 1499 females between the ages of 70 and 85 years randomly recruited by letter and was the source of 1200 study samples. Informed consent for DNA studies was obtained from 1387 of these subjects and genotype was obtained on 1078 of these. The study has been previously described (Dick *et al*, 2002). Aberdeen study subjects were postmenopausal women aged between 45 and 55 years and 991 study participants were drawn at random using Community Health Index records of Aberdeen, Scotland as previously described (MacDonald *et al*, 2001). Sydney subjects were obtained from the Northern Sydney Twin Study based at the Department of Rheumatology of the Royal North Shore Hospital as previously described (Makovey *et al*, 2005). 273 DZ twin pairs and 215 MZ twin pairs were genotyped from the Northern Sydney Twin Study. DZ twin pairs were considered as unique individuals for the analysis of BMD Z-scores. Q-repeat mutants identified in MZ twins were considered as a unit and the average twin pair BMD was considered for the analysis of BMD Z-scores. Individuals in all studies were Caucasian and

exclusion in all studies related to chronic conditions or medication known to influence bone density. Appropriate consent was obtained from subjects under procedures approved by the relevant ethics committees as previously described (Sanders *et al*, 1998; Dick *et al*, 2002; MacDonald *et al*, 2001; Makovey *et al*, 2005).

Table 4.1: Characteristics of the epidemiological studies of bone from which DNA samples were genotyped for gross variations within the poly Q/A domain of RUNX2.

Study	Region	Size	Bone measures
Geelong Osteoporosis Study (GOS)	Victoria, Australia	1531	BMD, fracture
Western Australia (WA)	Western Australia, Australia	1078	BMD, SOS, BUA, fracture
Aberdeen (ABDN)	Aberdeen, Scotland	991	BMD
Sydney twin study (SYD)	Sydney, Australia	273 DZ 215 MZ	BMD

4.2.2 Bone measures

Each population collection used different systems to measure bone densitometry by dual energy X-ray absorptiometry (DEXA). In the Aberdeen study a Norland XR26 or XR36 was used (Norland Corporation, Fort Atkinson, WI, USA). A Lunar DPX-L machine was used for the GOS. In Sydney, a QDR 4,500 W Hologic machine was used (Hologic, Waltham, Mass). The Western Australian study used a Hologic Acclaim 4500A fan beam densitometer to measure total BMD of the hip region. A Lunar Achilles ultrasound machine was used to measure the left calcaneus bone. The

average of two measures of speed of sound (SOS), broadband ultrasound attenuation (BUA) and bone stiffness (a variable that incorporates BUA and SOS) were available.

4.2.3 Detection of Q/A-variants

PCR was used to amplify RUNX2 exon 2 fragments harbouring the Q/A repeat using the primers forward 5′-CCGGCAAAATGAGCGACG-3′ and reverse 5′-GGGCGGTGTAGCCTCTTACCTT-3′. The PCRs were carried out in 20 µl reactions containing 5 x 10^{-7} M primers, PCR reaction buffer, 125 µM dNTPs, 80 ng genomic DNA, 0.5 units Qiagen HotStar *Taq* DNA polymerase and pure H_2O up to 20 µl as specified by the supplier (Qiagen, Sydney, Australia). The study populations were genotyped separately by differing means. For the GOS and Sydney twin study, the resulting 336 bp fragments were resolved via non-denaturing 10% polyacrylamide gel electrophoresis (PAGE). Heteroduplex analysis was used to determine the presence Q/A repeat variants. For the Aberdeen population the PCR fragment was digested with *MspA1I* (New England Biolabs) and resolved on 3% agarose. For the Western Australian samples, all PCR products were initially analysed via dHPLC (Varian Prostar 430, Varian Industries, Sydney, Australia) and subsequently by heteroduplex PAGE. All PCR amplified DNA fragments that displayed unique mobility patterns on polyacrylamide gels were sequenced using BigDye Terminator v1.1 ready mix according to the manufacture's protocol (Applied Biosystems, Foster City, CA, USA).

4.2.4 Cloning of the RUNX2-I coding region into pUC18

The expression vector containing the full length RUNX2-I cDNA (pEF-αA) was kindly donated by Dr Kosei Ito from the RUNX group / Institute of Molecular and Cell Biology, Singapore. The full length cDNA was excised from pEF-αA using *XbaI* (figure 4.1). The excised DNA was purified via agarose gel electrophoresis and ligated into the *XbaI* site of pUC18 to create pUC18-RUNX2. Ligated plasmid DNA was transformed into electrocompetent *E.coli* cells via electroporation and DNA minipreps were performed on resulting single colonies. Samples of plasmid DNA extracted from single clones were digested with *EcoRI* to confirm the successful cloning of the RUNX2 cDNA into pUC18 and the orientation of the cloned insert (figure 4.2).

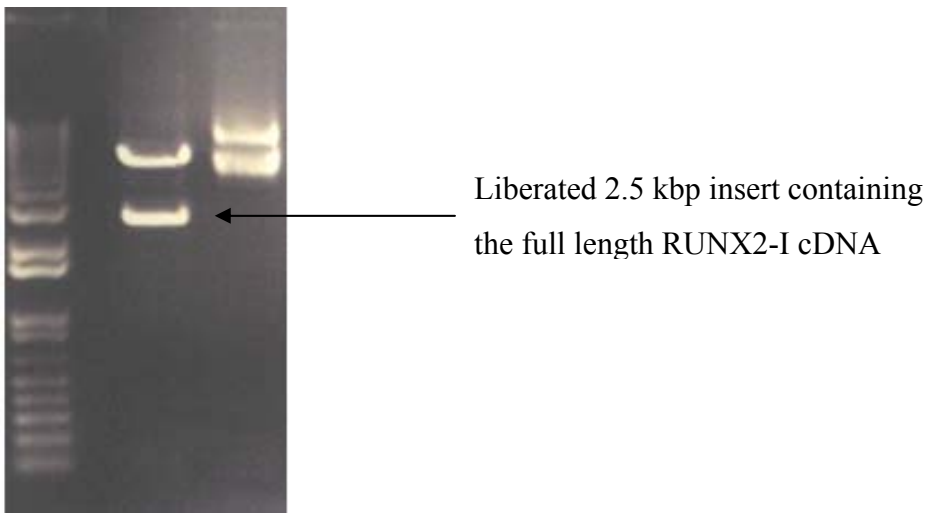

Figure 4.1: *XbaI* digestion of pEF-αA liberated a 2.5 kbp insert containing the coding region of RUNX2-I. Lane 1 contains DNA ladder, lane 2 is uncut pEF-αA and lane 3 contains pEF-αA digested with *XbaI*.

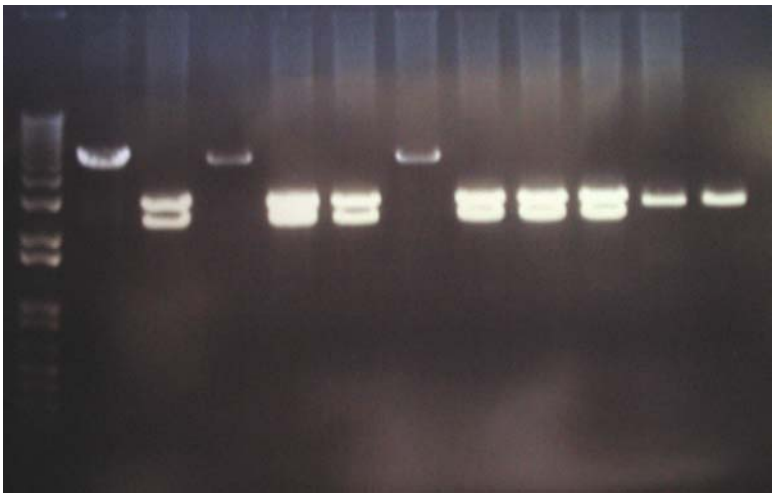

Figure 4.2: Plasmid DNA extracted from single colonies via DNA minipreps digested with *EcoRI*. Lane 1: DNA ladder, lanes 2-11: *EcoRI* digested miniprep DNA samples and lane 12: Positive control pUC18 digested with *EcoRI.* Lanes 2, 4 and 7 contain RUNX2 inserts cloned in pUC18 in the reverse orientation, lanes 3, 5, 6, 8, 9 and 10 contain RUNX2 inserts cloned in pUC18 in the forward orientation and lane 11 contains plasmid DNA from a blue colony (control).

4.2.5 Ligation of 16Q, 30Q and 11Ala containing poly Q/A domains into pUC18-RUNX2 and creation of RUNX2 expression vectors

Cloning of 16Q, 30Q and 11Ala polyQ/A domains into pUC18-RUNX2 was carried out using a PCR based cloning strategy. Partial RUNX2 P2 promoter and exon 2 fragments were PCR amplified from genomic templates harbouring 16Q, 30Q and 11Ala alleles using the oligonucleotide primers 5'-TTCACCACCGGACTCCAACT-3' for the 5' side and 5'-CATCTGGTACCTCTCCGAGGGCTACCACCTT GAAGGCCACGGGCAGGGTC -3' for the 3' side. The reverse primer contained an *EcoNI* tag facilitating the cloning of the PCR amplified product into the *BglII-EcoNI*

site of pUC18-RUNX2. The resulting PCR products were digested with *BglII* and *EcoNI* restriction enzymes and purified via agarose gel electrophoresis. The purified fragments were ligated into the corresponding sites of pUC18-RUNX2. The identities of the resulting plasmids were confirmed by DNA sequencing of the RUNX2 poly Q/A tract (figures 4.3, 4.4, 4.5 and 4.6).

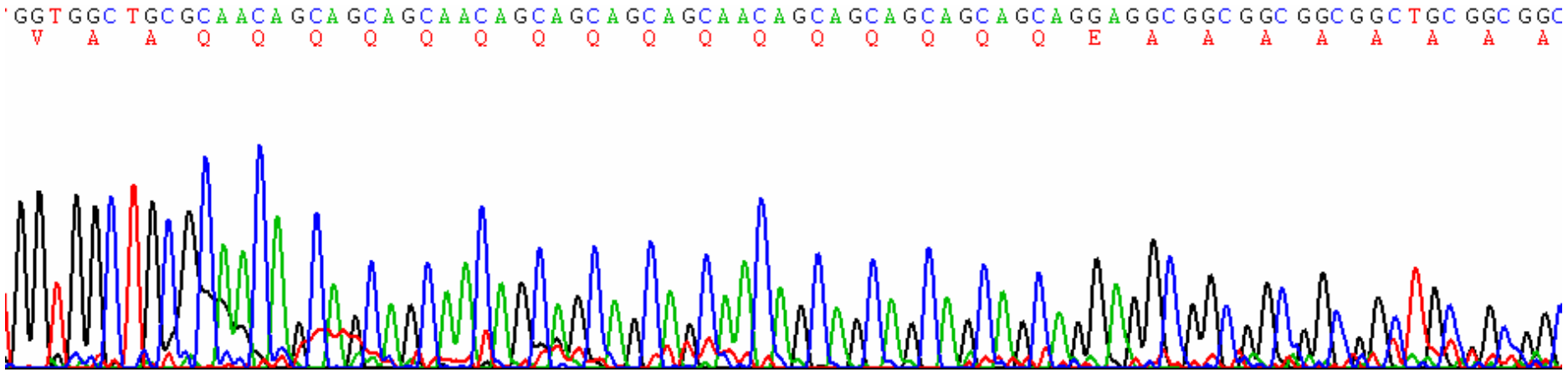

Figure 4.3: DNA sequence chromatogram for the glutamine repeat tract of the 16Q RUNX2 expression plasmid.

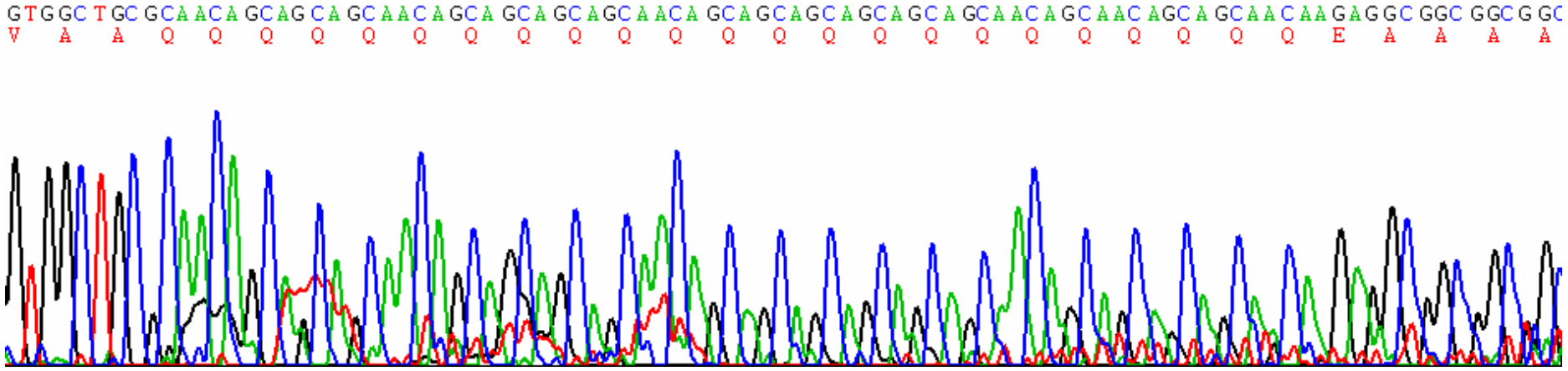

Figure 4.4: DNA sequence chromatogram for the glutamine repeat tract of the WT (23Q) RUNX2 expression plasmid.

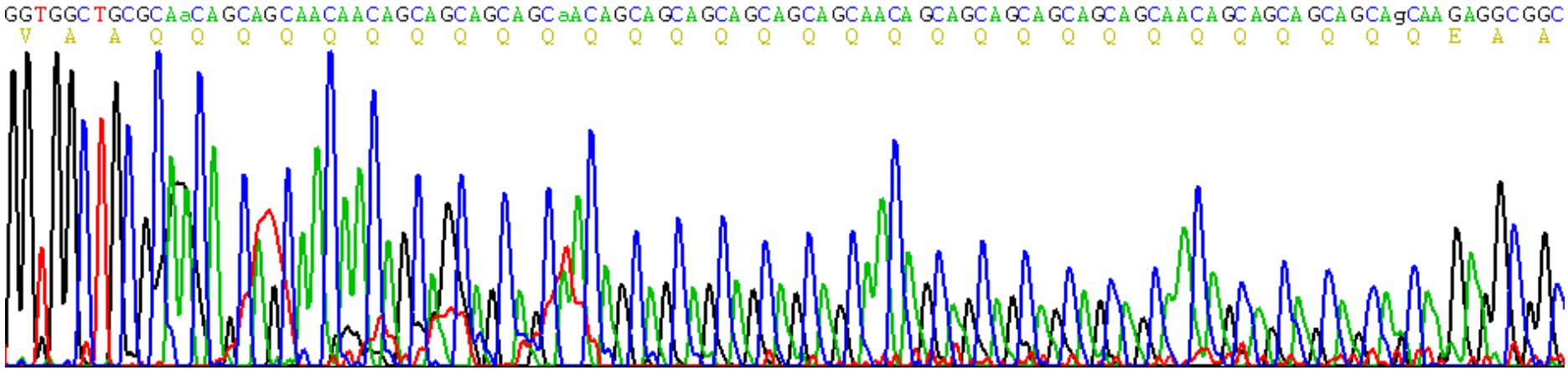

Figure 4.5: DNA sequence chromatogram for the glutamine repeat tract of the 30Q RUNX2 expression plasmid.

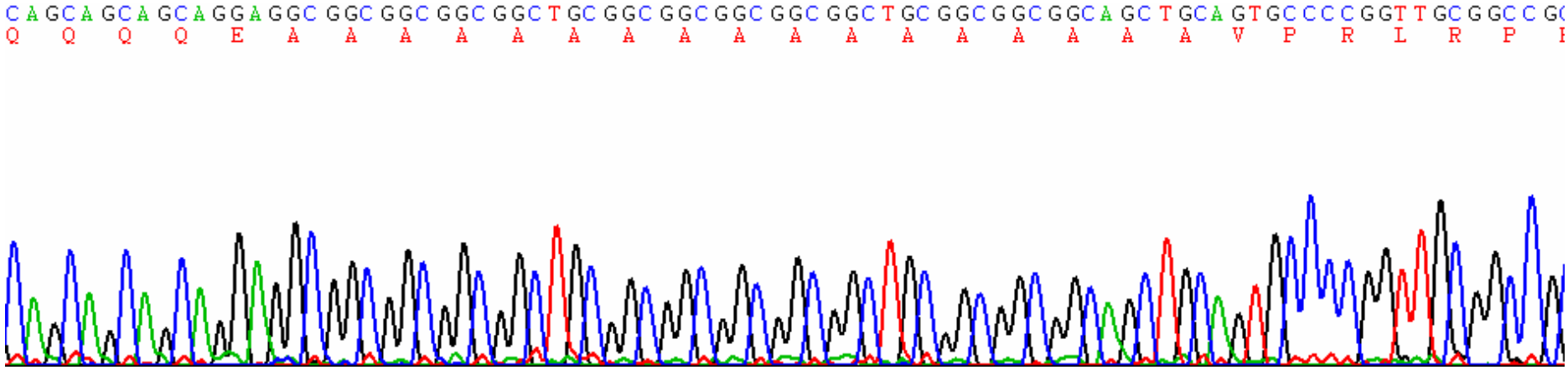

Figure 4.6: DNA sequence chromatogram for the alanine repeat tract of the WT (17Ala) RUNX2 expression plasmid.

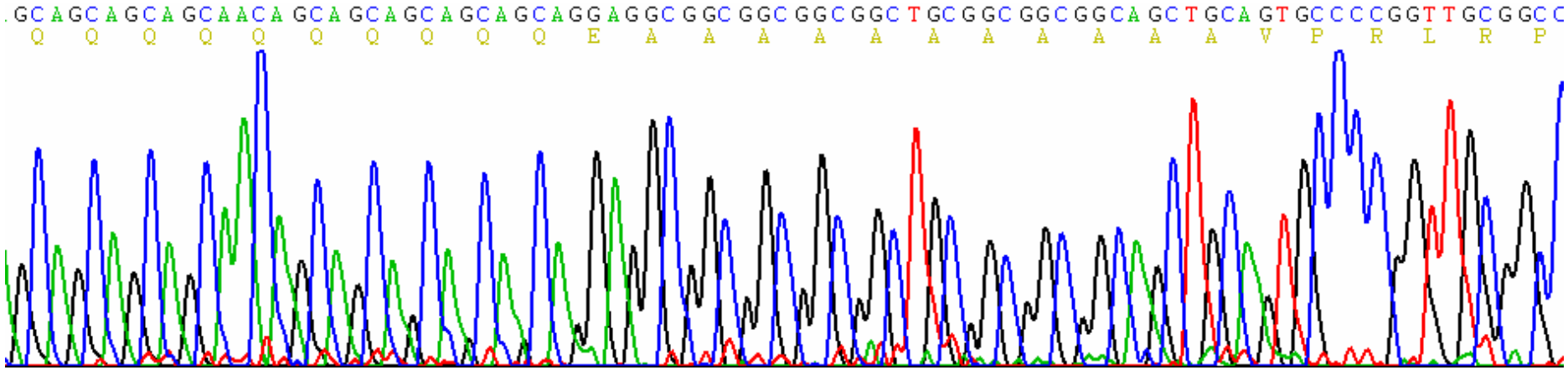

Figure 4.7: DNA sequence chromatogram for the alanine repeat tract of the 11Ala RUNX2 expression plasmid.

Once the pUC18-RUNX2 variant clones were confirmed by DNA sequencing the inserts were excised by *XbaI* digestion and cloned into the corresponding sites of the pEF-Bos expression vector to successfully create the RUNX2 expression plasmids containing 16Q, 30Q or 11Ala allele mutant Q/A domains. The orientation of the cloned inserts in pEF-Bos was confirmed via restriction enzyme digest with *EcoRI* (figure 4.8). Once confirmed, the expression plasmids for wild type (23Q/17Ala), 16Q, 30Q and 11Ala allele RUNX2 were produced in large quantities and purified via CsCl ethidium bromide equilibrium centrifugation.

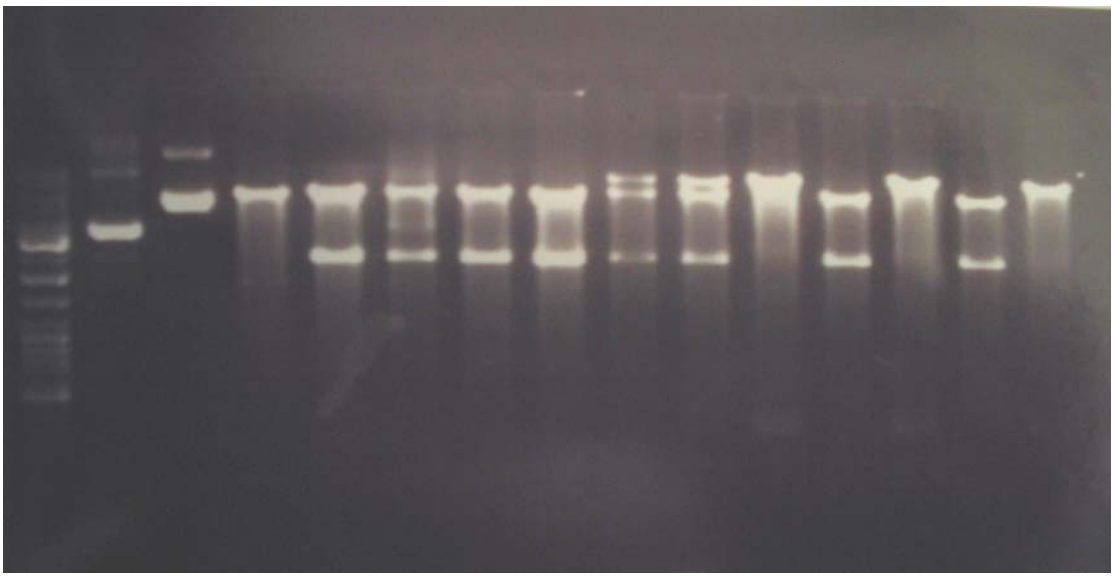

Figure 4.8: *EcoRI* digest of pEF-BosRUNX2 clones to confirm the successful cloning of RUNX2 into pEF-Bos and to determine the orientation in which the cDNAs were cloned. Lane: 1 DNA ladder, lane 2: pEF-Bos (uncut), lane 3 *EcoRI* digested pEF-bos, lane 4-15 *EcoRI* digested plasmid DNAs extracted from cloned colonies via DNA minpreps. Plasmid DNA samples in lanes 5-8, 12 and 14 contain RUNX2 inserts cloned in the correct (forward) orientation.

4.2.6 Creation of pOSLUC and p6OSE RUNX2 reporter plasmids

600 bp of the human osteocalcin promoter was amplified via PCR using the oligonucleotide primers 5'-CAGGAGATCTCTGACCGTCGAGCTG-3' for the forward and 5'-GGGCAAGCTTGGTGTCTCGGGTGGC-3' for the reverse. The oligonucleotides were engineered to contain *BglII* and *HindIII* restriction enzyme sites in the forward primer and the reverse primer respectively. Figure 4.8A shows a gel containing the PCR products for the amplification of the partial human osteocalcin promoter using annealing temperature gradients. Only one annealing gradient temperature produced a specifically amplified product (figure 4.9A, lane 5). A sample of the same PCR product was loaded and resolved through a polyacrylamide gel (figure 4.9B). The band was excised using a clean scalpel and the DNA was eluted in TE buffer. The resulting purified DNA was used as a template for PCR with the same original primers used for the amplification of the partial human osteocalcin promoter (figure 4.9C).

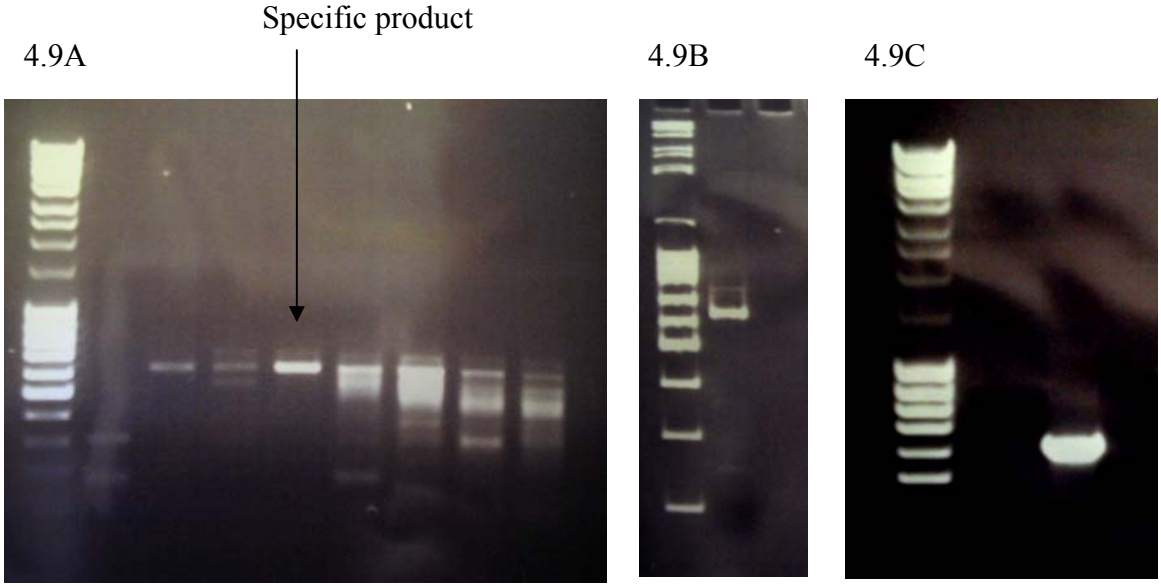

Figure 4.9: (A) Agarose gel of resolved PCR products for the amplification of the human osteocalcin promoter using annealing temperature gradients. Lane 1: DNA ladder, lanes 2-9: PCR products resulting from amplification reactions with annealing temperatures of 57ºC, 56.5ºC, 55.7ºC, 54.4ºC, 52.6ºC, 51.4ºC, 50.5ºC and 50ºC respectively. Only lane 5 contained a specifically amplified product. **(B)** PAGE of the specifically amplified osteocalcin promoter. Lane 1: DNA ladder, lane 2: Specifically amplified product. **(C)** Agarose gel of PCR product generated from a re-amplification reaction using the eluted PCR product obtained from the polyacrylamide gel as a template. Lane 1: DNA ladder, lane 2: -ve control and lane 3: Re-amp PCR product.

The re-amplified PCR product was purified and digested with *BglII* and *HindIII* restriction enzymes. The digested products were purified and ligated into the *BglII-HindIII* site of pGL3-basic. Colony clones resulting from the electrotransformation of ligated osteocalcin promoter with pGL3-basic were screened via DNA minipreps. The resulting plasmid DNAs were resolved via agarose gel electrophoresis to identify clones containing inserts (figure 4.10). Clones containing inserts were verified by DNA sequencing.

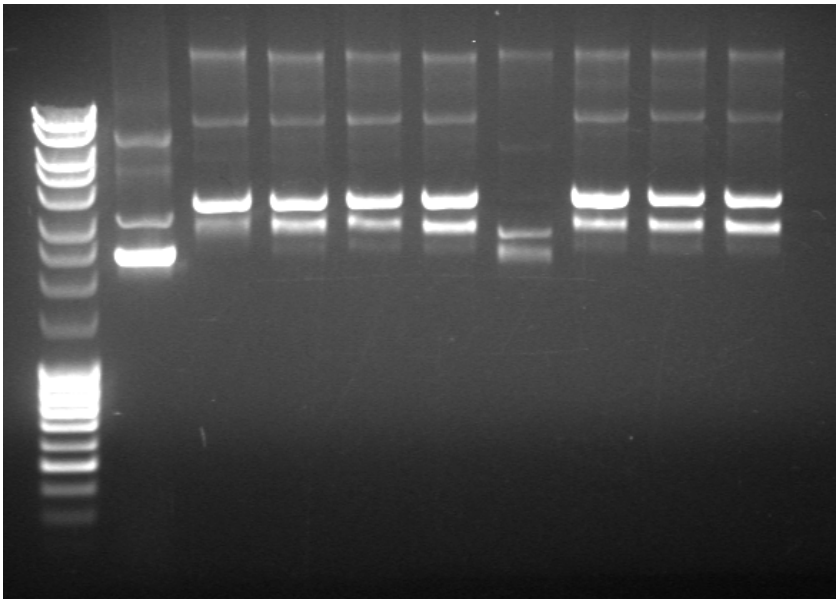

Figure 4.10: Agarose gel electrophoresis of pOSLUC clones. Lane 1: DNA ladder, lane 2: pGL3-basic, lanes 3-10: pOSLUC miniprep DNA samples. Lanes 2-5, 8-10 contained 600 bp of the human osteocalcin promoter.

The p6OSE reporter plasmid was created by annealing and multimerizing complementary 25mer oligonucleotides containing the core binding sequence for RUNX2 (OSE2, Ducy and Karsenty, 1995). The ligated oligonucleotides were purified and cloned into the *BglII* restriction site of pOSLUC. Resulting clones were screened via DNA sequencing for the presence of ligated oligonucleotides. The greatest number of consecutive oligonucleotides cloned into pOSLUC was six and thus the resulting plasmid was termed p6OSE and used for transfection experiments.

4.2.7 Tissue culture and transfection optimisation

NIH3T3 cells and HEK293 cells were maintained in DMEM (GIBCO) supplemented with 10% FBS (v/v) (GIBCO), 1% Penicillin-Streptomycin (v/v) (GIBCO) in a 5% CO_2 humidified atmosphere at 37˚C. For the transfection experiments NIH3T3 cells were seeded into 6-well plates at a density of 1 x 10^5 cells/well 24hrs prior to transfection. HEK293 cells were seeded into 12-well plates at a density of 1 x 10^5 cells/well 24hrs prior to transfection. Cells were transfected using the Fugene 6 transfection reagent (ROCHE).

The transfection conditions resulting in the highest amounts of gene transfer was determined via transfection optimisation. Transfections in HEK293 cells were carried out in 12-well plates at a cell density of 1 x 10^5 cells/well 24hrs prior to transfection. 100-600 ng of constitutive luciferase plasmid (pBOSLUX) was transfected into HEK293 cells with 1.5 µl of fugene 6 transfection reagent. Cell lysates were harvested 48 hours post-transfection and luciferase activities were quantitated (figure 4.11). The greatest amount of luciferase reporter activity was observed with 500 and 600 ng of plasmid DNA.

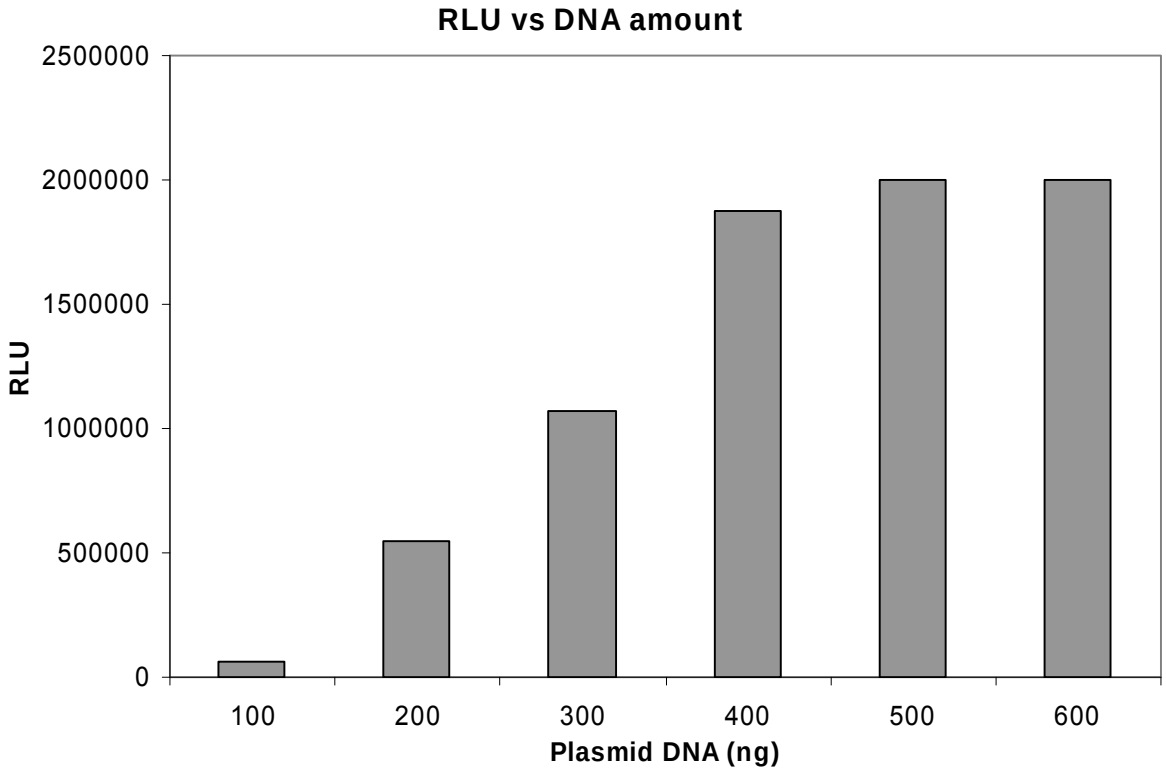

Figure 4.11: Transfection optimisation in HEK293 cells. Cells were transfected with 100-600 ng of pBOSLUX. The amounts of DNA showing the highest level of reporter luciferase activity was between 500-600 ng.

For NIH3T3 cells, transfections were carried out in 6-well plates using 1 μg of plasmid DNA and 3.0 μl of fugene 6. Optimisation of the transfection procedure was conducted by varying the cell density and the time point at which cell lysates were harvested. The cell density ranged from 0.5 x 10^5 to 5 x 10^5 cells/well 24 hours prior to transfection and cell lysates were harvested for analysis at 24 hours and 48 hours post-transfection (figure 4.12). Analysis of luciferase activities showed that harvesting cells 48 hours post-transfection as opposed to 24 hours post-transfection generated greater luciferase activities. The optimal cell density was determined to be 1.0 x 10^5 cells/well.

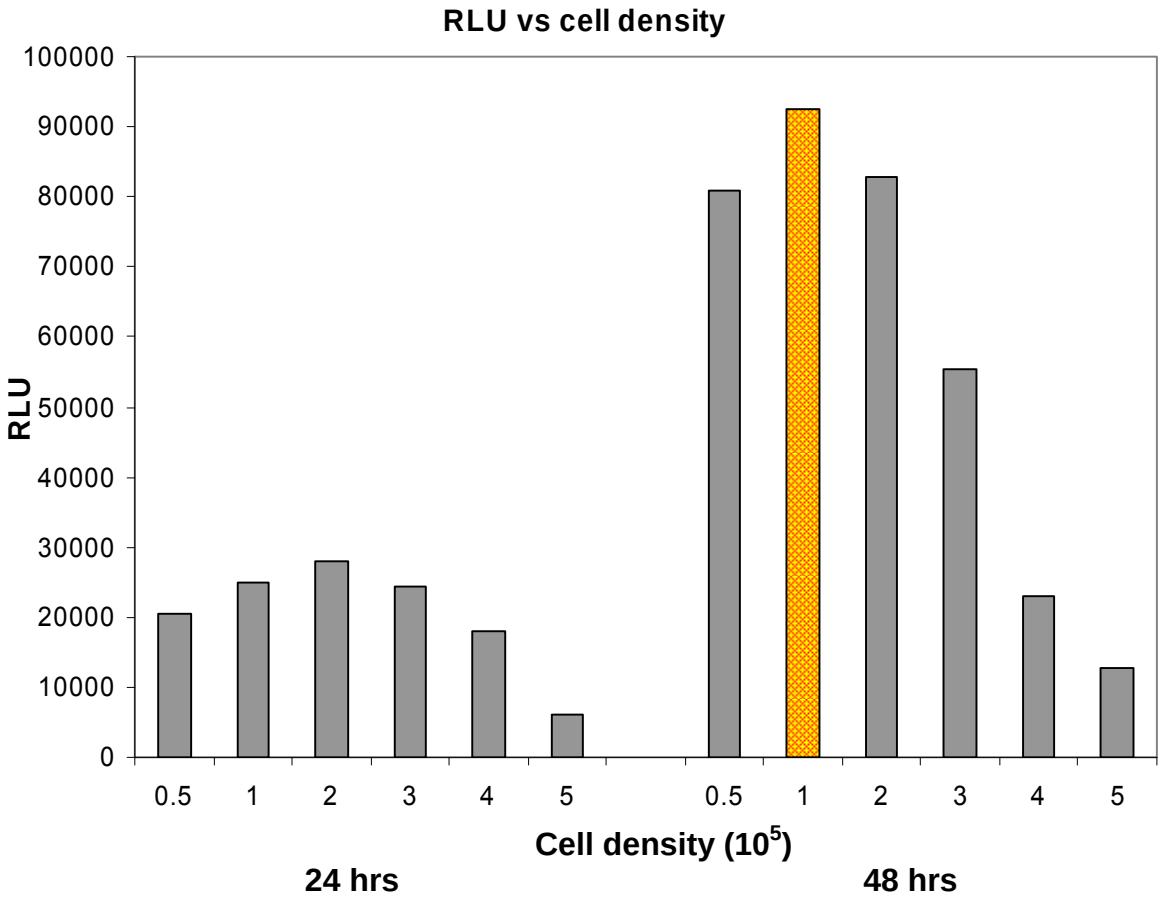

Figure 4.12: Transfection optimisation in NIH3T3 cells using cell density gradients and 24 hour and 48 hour analysis time points. Harvesting cells lysates at a cell density of 1.0 x 10^5 cells/well 48 hours post-transfection produced the highest levels of reporter activity (golden/red bar).

4.2.8 Transfection protocol for RUNX2 gene target reporter assay

For NIH3T3 cells, a total of 1.1 µg of plasmid DNA was transfected with 3.0 µl of Fugene 6 per well. For each well, 1.1 µg of pBOSLUX or 500 ng of RUNX2 expression plasmid, 500 ng of reporter plasmid and 100 ng of pRL-CMV were transferred to a microcentrifuge tube. TE buffer was added to the plasmid mix to a final volume of 20 µl. The DNA solution was vortexed for 15 seconds. 77 µl of

transfection media was pipetted into a separate microcentrifuge tube and 3 µl of fugene 6 transfection reagent was added. The tube was tapped gently on the side allowing the transfection reagent to mix with the media. The plasmid DNA was then pipetted into the media/fugene 6 solution and the solutions were mixed by tapping gently on the side of the tube. The DNA/media/fugene 6 solution was incubated for 15 minutes at room temperature prior to adding it drop wise to the tissue culture wells. For HEK293 cells, transfections were carried out using a total of 470 ng of plasmid DNA and 1.5 µl of fugene 6 per well. For each well, 470 ng of pBOSLUX or 215 ng of RUNX2 expression vector, 215 ng of reporter plasmid and 40 ng of pRL-CMV was pipetted into a microcentrifuge tube and TE buffer was added to a final volume of 10 µl. The DNA solution was vortexed for 30 seconds to mix thoroughly. To a separate microcentrifuge tube, 38.5 µl of transfection media was added followed by the addition of 1.5 µl of fugene 6. The tube was tapped gently on the side to evenly disperse the transfection reagent throughout the media. The plasmid DNA mixture was then pipetted into the media/fugene 6 solution and the tube was tapped gently on the side to mix the solutions. The plasmid DNA/media/fugene 6 solution was incubated at room temperature for 15 minutes before being added drop wise to the tissue culture wells. Negative control reactions contained TE instead of plasmid DNA.

4.2.9 Luciferase assay

NIH3T3 and HEK293 cells were harvested 48 hours post-transfection and the luciferase activities were determined using the Dual Luciferase Enzyme Assay System outlined by Dyer *et al.* (2000). The cells were harvested by removing the media from the wells and rinsing the transfected cells twice with phosphate buffered

saline (PBS). The cells were lysed via the addition of passive lysis buffer (promega corp.) (200 µl/well for 6-well plates and 100 µl/well for 12-well plates) followed by two freeze-thaw cycles at -80˚C. The resulting cell lysates were used directly for luciferase quantitation. 50 µl of each cell lysate sample was pipetted into the wells of a 96-well flat-bottom plate and placed into the tray of the FLUOstar OPTIMA light reader (BMG laboratories). 100 µl of luciferase buffer (25 mM glycylglycine, 15 mM KH_2PO_4 (pH 8.0), 4 mM EGTA, 2 mM ATP, 1 mM DTT, 15 mM $MgSO_4$, 0.1 mM Coenzyme A, 75 µM luciferin, with the final pH adjusted to 8.0) was added to each well and the plate was inserted into the light reader for luminescence detection and quantitation of firefly luciferase. After the light reader had completed acquiring the firefly luciferase activities, the plate was ejected and a 100 µl of renilla luciferase buffer (1.1 M NaCl, 2.2 mM Na_2EDTA, 0.22 M KH_2PO_4 (pH 5.1), 0.44 mg/ml BSA, 1.3 mM NaN_3, 1.43 µM coelenterazine, with the final pH adjusted to 5.0) was added to each well. The plate was re-inserted into the light reader and the light output recorded to quantitate renilla luciferase activity.

4.2.10 Statistical methods

Age adjusted values of bone density parameters were produced using regression analysis, of linear and higher than linear adjustments. Incident fracture during five years of observation was available for the Western Australian study. Incident fracture was categorised as zero and one for the absence and presence of fracture for analysis by logistic regression. Results of the logistic regression are presented as p values and odds ratios (OR) with 95% confidence intervals (CI). For BUA and SOS, age adjusted Z-scores were generated using regression analysis. The Z-scores of Q-variants was

assessed in a one sample t-test against the null hypothesis which states that the Z-scores would be normally distributed around a mean of zero.

In order to pool the femoral neck BMD data from all studies, each individual was expressed within a study as a Z-score of femoral neck BMD around the appropriate age-mean with a linear adjustment for age in each case. These Z-score values were then tested collectively for deviation from the expectation under the null hypothesis that they would be normally distributed around zero. This was established using a one-sample approach. Monte Carlo simulations were conducted to replicate experimental results with 10,000 iterations to determine the probability of obtaining bone density Z-scores by chance. Monte Carlo simulations were performed in Microsoft excel using the add-in PopTools. PopTools was created by the commonwealth scientific and industrial research organisation (CSRIO), Canberra, Australia and is freely available at http://www.cse.csiro.au/poptools/. For the luciferase assay, luciferase activities were analysed using analysis of variance (ANOVA) to determine the presence of any significant differences. The data was first normalized by dividing the raw firefly luciferase activity with the renilla luciferase internal control. LSD post-hoc tests were used to determine which groups were significantly different from each other.

4.3 Results

4.3.1 Q/A-variants identified

Characteristics of Q-variant carriers are presented in Table 4.2. Heteroduplex PAGE was used to detect mutant RUNX2 alleles via their altered and unique migration through polyacrylamide matrices. In the GOS population 7 glutamine repeat mutants were obtained in the 1531 samples screened. All mutations were heterozygous and included one 15Q allele, four 16Q alleles and two 30Q alleles. The frequency of the rare Q mutations was approximately 0.5% for the GOS. In the Scottish cohort, three rare variations were detected. Subsequent sequencing revealed the presence of two 16Q variants and one insertion of the polyalanine tract (23Ala). For the Western Australian study, dHPLC analysis of the PCR fragments determined that glutamine variants displayed specific retention peaks. These were easily identified and matched with PAGE patterns. From the 1078 individuals genotyped, there were a total of 8 variations, including five 16Q alleles, one 18Q allele and two 30Q alleles. The 8 Q-variants were found from a total of 1078 subjects and gives an approximate allele frequency of 0.74% in the Western Australian population. In the Sydney Twin study, one member of DZ twin pair contained a 30Q allele, one MZ twin pair was heterozygous for the 18Q allele and one MZ twin pair was heterozygous for the 16Q allele as identified by PAGE and DNA sequencing. All Q-repeat variants were heterozygous and associated with a 23Q/17Ala wild type allele.

Table 4.2: Age, weight, height, FN-BMD Z-score and fracture status of Q/A repeat mutants from the CAIFOS (WA), Geelong Osteoporosis Study (GOS), Aberdeen (ABDN) and Sydney Twin Study (SYD).

Allele	Age (yrs)	Weight (kg)	Height (cm)	Z-FN	fracture
WA					
16Q	76	52	156	-0.91	
16Q	78	61	151	-0.70	
16Q	79	65	167	-0.32	Femur
16Q	75	71	165	-1.68	Foot, humerus
16Q	72	80	168	0.85	Elbow, wrist, spinal deformation
18Q	74	69	157	-0.25	Femur, spinal deformation
30Q	74	54	161	-0.04	
30Q	72	57	161	0.05	Radius
GOS					
15Q	41	69	159	-0.33	
16Q	30	79	171	-1.42	
16Q	45	56	166	0.07	
16Q	70	56	152	-0.34	Spine
16Q	85	70	147	-0.13	Hip
30Q	39	97	161	-1.34	Humerus
30Q	87	50	155	-1.18	Hip
ABDN					
16Q	47	68	174	-1.82	
16Q	49	66	161	-0.85	
23A	49	52	154	-1.33	
SYD					
16Q	65	95	163	-0.33	
18Q	69	71	165	-0.16	
30Q	48	62	160	-1.37	

4.3.2 Fracture and Q-variant carrier status in the Western Australian study

Incident fracture during the study period was coded as 0 or 1 for absence and presence of fracture respectively and the type of fracture was ignored. Q-variant carriers were significantly (p=0.026) more likely to be in the fracture category (OR 4.932 95% CI 1.2 to 20.1). Four of 8 Q-variant carriers sustained incident fracture whereas the fracture rate was 17.8% in 1036 subjects with the normal 23Q RUNX2 allele.

Logistic regression showed that both femoral neck BMD and stiffness were independent predictors of fracture, each with similar effects as indicated by the logistic odds ratios (e^{β}) against the standard scores of FN-BMD and stiffness (0.72 and 0.67 with p=0.005 and p=0.001, respectively). The analysis indicated that FN-BMD and ultrasound data measure some different properties of bone that contribute to fracture risk. In the presence of these two strong variables, Q-variant status was rejected as a predictor from the logistic regression. Therefore, although Q-variant status is significantly associated with fracture likelihood, a reasonable proposition is that the increased fracture risk associated with Q-variant carrier status stems from the effect of Q-variants on bone density, as measured by DEXA or ultrasound.

4.3.3 Bone density of Q-variants

The Q-variant carriers in the Western Australian study were compared to non carriers (N=1021) for differences in the ultrasound measures of bone density: broadband ultrasound attenuation (BUA) and speed of sound (SOS) (Table 4.3). Q-variants were mostly below the mean for both BUA and SOS in their joint distribution (Figure 4.13). Q-variants had significantly lower broadband ultrasound attenuation measures (n=8, BUA, p=0.031) at the calcaneus, with a difference of 0.79 SD. The speed of sound showed a trend for a decrease with Q-variants presenting with an average 0.69 SD decrease (SOS, p=0.190). The variable, bone stiffness also showed a trend for a decrease in Q-variants (mean decrease of 0.80 SD, p=0.085). Weight, height and age were not significantly different in Q-variants (data not shown).

Table 4.3: Q/A-variants and measures of bone density as analysed via one-sample t-tests.

					95% CI	
Parameter	N	Mean	T-score	p-value	Lower	Upper
BUA (WA)	8	-0.79	-2.70	**0.031**	-1.48	-0.10
SOS (WA)	8	-0.69	-1.45	0.190	-1.81	0.43
Stiff (WA)	8	-0.80	-2.00	0.085	-1.74	0.14
FN (WA)	8	-0.38	-1.42	0.199	-1.00	0.25
HIP (WA)	7	-0.94	-2.85	**0.029**	-1.75	-0.13
Troch (WA)	7	-0.88	-2.89	**0.028**	-1.63	-0.13
Int (WA)	7	-0.87	-2.03	0.089	-1.92	0.18
LS (GOS)	7	-0.24	-0.95	0.381	-0.86	0.38
FN (GOS)	7	-0.67	-2.83	**0.030**	-1.24	-0.09
WrT (GOS)	7	-0.49	-1.68	0.144	-1.19	0.22
Troch (GOS)	7	-0.85	-3.16	**0.019**	-1.51	-0.19
LS (ABDN)	3	-0.92	-2.45	0.134	-2.54	0.70
FN (ABDN)	3	-1.33	-4.76	**0.041**	-2.54	-0.13
FN (SYD)	3	-0.62	-1.64	0.243	-2.25	1.01
Weight mean	90	**-0.72**				
FN dels	15	-0.56	-3.08	**0.008**	-0.94	-0.17
FN ins	6	-0.87	-3.12	**0.026**	-1.58	-0.15
FN all	21	-0.65	-4.27	**0.0004**	-0.96	-0.33

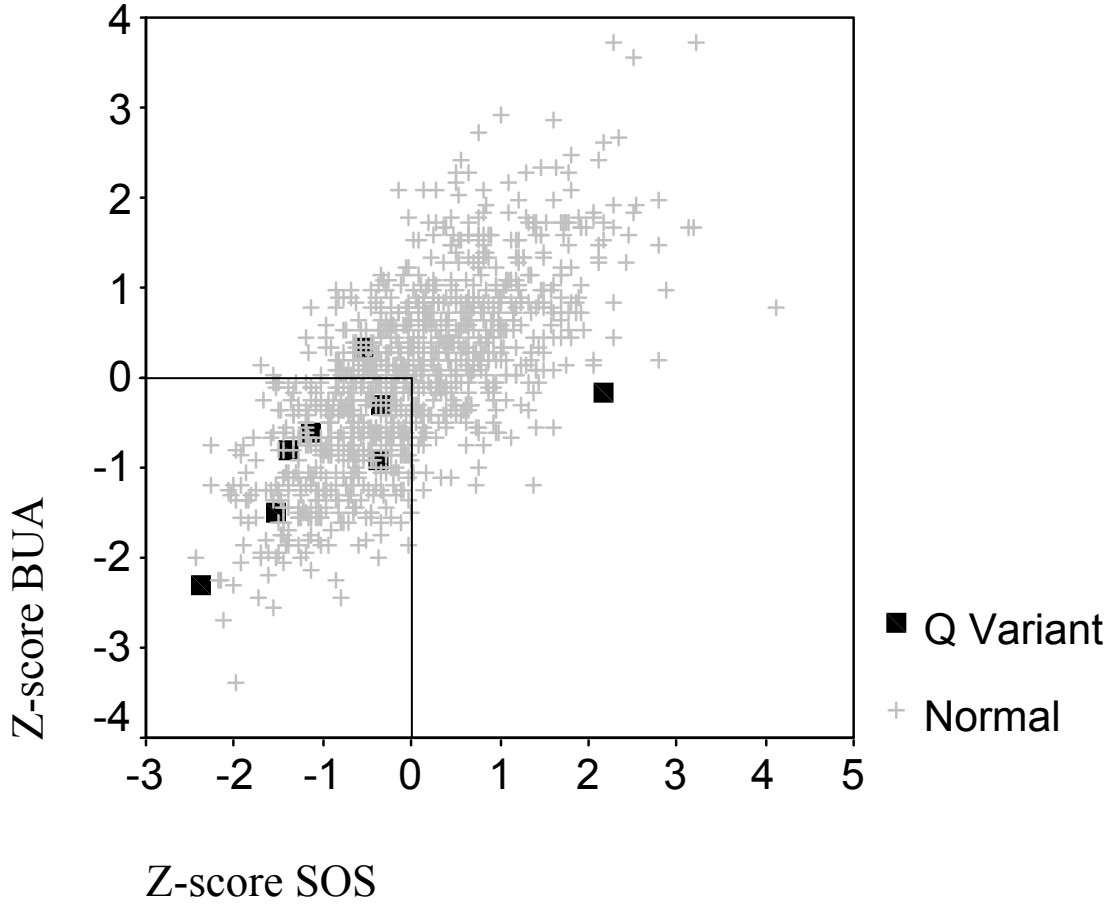

Figure 4.13: Position of CAIFOS Q-variants and non-carriers within the joint distribution of BUA and SOS Z-scores. Q-repeat carriers mostly have negative BUA and SOS Z-scores reflecting lower bone density.

4.3.4 Q/A-variant BMD and fracture in GOS, Aberdeen and Sydney studies

In the GOS, seven variants were identified. These included two 30Q alleles, four 16Q alleles and one 15Q allele. When Z-scores of BMD were examined at multiple sites, there was a strong trend for these individuals to have negative Z scores (BMD below the population mean value, table 4.3). This analysis showed a significant effect of Q-

variants on femoral neck BMD (p=0.03) and trochanteric BMD (p=0.02) but not spine (p=0.4). The magnitude of the effect at the femoral neck (0.67SD) was almost identical to that found in the Western Australian study with calcaneal BUA and BMD at the hip (Table 4.3). Of the seven Q-variants, four had osteoporosis related fractures. The three variant subjects from the Aberdeen study had negative Z-scores for both femoral neck and lumbar spine BMDs (averaging -0.92SD and -1.33SD, respectively). The 23Ala individual was 49 years old, 52 kilograms in weight and had low BMD values: -1.07 and -1.33 Z-scores (lumbar spine and femoral neck respectively). In the Sydney Twin study, three unique genomes were identified as containing Q-mutants. A 30Q was identified in a DZ twin pair whereas two heterozygous deletions of the Q-repeat tract were observed in two MZ twin pairs (18Q and 16Q). The average FN-BMD Z-score for Sydney Q-mutants was -0.62.

4.3.5 Combining the effect of Q/A-variants over different studies

Femoral neck BMD was the only measure in common between the GOS, Aberdeen, Western Australian and Sydney studies. In order to combine the effects of these studies, Z-scores around the age-adjusted population mean for each study were taken. The null hypothesis was that the mean Z-score of femoral neck BMD for Q-variants would be zero and not different from the population mean. This hypothesis was tested using a one sample t-test assuming that the population mean is measured without error and that normalizing BMD values eliminates any differences between studies.

A total of 21 variants were available who had measures of femoral neck BMD, including five 30Q, two 18Q, twelve 16Q, and one 15Q and the 23Ala. The result was a highly significant decrease in femoral neck BMD overall (p=0.0004) with an average effect of 0.65 SD. All insertions pooled (30Q and 23A) had significantly reduced FN-BMD (p=0.026) with a decrease of -0.87 SD. All deletions pooled showed significantly lower femoral neck BMD (p=0.008); an effect compatible with a decrease of -0.55 SD in femoral neck BMD being associated with heterozygous Q-deletion status. Although the insertion variants had an overall greater reduction in bone density compared to the deletions, this difference was not significant (p=0.36), possibly due to low numbers.

Using a one sampled t-test approach to test the null hypothesis that bone density Z-scores of Q-variant carriers would be normally distributed around a mean of zero was a conservative approach as only the data from Q-variants were considered for the analysis. This greatly reduced the degrees of freedom heightening the risk of committing type II errors but protecting against type I errors. An alternate means of analysis was to conduct Monte Carlo simulations of the experimental results. Corresponding Monte Carlo simulations were conducted for each of the one-sample t-tests performed (table 4.4). In the CAIFOS, Monte Carlo simulations revealed that the probability of obtaining the bone density results by chance was less than 5 in two hundred for BUA, SOS, Stiff, HIP, Troch and Int confirming the association of Q-variants with lower bone density. Only the BMD at the FN for the CAIFOS did not produce a significant result. FN BMD was significantly lower in the GOS and Aberdeen populations. Collectively, all deletions pooled had significantly lower FN BMD and significantly decreased FN BMD was observed when only insertions were

considered for the simulations. All Q-variants combined for FN BMD produced the most significant result where the data would have been observed only 18 times in 10,000 by chance providing strong evidence to indicate the Q-repeat variants were associated with lower FN BMD.

Table 4.4: Q/A-variants and measures of bone density as analysed via Monte Carlo simulations.

Parameter	N	Mean	Iterations	Observations	p-value (1-tailed)
BUA (WA)	8	-0.79	10000	118	**0.012**
SOS (WA)	8	-0.69	10000	234	**0.023**
Stiff (WA)	8	-0.80	10000	104	**0.010**
FN (WA)	8	-0.38	10000	1496	0.150
HIP (WA)	7	-0.94	10000	59	**0.006**
Troch (WA)	7	-0.88	10000	109	**0.011**
Int (WA)	7	-0.87	10000	117	**0.012**
LS (GOS)	7	-0.24	10000	2576	0.258
FN (GOS)	7	-0.67	10000	395	**0.040**
WT (GOS)	7	-0.49	10000	954	0.095
Troch (GOS)	7	-0.85	10000	139	**0.014**
LS (ABDN)	3	-0.92	10000	525	0.0525
FN (ABDN)	3	-1.33	10000	111	**0.011**
FN (SYD)	3	-0.62	10000	8563	0.856
FN dels	15	-0.56	10000	149	**0.015**
FN ins	6	-0.87	10000	156	**0.016**
FN all	21	-0.65	10000	18	**0.002**

4.3.6 RUNX2 reporter gene assay: transactivation function of 16Q, 30Q, 11Ala and wild type RUNX2

The transactivation function of 16Q, 30Q, 11Ala allele and wild type RUNX2 proteins was assessed using a RUNX2 gene target reporter assay (figure 4.13). The experiment was conducted in mouse NIH3T3 embryonic fibroblasts and human embryonic kidney 293 (HEK293) cells. Transactivation function was assessed by measuring the levels of a luciferase reporter driven from known RUNX2 target promoters. The results were derived from the average of 9 independent experiments in NIH3T3 cells and 6 independent experiments in HEK293 cells. In NIH3T3 cells using the p6OSE reporter plasmid, the mean transcriptional activities ± SE were 100 ± 6.3 for WT, 76 ± 4.9 for 16Q, 83 ± 7.3 for 30Q and 105 ± 6.8 for 11Ala. The 16Q and the 30Q RUNX2 proteins had significantly lower transactivation function compared to WT ($p = 0.002$ and 0.016, for 16Q and 30Q, respectively). In contrast, 11Ala allele RUNX2 had similar potential to transactivate p6OSE compared to WT ($p = 0.54$). In the highly transfectable HEK293 cell line using the p6OSE reporter plasmid, the mean transcriptional activities ± SE were 100 ± 4.8 for WT, 84 ± 3.2 for 16Q, 93 ± 2.6 for 30Q and 93 ± 4.6 for 11Ala. The 16Q variant was found to have significantly decreased reporter activity ($p = 0.036$). The 30Q also had decreased transactivation function however it failed to reach statistical significance ($p = 0.23$). The 11Ala allele RUNX2 protein also displayed decreased transcriptional capacity however the effect was not significant ($p = 0.20$). The final series of transfections were conducted in HEK293 cells using the pOSLUC reporter plasmid. The mean transcriptional

activities ± SE were 100 ± 0.96 for WT, 89 ± 3.1 for 16Q and 90 ± 5.2 for 30Q. Both the 16Q and 30Q variants had significantly decreased transcriptional activity in relation to wild type RUNX2 at an $\alpha = 0.10$ ($p=0.007$ and 0.066 for 16Q and 30Q respectively).

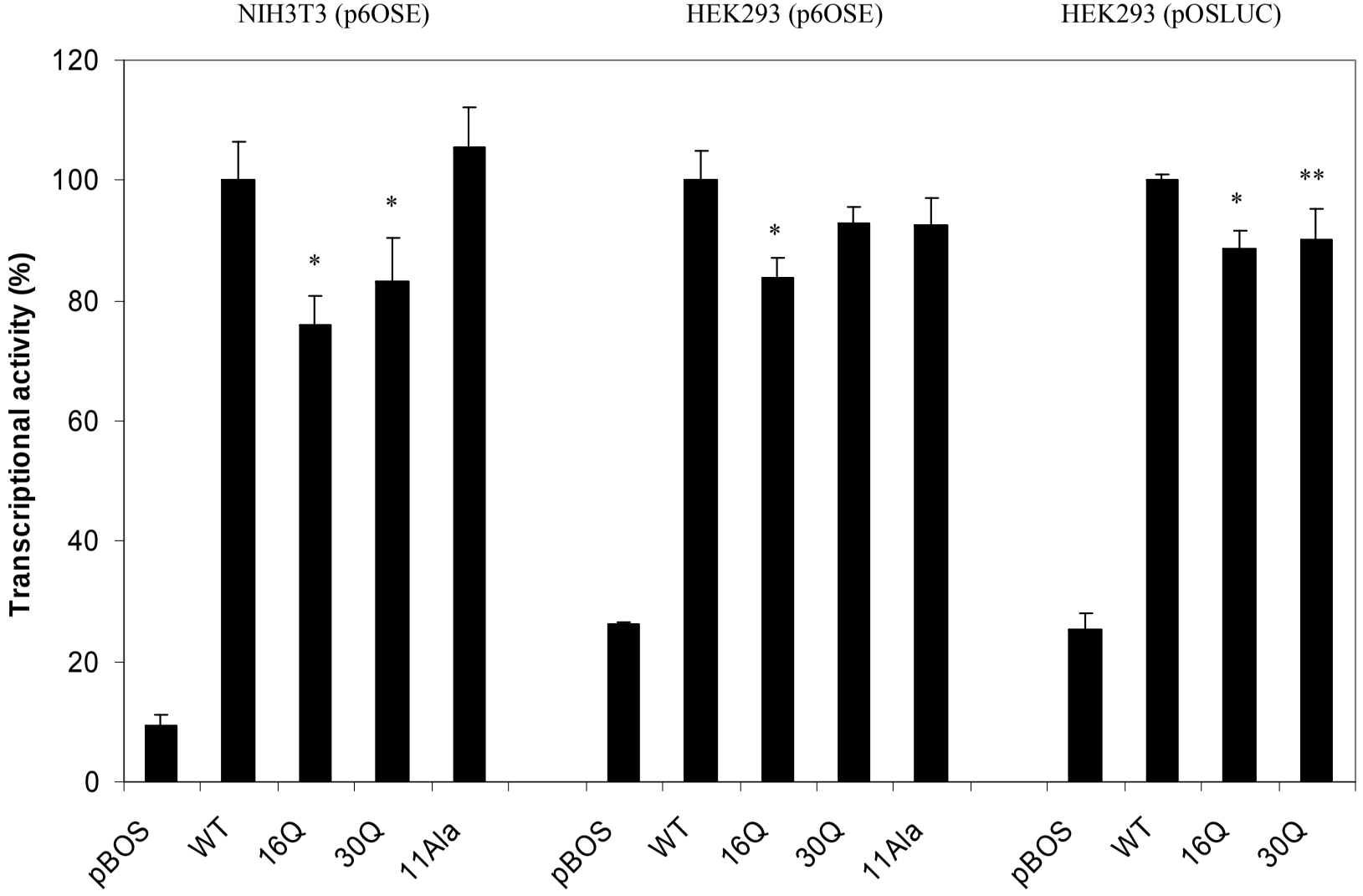

Figure 4.14: Quantitative transactivation function of WT, 16Q, 30Q and 11Ala RUNX2 proteins. * Significantly different from WT ($p = < 0.05$), ** significantly different from WT ($p = < 0.10$)

4.4 Discussion

DNA samples from four epidemiological studies of bone density were screened for glutamine repeat mutations. A total of 20 glutamine repeat and one alanine repeat variants were identified occurring at a collective frequency of approximately 0.5%. We had hypothesized that Q-mutant individuals derived from normal populations would not present with CCD (severe bone phenotype) but rather Q-mutants would present with another altered skeletal phenotype. Our hypothesis was proven to be true as the Q-variants presented with significantly decreased bone density as measured by broadband ultrasound attenuation at the calcaneus and by DEXA at the femoral neck. Collectively, Q-repeat variants identified in CAIFOS presented with significantly decreased BUA and marginally significantly decreased stiffness. When FN BMD measures were combined across all four studies by converting the BMD data into Z-scores, Q-repeat mutants had significantly decreased BMD with an average reduction of 0.65 SD. The 0.65 SD reduction in BMD is comparable to the 0.79 SD reduction in BUA observed in Q-mutants identified from CAIFOS. If the genetic effect of Q-variants on bone density were additive, we would expect to see a 1.3-1.6 SD decrease in bone density in Q-variant homozygotes. When only deletion Q-mutants were considered for the analysis of FN BMD, they presented with significantly decreased BMD with an average effect of -0.55 SD. Insertion mutants also presented with significantly decreased BMD with a somewhat stronger effect than the deletions. However the difference in BMD between deletion and insertion Q-mutants was not significant, possibly due to low numbers.

Analysis of incident fracture in CAIFOS suggested that Q-mutants had a greater than expected fracture rate. Considering the lower bone density phenotype in Q-mutants, it makes sense that Q-variants were found to have had an increased risk of fracture. According to the model that for every 1 SD reduction in BMD the risk of fracture increases by 1.5-3.0 fold (Kanis, 2002), we observed a greater than expected increased risk of fracture than would be explained by a 0.65 SD decrease in BMD. However, it is important to point out that the fracture analysis was only conducted on a small sample of Q-mutants and the expected increased risk of fracture associated with a 0.65 SD decrease in BMD lies within the 95% CI for the odds ratio of the fracture analysis.

Based on the low frequency of occurrence and the variety observed, the Q-repeat mutants are likely to have been generated as new mutations via strand slippage during DNA replication of the repeat sequence which encodes the Q/A domain. Expansion of Q-repeats is known in other diseases such as Kennedy's disease where androgen receptor repeats expand to a point of pathology. Diseases of this kind show the genetic characteristic of anticipation, where subsequent generations develop more severe disease through repeat expansion (Cummings and Zoghbi, 2000). There is currently no evidence of anticipation in fracture and osteoporosis. The repeat lengths that we observe do not exceed 30Q, below the size limit where Q-repeat disease has been observed. Despite this, it seems possible that longer repeat expansion may be observed and these may be associated with some other pathology. Repeat deletions of 18Q, 16Q and 15Q seem reasonable candidates for involvement in severe cases of osteoporosis/osteopenia and fracture.

Multiple types of glutamine insertion and deletion mutations were identified via the genotyping studies (15Q, 16Q, 18Q and 30Q). To assess the transactivation function of insertion glutamine mutants a RUNX2 expression vector harbouring the 30Q mutation was created, whereas a 16Q expression vector was created and used to represent the function of deletion variants. The function of the common 18 bp deletion was assessed by creating a RUNX2 expression vector containing the 11Ala allele. The ability of the mutant and wild type RUNX2 proteins to transactivate target promoters was assessed in NIH3T3 and HEK293 cell lines. In NIH3T3 cells, all mutant forms of RUNX2 were capable of transactivating the p6OSE luciferase reporter plasmid. However when compared to wild type RUNX2 the 16Q and 30Q mutants had significantly lower transcriptional activity. The activity of the 16Q and 30Q were 76 % and 83 % that of wild type respectively. The transcriptional activity of the 11Ala allele RUNX2 protein was not significantly different to WT. Similar results were obtained in HEK293 cells using the p6OSE reporter plasmid. The 16Q and 30Q had lower transactivation function (84 % and 93 % that of WT respectively) however only the 16Q reached statistical significance. Again, the 11Ala allele had no material effect on the transactivation potential of RUNX2. The final series of transfections focused on the transactivation function of the 16Q and 30Q mutants in HEK293 cells using the pOSLUC reporter vector. Both mutant forms of the protein had a significantly diminished capacity to transactivate the reporter plasmid compared to WT RUNX2 with mean relative transcriptional activities of 88 % and 90 % for the 16Q and 30Q respectively. In summary, the transfection experiments demonstrated that the 16Q and 30Q mutations had detrimental effects on the transactivation function of RUNX2 with respect to the two reporter plasmids used in the study. In contrast, the 11Ala deletion polymorphism appeared to have little effect on RUNX2 function presenting with

similar transcriptional activity compared to WT. A possible limitation of the analysis is that the significantly lower transactivation capacity of the 16Q and 30Q RUNX2 could have been due to differing protein levels. If differences in protein levels were responsible for lowering transcriptional activity it would still reflect a functional alteration in RUNX2 activity possibly due to reductions in mRNA and/or protein stability.

The decreased transcriptional activity of the 16Q and 30Q variants was consistent with the decreased bone density observed in individuals carrying Q-repeat mutations. It seems plausible that accumulated over a lifetime the decreased transcriptional activity could compromise bone density and lead to an increased risk of fracture. However, only two target genes using the same response element were used in the study and the effect of the Q-repeat variants on other target genes is unknown. Repeating the transfections in an osteoblastic cell line could also provide more information on the mutations by demonstrating how the variant proteins would function within the context of an osteoblast which is the cell type where RUNX2 is naturally found. In addition, the transactivation analysis was conducted in the context of the RUNX2-I isoform and the effect of the mutations on the type-II isoform driven from the first promoter is not known. However, the results do provide support for the role of the glutamine tract in contributing to the transactivation function of RUNX2 as indicated by Thirunavukkarasu *et al* (1998). Disruption of the Q/A domain (16Q and 30Q mutations) was capable of decreasing transactivation function, however the exact mechanism via which the mutations impose their detrimental effects is not known. It is possible that the mutations confer a change in protein conformation or may disrupt the binding of RUNX2 to accessory proteins required for the regulation of target

genes. RUNX2 acts as a scaffolding protein and regulates the transcription of target genes by interacting with accessory proteins such as VDR, SMADs, HDACs, AP1, TLE/Groucho and other co-factors (Schroeder *et al*, 2005). It seems plausible that a change in protein conformation could alter the ability of RUNX2 to interact with cofactors impacting on the regulation of target genes. The disruption in the regulation of target genes could lead to compromised bone quality which would ultimately lead to fracture.

A similar logic could be used to explain the effects of the 11Ala allele on fracture and serum osteocalcin even though the transactivation analysis failed to show a negative impact of the mutation on transcriptional activity. Since only one target promoter was used in the analysis of the 11Ala allele, it would be fair to say the reporter plasmid would not adequately represent the myriad of genes regulated by RUNX2. Therefore it would be possible to envisage that the deletion mutation could disrupt the ability of RUNX2 to interact with proteins and cofactors leading to a diminished capacity to transactivate target genes other than the one used in the study. Alternatively, the mutation could be linked to a nearby intronic sequence which could alter splicing and/or mRNA processing ultimately influencing protein function.

Chapter 5

Identification of genes regulated by RUNX2 and cooperatively regulated by RUNX2 and BMP2

5.1 Introduction

RUNX2 is one of the three members of the RUNT domain family of transcription factors found in humans. RUNX proteins participate in the regulation of genes involved in cellular growth, differentiation and survival (Durst and Hiebert, 2004). RUNX2 plays an essential role during embryonic development by directing the differentiation of osteoblasts from mesenchymal precursors and promoting osteogenesis (Ducy *et al*, 1997). In addition to its role on osteoblasts, RUNX2 is expressed in hypertrophic chondrocytes and participates in chondrocyte maturation (Kim *et al*, 1999; Enomoto *et al*, 2000). RUNX2 is important beyond development as it serves to maintain the osteoblast phenotype and thus the integrity of the skeleton in adults (Ducy, 2000). Genetic ablation of RUNX2 in mice resulted in a complete lack of endochondral bone formation due to the maturational arrest of osteoblasts (Komori *et al*, 1997; Otto *et al*, 1997). Further confirming the functional of importance of RUNX2 in contributing to skeletal development was the discovery that heterozygous mutations in the RUNX2 gene of humans and mice caused the syndrome Cleidocranial Dysplasia which is characterized by gross dysgenesis of the skeleton and dental abnormalities (Mundlos *et al*, 1997; Lee *et al*, 1997).

RUNX2 is required for proper skeletal development and the identification of RUNX2 downstream gene targets would yield an insight into how RUNX2 facilitates osteoblast development and contributes to skeletal formation. RUNX2 has been implicated in the regulation of numerous genes such as osteocalcin, collagen α1(I), MMP-13, bone sialoprotein and osteopontin (Geoffory *et al*, 1995; Ducy *et al*, 1997; Jimenez *et al*, 1999). RUNX2 associates with several factors such as co-repressors,

co-activators and transcription factors to regulate target genes (Schroeder *et al*, 2005). The binding of accessory factors to RUNX2 dictate whether RUNX2 will positively or negatively regulate target genes and thus RUNX2 functions as a context-dependent transcriptional regulator of gene expression. For example, the VDR acts in synergy with RUNX2 to transcriptionally activate the osteocalcin and osteopontin genes (Paredes *et al*, 2005; Shen and Christakos, 2005). The binding of HDAC, TLE and YAP co-repressors to RUNX2 promote repressor function (Westendorf, 2006). Other co-regulatory molecules known to interact with RUNX2 include p300, MOZ, MORF, TLE/Groucho, HDACs, and SMADs (Sierra *et al*, 2003; Pelletier *et al*, 2002; Wang *et al*, 2004; Javed *et al*, 2000; Thirunavukkarasu *et al*, 1998; Vega *et al*, 2004; Schroeder *et al*, 2004; Westendorf *et al*, 2002; Zhang *et al*, 2000a; Afzal *et al*, 2005; Zaidi *et al*, 2002).

SMAD transcription factors are downstream signal transducers of the TGF-β superfamily and have been shown to physically interact with RUNX2 (Zhang *et al*, 2000a; Afzal *et al*, 2005; Massague *et al*, 2005). The interaction between RUNX2 and SMADs is facilitated by the SMAD interacting domain (SMID) which is embedded in the NMTS of RUNX2 (Afzal *et al*, 2005). The interaction between BMP2 activated SMADs and RUNX2 is of great interest for bone biology as both RUNX2 and BMP2 are important regulatory factors required for successful bone development. It was demonstrated that the association between RUNX2 and BMP2 activated SMADs synergistically regulated alkaline phosphate activity during the transdifferentiation of premyoblastic C2C12 cells into osteoblasts (Lee *et al*, 2000); alkaline phosphatase is one of potentially many genes cooperatively regulated by RUNX2 and BMP2.

BMP2 is a powerful osteogenic factor that was originally characterized by its ability to induce ectopic bone formation when implanted under the skin of rodents (Ducy and Karsenty, 2000). BMP2 belongs to the family of bone morphogenic proteins (BMPs) which are small secreted molecules that function as multifunctional growth factors (Ducy and Karsenty, 2000; Chen *et al*, 2004). BMP2 is able to drive the differentiation of C2C12 cells and stromal cells towards the osteoblast lineage and is responsible for the regulation of several osteoblast specific genes such as alkaline phosphatase and type I collagen (Katagiri *et al*, 1994; Takuwa *et al*, 1991; Thies *et al*, 1992). BMP2 acts by binding to a heterodimeric complex of two transmembrane receptors, termed type I and type II. The receptors possess serine-threonine kinase activity, which upon ligand stimulation phosphorylate members of the SMAD family of transcription factors. Once phosphorylated, the SMADs are activated and translocated to the nucleus to transduce their signals (Ducy and Karsenty, 2000). SMADS 1, 5 and 8 are activated in response to BMP signaling (Ducy and Karsenty, 2000).

The identification of novel RUNX2 gene targets and genes cooperatively regulated by RUNX2 and BMP2 would aid in elucidating the complex functions carried out by RUNX2 within the context of regulating gene expression. To achieve the successful identification of legitimate target genes, an overexpression approach was implemented. Stably transfected NIH3T3 cells overexpressing RUNX2, BMP2 and both RUNX2 and BMP2 were created and gene expression investigations via microarray and RT-PCR analyses were used to identify regulated genes.

5.2 Methods

5.2.1 BMP2 and RUNX2 expression vectors

The BMP2 expression plasmid was created by cloning the BMP2 cDNA into the pEGFP-C1 expression vector. This was achieved by first amplifying the full length BMP2 cDNA from HeLa cell cDNA using the oligonucleotide primers 5'-CTAAAGGAGATCTATGGTGGCCGGG-3' for the forward and 5'-GACTGGAATTCCTAGCGACACCCACAACCCT-3' for the reverse. The oligonucleotides were designed to contain an *XbaI* restriction site in the forward primer and an *EcoRI* restriction site in the reverse primer to facilitate the cloning of the cDNA into the *NheI* and *EcoRI* sites of pEGFP-C1. The successfully amplified BMP2 cDNA fragments were digested with *XbaI* and *EcoRI* and ligated into the *NheI* and *EcoRI* sites of pEGFP-C1. The cloning strategy resulted in the replacement of the EGFP cDNA with the human BMP2 coding region creating pCMV-BMP2. For the generation of the RUNX2 expression vector, the *BglII-SalI* fragment from pEF-αA was excised via restriction enzyme digestion and ligated into the *BamHI-SalI* sites of pBABE-puro. The resulting plasmid was termed pBABE-RUNX2.

5.2.2 Tissue culture

NIH3T3 cells and NIH3T3 cells stably transfected with RUNX2, BMP2 and both RUNX2 and BMP2 were maintained in DMEM (GIBCO) supplemented with 10% FBS (v/v) (GIBCO), 1% Penicillin-Streptomycin (v/v) (GIBCO) in a 5% CO_2 humidified atmosphere at 37˚C. For affymetrix microarray analysis and subsequent RT-PCR, cells were grown to 80% confluence in 25-cm^2 flasks prior to RNA extraction. For the codelink microarray and subsequent RT-PCR analysis, standard NIH3T3 cells and NIH3T3 cells stably transfected with RUNX2, BMP2 and both RUNX2 and BMP2 were grown to confluence and subsequently cultured for a further 12-days in media supplemented with 50 µg/ml AA prior to RNA extraction.

5.2.3 Generation of stable transfectants

Stably transfected cell lines overexpressing RUNX2 and/or BMP2 were generated by transfecting NIH3T3 cells with either pBABE-RUNX2 and/or pCMV-BMP2. Cells containing plasmids integrated within their genomes were selected by supplementing culture media with the appropriate antibiotics. For transfection, NIH3T3 cells were seeded into 6-well plates at a density of 1 x 10^5 cells/well 24-hours prior to transfection. The cells were transfected with 1.0 µg of pBABE-RUNX2 and/or 1.0µg pCMV-BMP2 using 3.0 µl of fugene 6 transfection per well. 48 hours post-transfection, the culture media was removed and replaced with fresh DMEM containing selective antibiotics. Cells transfected with pBABE-RUNX2 were supplemented with puromycin at 2 µg/ml and cells transfected with pCMV-BMP2

were treated with G418 at a concentration of 400 μg/ml. The cells were maintained in selective media for three weeks permitting non-stably transfected cells to die leaving only cells with permanently integrated plasmids. Once established, the cell lines were maintained in DMEM supplemented with 2 μg/ml of puromycin for cells permanently transfected with pBABE-RUNX2 and with 200 μg/ml of G418 for cells transfected with pCMV-BMP2.

5.2.4 RNA extraction

The total RNA from tissue culture cells was extracted for use in RT-PCR and microarray experiments. RNA extraction for cells grown in a 25-cm^2 flask was performed by removing the media and washing the cells twice with 5 ml of fresh PBS. 400 μl of 4.0 M guanidium isothiocyanate, 1% lauryl sarcosine (SLS) solution was added to the flask and allowed to spread across the bottom of the flask until all the cells were covered allowing cell lysis to occur. The viscous cell lysate was removed using a pipette and transferred into a microcentrifuge tube. 150 μl of 10% SLS solution was added to the lysate solution and the proteins were sheared by pipetting the solution with a 200 μl pipette tip 10-20 times. The lysate sample was layered onto a cushion of 5.7 M CsCl, 0.01 M EDTA solution in a small polyallomer ultracentrifuge tube (Beckman). 4.0 M Guanidium isothiocyanate, 1% SLS solution was used to fill the tube and equalize its weight ready for centrifugation with other samples or with a balance tube. The sample was centrifuged at 55,000 rpm for 3 hours in an ultracentrifuge allowing the RNA to form a pellet at the bottom of the tube. The sample was removed from the centrifuge and the supernatant was carefully removed using a pipette making sure not to disturb the RNA pellet. The tube was tipped upside

down allowing the remainder of the supernatant to run down the tube onto paper. Using a sterile scalpel, the bottom of the tube containing the RNA pellet was cut and the top part was discarded. 100 µl of diethyl pyrocarbonate treated 70 % ethanol was gently added to the bottom of the cut tube and subsequently removed to rinse the RNA. To dissolve the RNA, 60 µl of TE, 0.1 % SDS solution was added to the bottom of the tube and the resulting solution was transferred to a fresh microcentrifuge tube. 40 µl of TE buffer was added to the bottom of the tube to dissolve the remaining RNA and the solution transferred to the microcentrifuge tube containing the RNA. 10 µl of 3 M NaAc and 200 µl of ice cold 100 % ethanol were added to the solution containing the RNA and mixed via inversion. The precipitated RNA was collected via centrifugation at 14,000 rpm for 20 minutes at 4°C. The supernatant was removed and the RNA pellet was washed with 100 µl of diethylpyrocarbonate (DEPC) treated 70 % ethanol to remove excess salt and centrifuged @ 14, 000 rpm for 5 minutes at 4°C. The supernatant was discarded and the RNA pellet was allowed to dry on ice before being resuspended in 50 µl of TE buffer containing 40 units of RNaseOUT^{TM} RNase inhibitor (Invitrogen corp.).

5.2.5 cDNA synthesis

Synthesis of cDNA from total RNA was conducted using the Improm-II^{TM} Reverse Transcription System (Promega). 1 µg of total RNA was added to a microcentrifuge tube and placed on ice. 1 µl of random hexamer primers (500 ng/µl) and 2 µl of 20mer oligoDT primers (200 ng/µl) were added to the RNA. Pure H_2O was added to the RNA/primer mix to a total volume of 5 µl and the contents were mixed by gently tapping the side of the tube. The RNA/primer mix was incubated at 70°C for 5

minutes to denature RNA secondary structures. After the incubation period at 70°C, the tube was placed on ice for 5 minutes followed by centrifugation for 10 seconds in a microcentrifuge to collect the condensate. In a separate tube, the reverse transcriptase mix was prepared by pipetting 4 µl of 5x reaction buffer, 2.4 µl of 25 mM $MgCl_2$, 2 µl of 5 mM dNTPs, 1 µl (20U) of RNasin RNase inhibitor (Promega) and 4.6 µl of pure H_2O. The contents were mixed by vortexing for 10 seconds and added to the RNA/primer mix on ice. 1 µl of Improm-II reverse transcriptase was added to the reaction tube and the contents were mixed by gently tapping the side of the tube. The tube was removed from the ice and placed in a controlled temperature heating block set at 25°C for 5 minutes allowing the primers to anneal to the RNA template. Following the annealing period, the reaction mix was incubated at 42°C for 1 hour allowing extension to occur. The reverse transcriptase was inactivated via incubation at 70°C for 15 minutes. The resulting cDNA was either stored at -80°C or diluted and used directly as a template in RT-PCR.

5.2.6 RT-PCR primers

Primers were used for RT-PCR gene expression analysis. Oligonucleotides were designed using the blast server from The National Centre for Biotechnology Information (NCBI). The server was used to test short nucleotide sequences for their binding specificity to target genes and thus facilitated the successful design of suitable oligonucleotide pairs to specifically amplify target genes during PCR. Primers were designed to specifically amplify coding regions of DNA residing within the 3' end of genes. The amplicons were generally 200-400 bp in size and individual oligonucleotides ranged from 17-26mers. All oligonucleotides were designed from

mouse gene templates with the exception of 18s, BMP2 and RUNX2 which were of human origin. Table 5.1 lists the primers used during the study.

Table 5.1: RT-PCR primers used for quantitative gene expression analysis.

Gene	Forward 5'-3'	Reverse 5'-3'	cDNA product (bp)
BMP2	GATGCGGTGGACTGCACAGGGACAC	GACCAACGTCTGAACAATGGCATG	409
IGF-II	TGGAGACTATGAATTGGCCTGGTAT	AGAGGGGATCCCACTGAAGACAGTA	262
N-MYC	GGTCGTCGAGTGCTAGCCACACCGG	CGTCTTGGGACGCACAGTGATCGTG	416
MMP-13	GTTGGTCATTACTCAAGGCTATGCA	GGCTTGCTGTGTCTTAGCTGGATC	330
OSC	GCAGACACCATGAGGACCC	GGTCTGATAGCTCGTCACAAGC	230
RUNX2	AGCCTGCAGCCCGGCAAAATGAGC	GGTGGTCGGCGATGATCTCCACCATG	237
SCYA11	TCTGAGGGAATATCAGCACCAGTC	GTTACTCCTAACTCGTCCCATTGTG	198
SFRP2	TAGCTGTAGTACTTTGACCCGAGGG	ATGAGGAATGGTTACTGTGTGCTTA	326
CCL9	CTGAAGCTGACCTCAATGACTACAC	CTTGAGTGATTCTGAGGCAGTTAGG	281
CSF2	AAGTTACCACCTATGCGGATTTCAT	AGTCAGCGTTTTCAGAGGGCTATAC	242
EHOX	CAACCAAGAGGACCAGGACACCAG	AAGTGATTCTGCTGGAAAATGCGC	225
OSF-1	CACCTAGACTTTTTTTCCCAAATCAG	AACATTTCACTACATCGTTGCTCTG	171
18S	ACGCTGAGCCAGTCAGTGTA	CTTAGAGGGACAAGTGGCG	106

5.2.7 Quantitative RT-PCR

Quantitative RT-PCR analysis was conducted to confirm microarray results and identify RUNX2 and BMP2 gene targets. The PCRs were conducted using the Bio-Rad iCycler real-time PCR detection system and data generated from real-time experiments were analysed using iCycler software. The program permitted the calculation of threshold cycles which were subsequently used for quantitative calculations. The software allowed the examination of melt-curves which provided information on the specificity and the integrity of amplified PCR products. RT-PCRs were carried out in 20 µl reactions and contained 2.5 x 10^{-7} M of each primer, 1 µl of Qiagen 10 x PCR buffer, 0.4 µl of 25 mM $MgCl_2$, 125µM dNTPs, 1:20000 SYBR Green I, 0.15% Triton-X 100, 10 nM fluorescein, 0.5 units Qiagen HotStar *Taq* DNA polymerase, 2µl cDNA and nuclease free water up to 20µl. The thermal cycler conditions were: step 1: 95°C for 15 min (1 cycle); step 2: 95°C for 30 s, 59°C for 30 s and 72°C for 30 s (45 cycles); step 3: melt curve analysis from 60°C to 96°C in 0.5°C increments. 18s ribosomal RNA was used as an internal control housekeeping gene and relative gene expression was calculated using the $2^{-\Delta\Delta CT}$ method outlined by Livak and Schmittgen, 2001.

5.2.8 Affymetrix gene-chip microarray analysis

RNA samples extracted from standard NIH3T3 cells and NIH3T3 cells stably transfected with RUNX2 were sent to the Australian Genome Research Facility (AGRF) for microarray analysis using affymetrix gene-chips. The RNA samples were

prepared and hybridized to full mouse genome microarrays. The major steps followed during the Gene-Chip analysis procedure was as follows: Step 1: target preparation; step 2: target hybridization; step 3: fluidics station setup; step 4: probe array washing and staining; step 5: probe array scan and step 6: data analysis. Steps 1-5 were conducted by the AGRF whereas as step 6 was conducted in our laboratory. The experiment involved sending to the AGRF 15-20 μg of CsCl purified total RNA for each sample to be analysed. The samples served as templates for 1st strand cDNA synthesis and the newly formed cDNAs were then used in a subsequent reaction for secondary strand cDNA synthesis. The double stranded cDNA samples were purified and used for the generation of biotin labeled cRNA via in vitro transcription. The biotinylated cRNA samples were purified and fragmented prior to being hybridized to Mouse Genome 430A 2.0 arrays. Following hybridization, the chips were washed several times and stained enabling detection of hybridized cRNA. The chips were scanned and the images were saved on CD. The image files were sent back to our laboratory for data analysis. Data analysis was carried out using the affymetrix GeneChip® Operating Software (GCOS). Once installed the software was used to compute cell intensity data from the image files of each affymetrix chip. The saved cell intensity data files were then used for expression analysis where every probe-pair in a probe set was qualitatively and quantitatively analysed. The resulting files were saved and used for comparison analysis where every probe-pair from each of the probe sets of one experiment were compared to the corresponding probe-pairs of the second experiment via algorithms and statistical analysis. The resulting data was exported to an excel file where comparative gene expression analysis was carried out.

5.2.9 Codelink gene-chip microarray analysis

Codelink gene-chip microarray analysis was used to identify genes cooperatively regulated by RUNX2 and BMP2. RNA extracted from NIH3T3 and NIH3T3-BMP2-RUNX2 cells was used for the experiment which was conducted by Dr Ivan Biros from GE healthcare. The major steps followed during the procedure were as follows: step 1: Preparation of total RNA and bacterial controls; 2: first-strand cDNA synthesis at 42 °C for 2 hours; 3: second-strand cDNA synthesis at 16 °C for 2 hours; 4: cDNA purification; 5: in vitro transcription and biotin labeling of cRNA at 37 °C for 14 hours; 6: purification of in vitro transcribed and biotin labeled cRNA; 7: fragmentation of cRNA at 94 °C for 20 min; 8: hybridization of labeled target to codelink gene chip at 37 °C for 18 hours; 9: wash and stain microarray with fluorophore; 10: scan and save image. The Scanned images were saved on CD and sent back to the laboratory for analysis. The scanned images were analysed via Codelink Expression Analysis v4.0 software from which an expression plot and a gene list was created. The gene list was analysed for legitimate and interesting targets.

5.2.10 Statistical analysis

Real-time PCR data was analysed using the $2^{-\Delta\Delta CT}$ method to calculate relative mRNA levels. Standard or ln + 1 transformed relative mRNA levels were analyzed by student's t-test or ANOVA with Fisher's post-hoc *t*-test to determine final p-values.

5.3 Results

5.3.1 Identification of RUNX2 gene targets using Affymetrix microarray analysis

The search for RUNX2 gene targets was initiated by performing microarray analysis on RNA extracted from NIH3T3 cells and NIH3T3 cells stably transfected with RUNX2. The cells were grown to 80% confluence prior to RNA extraction. The expression of RUNX2 mRNA in NIH3T3 and NIH3T3-RUNX2 cells was verified via RT-PCR analysis. NIH3T3-RUNX2 cells had significantly increased levels of RUNX2 mRNA ($p = 2.7E-08$) displaying a 28 fold increase compared to NIH3T3 cells (figure 5.1). The gene expression profile of NIH3T3-RUNX2 cells was compared to that of NIH3T3 cells via microarray analysis. The expression plot (data not shown) demonstrated that very few genes were differentially regulated at expression levels above background. The microarray analysis confirmed that RUNX2 levels were increased in NIH3T3-RUNX2 cells compared to NIH3T3 cells displaying a 12.6 fold up-regulation. The most differentially regulated genes were summarized in table form and analysed to determine the presence of interesting and legitimate gene targets. From the gene list, 6 differentially regulated genes were further analysed by RT-PCR. The genes were v-myc myelocytomatosis viral related oncogene, neuroblastoma derived (avian) (N-MYC), secreted frizzled-related protein 2 (SFRP2), matrix metalloproteinase-13 (MMP-13), osteocalcin (OSC), insulin like growth factor-II (IGF-II), and small inducible cytokine A11 (SCYA11).

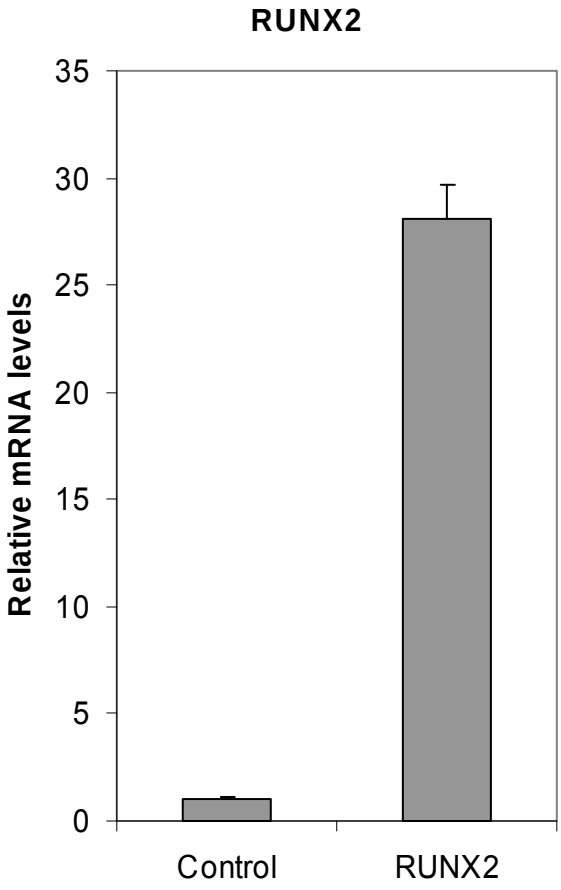

Figure 5.1: Relative mRNA levels of RUNX2 in NIH3T3 (control) and RUNX2 stably transfected cells. Permanent integration of pBABE-RUNX2 resulted in a 28 fold increase in RUNX2 mRNA levels compared to NIH3T3 control cells.

5.3.2 RT-PCR analysis of N-MYC, SFRP2, IGF-II, SCYA11, MMP-13 and OSC

RT-PCR was conducted on the 6 differentially regulated genes and compared to the fold regulation results obtained from the microarray analysis (table 5.2). The RT-PCR results were representative of four independent PCRs using cDNA derived from the same RNA samples used for the microarrays.

Table 5.2: Differentially regulated genes identified by microarray analysis. Microarray fold regulation and fold regulation calculated via quantitative RT-PCR.

Gene	Microarray fold regulation	RT-PCR fold regulation (mean ± SE)
N-MYC	267.0	-1.18 ± 0.16
SFRP2	18.5	-3.4 ± 0.60
IGF-II	-11.0	-27.6 ± 6.64
SCYA11	-6.4	-10.1 ± 1.57
MMP-13	6.4	2.1 ± 0.178
OSC	2.6	2.5 ± 0.185

N-MYC was determined to be the most highly induced gene as a consequence of RUNX2 over-expression. The microarray analysis indicated that N-MYC was up-regulated 267 fold. However, RT-PCR analysis indicated that N-MYC was not differentially regulated between NIH3T3 and NIH3T3-RUNX2 cells showing a non-

significant 1.18 fold decrease in NIH3T3-RUNX2 cells ($p = 0.91$). The RT-PCR data confirmed that N-MYC was not actually up-regulated by RUNX2 and that the microarray result was a false positive. SFRP2 was determined to be up-regulated 18.5 fold via the microarray analysis. In contrast, RT-PCR analysis determined that SFRP2 was significantly down-regulated 3.4 fold ($p = 0.0032$) in NIH3T3-RUNX2 cells again showing inconsistency between the microarray data and RT-PCR gene expression results. IGF-II and SYCA11 were both down-regulated in the presence RUNX2 as quantitated by the microarray analysis. RT-PCR confirmed the results demonstrating that IGF-II and SYCA11 were significantly down-regulated 27.6 fold ($p = 1.95 \times 10^{-6}$) and 10.1 fold ($p = 0.0002$) respectively. MMP-13 and OSC were both modestly up-regulated in the microarray. The results were confirmed with RT-PCR revealing that MMP-13 mRNA levels were significantly induced 2.1 fold ($p = 0.002$) and that OSC was increased 2.5 fold ($p = 0.00017$).

5.3.3 Identification of genes regulated via the functional cooperation between RUNX2 and BMP2: codelink microarray analysis

The search for genes cooperatively regulated by RUNX2 and the powerful bone-promoting agent BMP2 was initiated by performing microarray analysis using codelink gene chips (GE Healthcare). RNA extracted from standard NIH3T3 cells and NIH3T3-BMP2-RUNX2 cells were used as templates for microarray analysis. Each cell line was first grown to confluence and subsequently cultured for a further 12 days in the presence of AA prior to RNA extraction. The expression of RUNX2 and BMP2 in the stably transfected cell line was verified via RT-PCR and standard PCR respectively (figure 5.2).

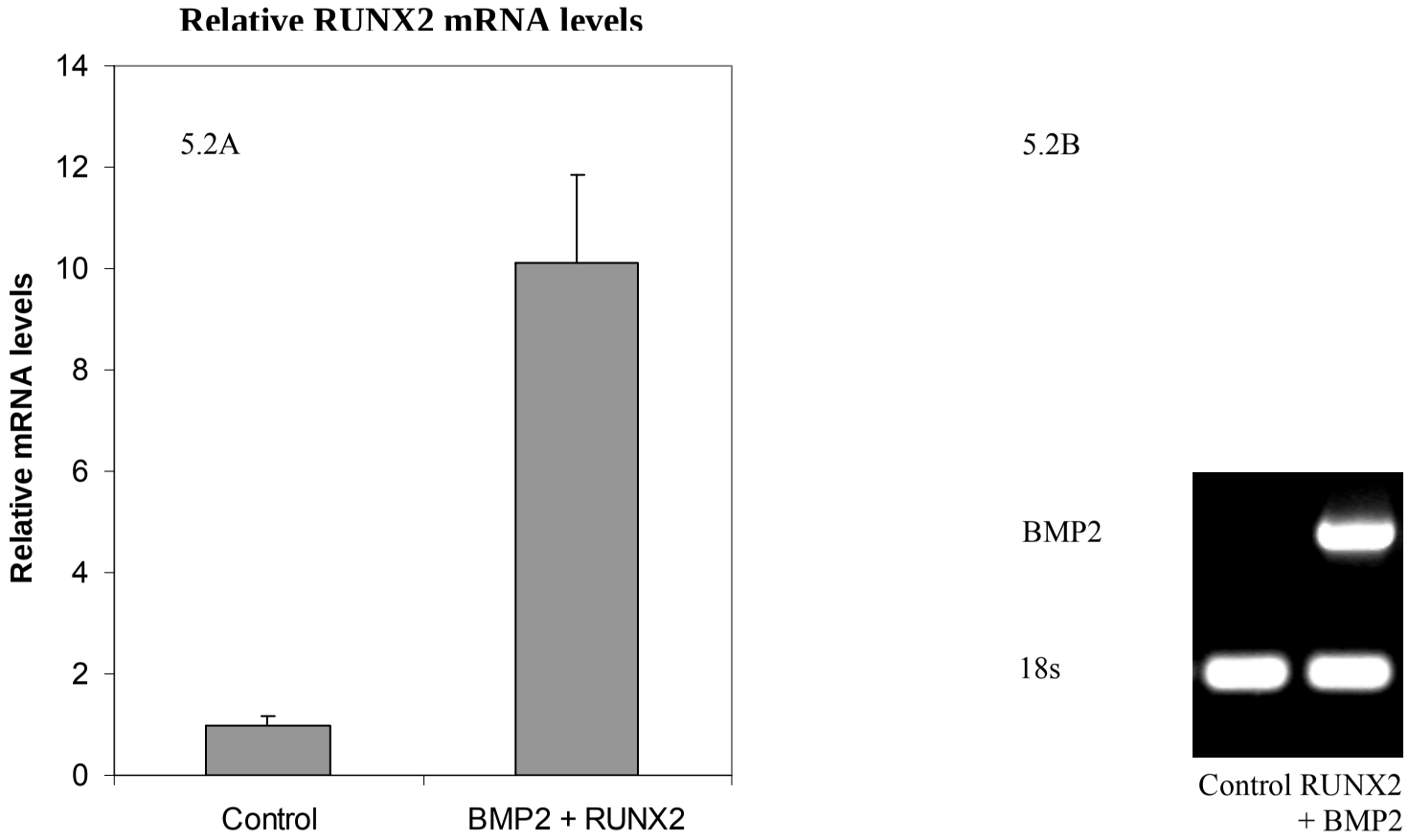

Figure 5.2: (5.2A) RT-PCR analysis of RUNX2 gene expression in control and cells stably transfected with BMP2 and RUNX2 verified the overexpression of RUNX2 in stably transfected cells. (5.2B) Non-saturating conventional PCR demonstrated the presence of BMP2 transcripts in the cDNA derived from NIH3T3-BMP2-RUNX2 cells but not control NIH3T3 cells.

RT-PCR revealed that RUNX2 was significantly up-regulated 10.1 ± 1.74 fold ($p = 0.001$) in NIH3T3-BMP2-RUNX2 cells. Non-saturating conventional PCR demonstrated the presence of BMP2 transcripts in cDNA derived from NIH3T3-BMP2-RUNX2 cells only, thereby confirming BMP2 mRNA induction.

The gene expression data derived from NIH3T3-BMP2-RUNX2 cells was compared to the gene expression profile of NIH3T3 cells. The analysis of RUNX2 mRNA levels revealed it was induced 14.5 fold in the stably transfected cells confirming the results obtained from the RT-PCR. Observation of the expression plot (figure 5.3) revealed a large number of genes were differentially regulated above background levels and indicated the presence of many possible gene targets. To simplify the analysis, only genes differentially regulated greater than or equal to 4 fold (either up or down-regulated) were examined for the presence of interesting gene targets. 4 differentially regulated genes were chosen to be further analysed via RT-PCR. The genes were ES cell derived homeobox containing gene (EHOX), colony stimulating factor 2 (granulocyte-macrophage) (CSF2), osteoblast specific factor-1 (OSF-1) and chemokine (C-C motif) ligand 9 (CCL9). EHOX and CSF2 were up-regulated 52.5 fold and 4.6 fold respectively whereas OSF-1 and CCL9 were down-regulated 11.5 and 11.0 fold respectively as indicated by the microarray analysis.

Expression plot of NIH3T3-RUNX2-BMP2/NIH3T3

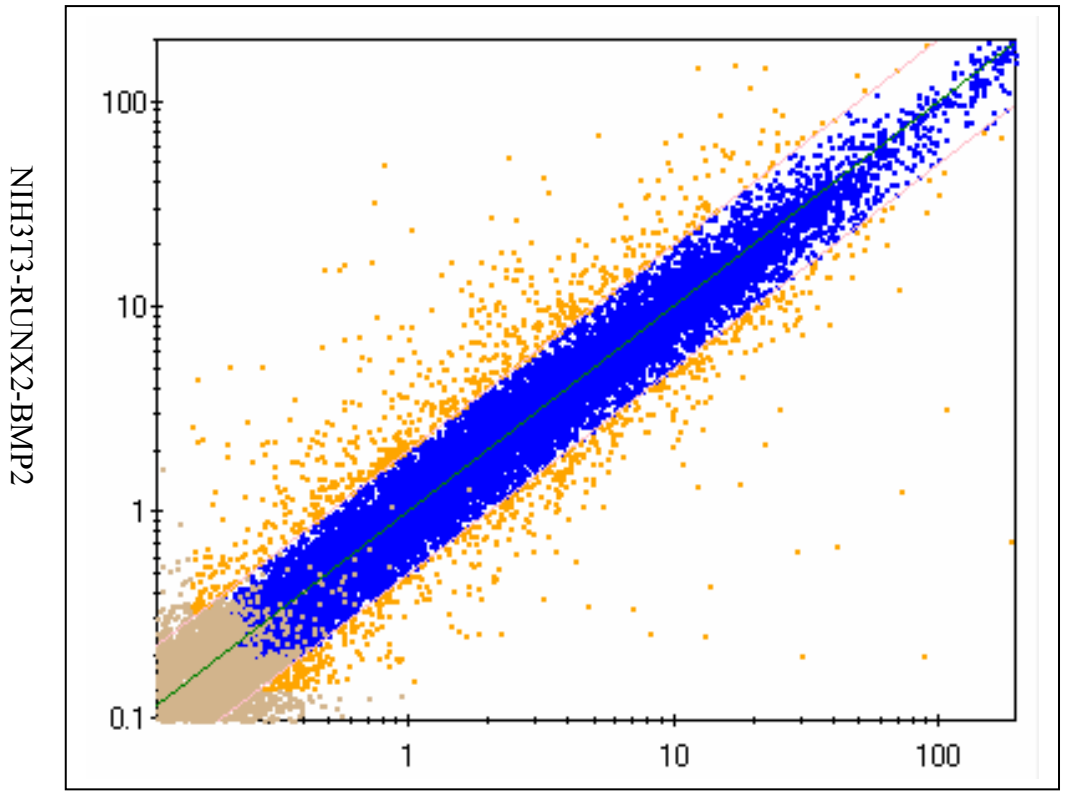

Figure 5.3: Expression plot of NIH3T3-BMP2-RUNX2 over NIH3T3. Genes regulated greater than or equal to 2-fold are represented by the yellow dots. Blue dots represent genes differentially regulated less that 2-fold and light brown dots represent genes with expression levels near background.

5.3.4 RT-PCR analysis of EHOX, CSF2, OSF-1 and CCL9

EHOX, CSF2, OSF-1 and CCL9 were analysed via RT-PCR to verify the microarray results. To determine if the genes were dependent on BMP2, RUNX2 or both BMP2 and RUNX2, RT-PCRs were conducted on cDNA derived from NIH3T3 cells and NIH3T3 cells stably transfected with RUNX2 (NIH3T3-RUNX2), BMP2 (NIH3T3-BMP2) and both RUNX2 and BMP2 (NIH3T3-BMP2-RUNX2). The results from the RT-PCR analyses were representative of 3 reactions and were conducted on cDNA derived from the same RNA samples used for the microarray analysis with respect to NIH3T3 and NIH3T3-BMP2-RUNX2 cells. The expression of RUNX2 in NIH3T3-RUNX2 cells and BMP2 in NIH3T3-BMP2 cells was verified by RT-PCR and non-saturating conventional PCR respectively (figure 5.4).

RT-PCR analysis revealed that RUNX2 was significantly induced 8.7 fold in NIH3T3-RUNX2 cells ($p = 0.0009$). Non-saturating conventional PCR analysis confirmed that BMP2 transcripts were only detected in the cDNA derived from NIH3T3-BMP2 cells.

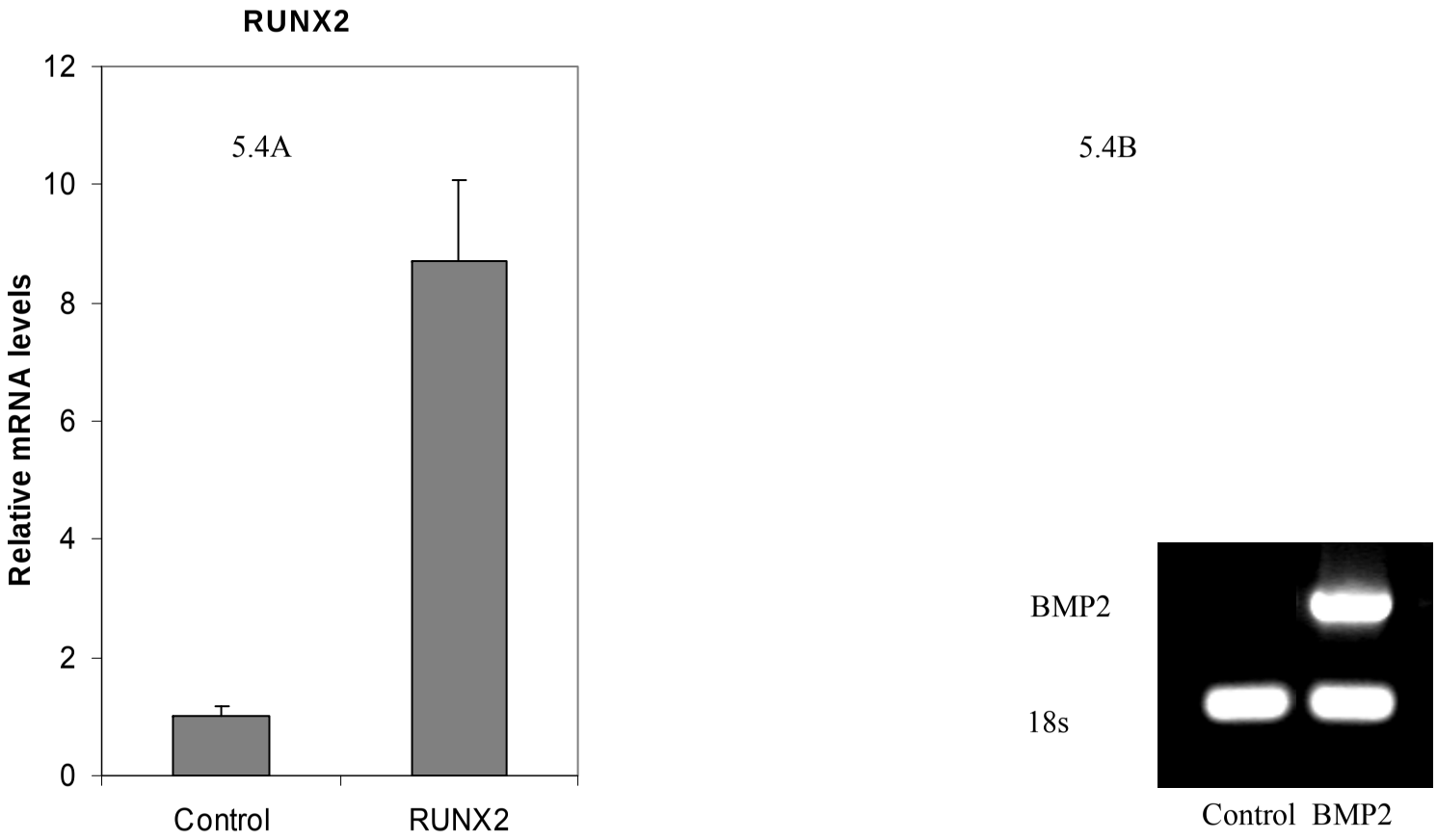

Figure 5.4: (5.4A) RT-PCR analysis of RUNX2 mRNA levels confirmed RUNX2 was significantly induced in NIH3T3-RUNX2 cells. (5.4B) Non-saturating conventional PCR indicated BMP2 transcripts were detected in the cDNA derived from the RNA of NIH3T3-BMP2 cells only.

EHOX mRNA levels were determined to be induced in the microarray. RT-PCR analysis revealed that EHOX was not significantly differentially regulated in cells stably transfected with RUNX2 (1.3 fold, p = 0.36) or BMP2 (0.31 fold, p = 0.06) (figure 5.5). However, when both RUNX2 and BMP2 were overexpressed, EHOX transcripts were significantly upregulated 26.6 fold (p = 0.004, figure 5.5).

CSF2 was determined to be up-regulated 4.6 fold in NIH3T3-BMP2-RUNX2 cells through the microarray. RT-PCR analysis of CSF2 transcript levels in all four cell lines indicated it was modestly up-regulated in both RUNX2 and BMP2 stably transfected cells (5.2 fold, p = 0.044 and 2.1 fold, p = 0.03 in NIH3T3-RUNX2 and NIH3T3-BMP2 respectively, figure 5.6). In NIH3T3-BMP2-RUNX2 cells, the RT-PCR results revealed CSF2 was induced 31.3 fold ($p = 6.6 \times 10^{-7}$) confirming the general direction but not the magnitude of the microarray analysis (figure 5.6).

OSF-1 mRNA levels were determined to be suppressed in NIH3T3-BMP2-RUNX2 cells through the microarray. RT-PCR revealed a trend for decreased OSF-1 mRNA levels in NIH3T3-RUNX2 cells (-2.3 fold, p = 0.10) (figure 5.7). In the cell lines stably transfected with BMP2, OSF-1 mRNA levels were dramatically reduced. In NIH3T3-BMP2 cells, OSF-1 mRNA was decreased 48.0 fold (p = 0.0008) and in NIH3T3-BMP2-RUNX2 cells OSF-1 mRNA levels were decreased 308.0 fold (p = 0.0003, figure 5.7).

CCL9 was determined to be down-regulated 11.0 fold in the microarray. RT-PCR analysis of CCL9 revealed there were no significant differences in CCL9 mRNA levels between control and NIH3T3-RUNX2 cells (1.6 fold, p = 0.48, figure 5.8).

However, in both NIH3T3-BMP2 and NIH3T3-BMP2-RUNX2 cell lines, CCL9 levels were significantly suppressed. CCL9 was decreased 6.1 fold ($p = 0.018$) and 22.8 fold ($p = 0.003$) in NIH3T3-BMP2 and NIH3T3-BMP2-RUNX2 cells respectively (figure 5.8).

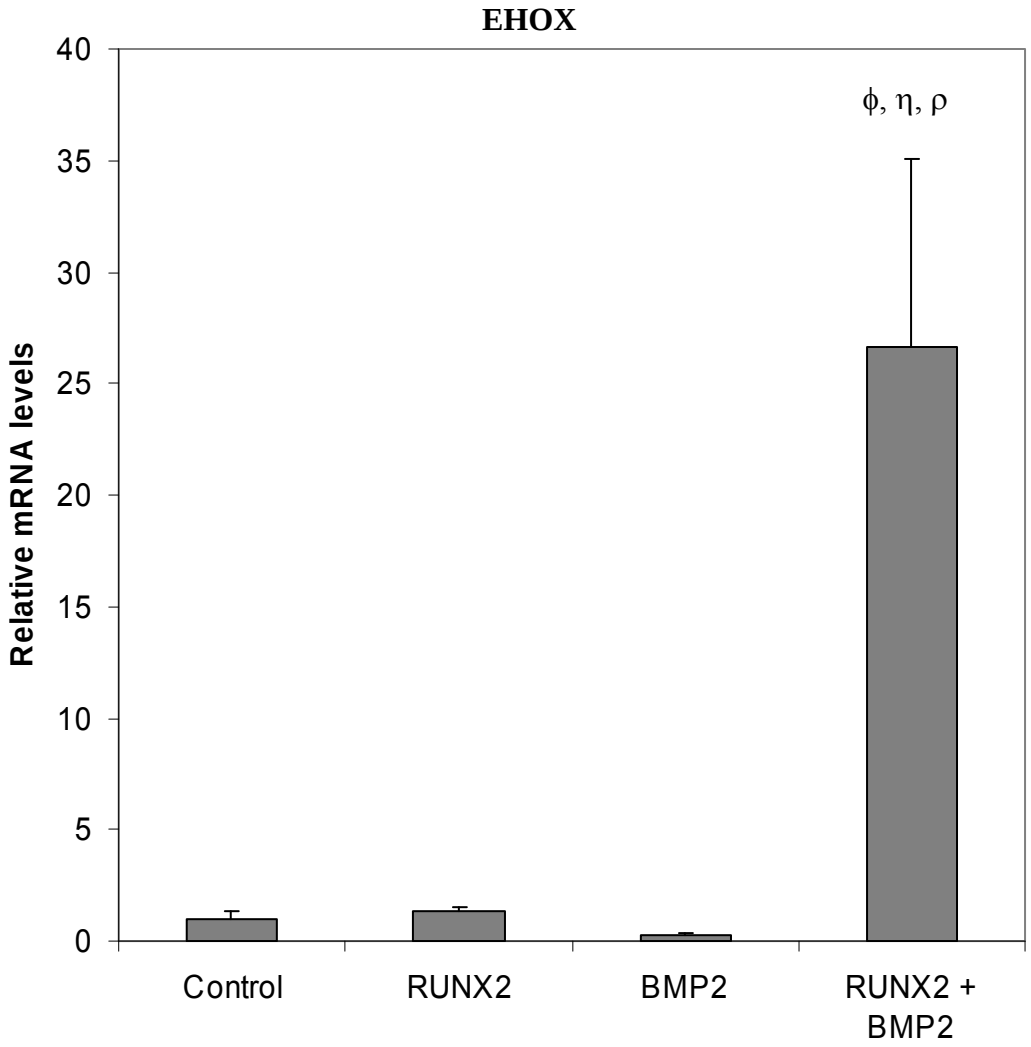

Figure 5.5: RT-PCR analysis of EHOX mRNA levels in control and stably transfected cell lines. There were no significant differences in EHOX mRNA levels between control and cells stably transfected with RUNX2 or BMP2. However, in the presence of both factors, EHOX transcripts were significantly up-regulated 26.6 fold compared to control cells.

ϕ = significantly greater than control ($p < 0.05$), η = significantly greater than RUNX2 ($p < 0.05$), ρ = significantly greater than BMP2 ($p < 0.05$)

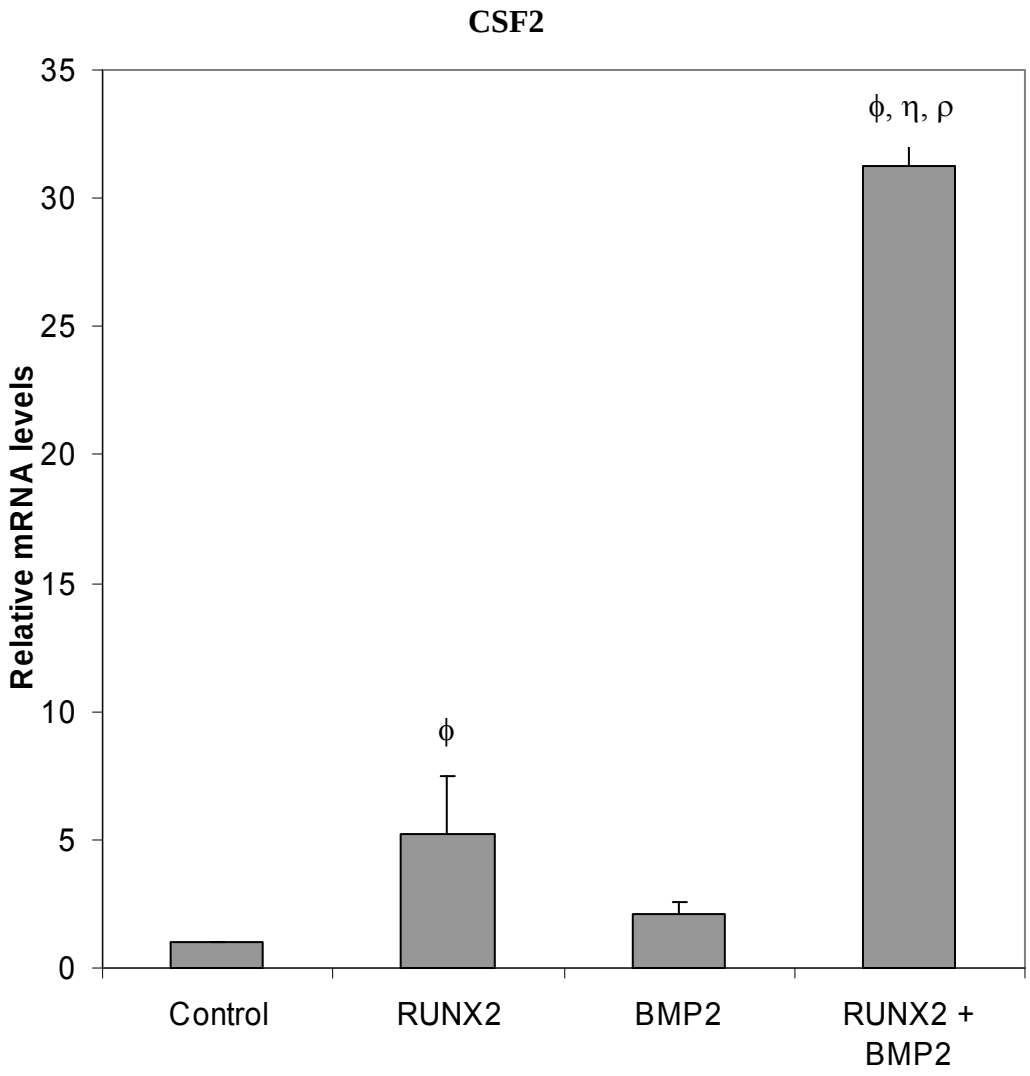

Figure 5.6: RT-PCR analysis of CSF2 mRNA levels in control and stably transfected cell lines. CSF2 mRNA levels were significantly induced in all three stably transfected cell lines compared to control cells. The greatest induction was observed in the cells stably transfected with both RUNX2 and BMP2.

ϕ = significantly greater than control ($p < 0.05$), η = significantly greater than RUNX2 ($p < 0.05$), ρ = significantly greater than BMP2 ($p < 0.05$)

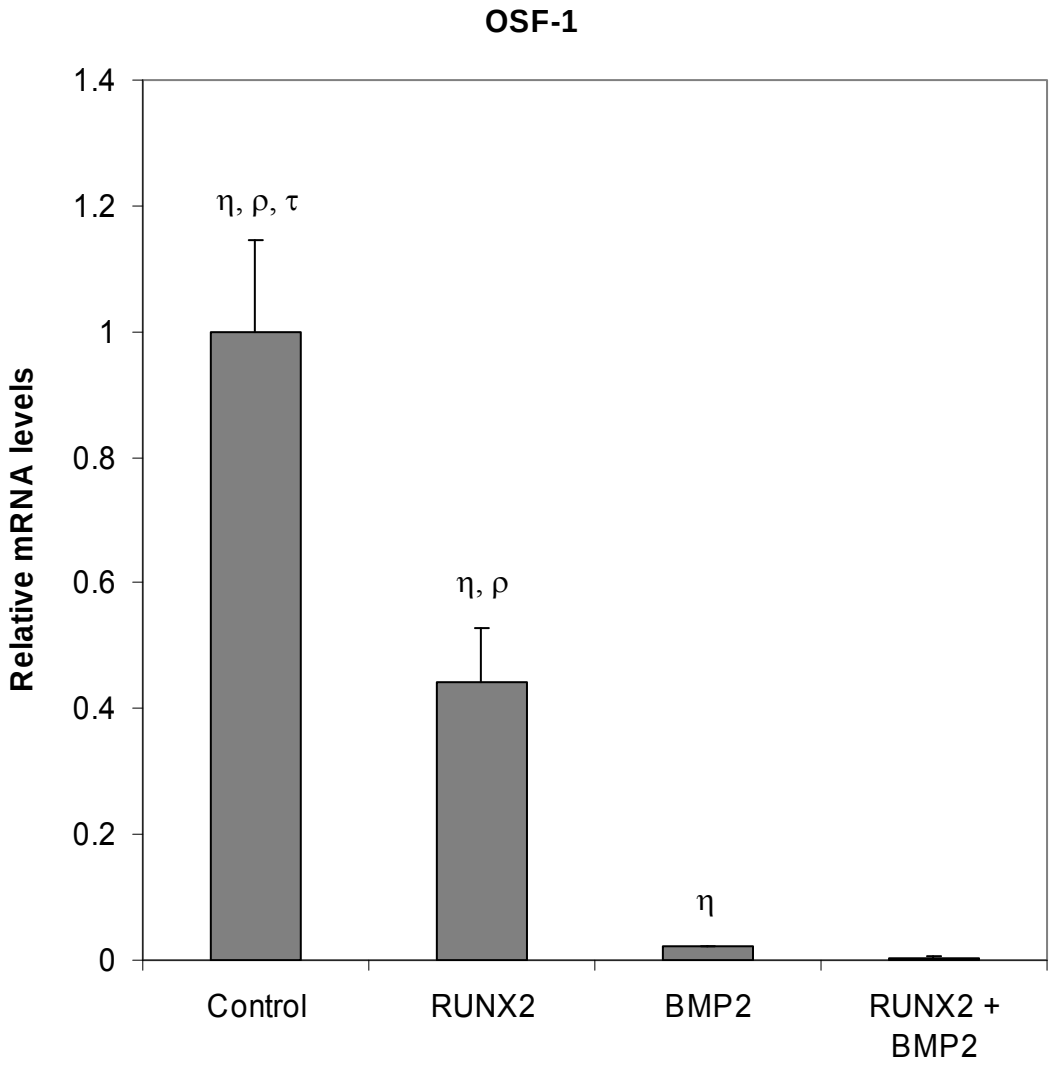

Figure 5.7: RT-PCR analysis of OSF-1 mRNA levels in control and stably transfected cell lines. OSF-1 showed a trend for a decreased expression in NIH3T3-RUNX2 cells. The levels of OSF-1 mRNA were more dramatically reduced in cells stably transfected with BMP2 with both cell lines showing significant declines in the expression of OSF-1.

η = significantly greater than RUNX2 ($p < 0.05$), ρ = significantly greater than BMP2 ($p < 0.05$), τ = significantly greater than RUNX2 + BMP2 ($p < 0.05$).

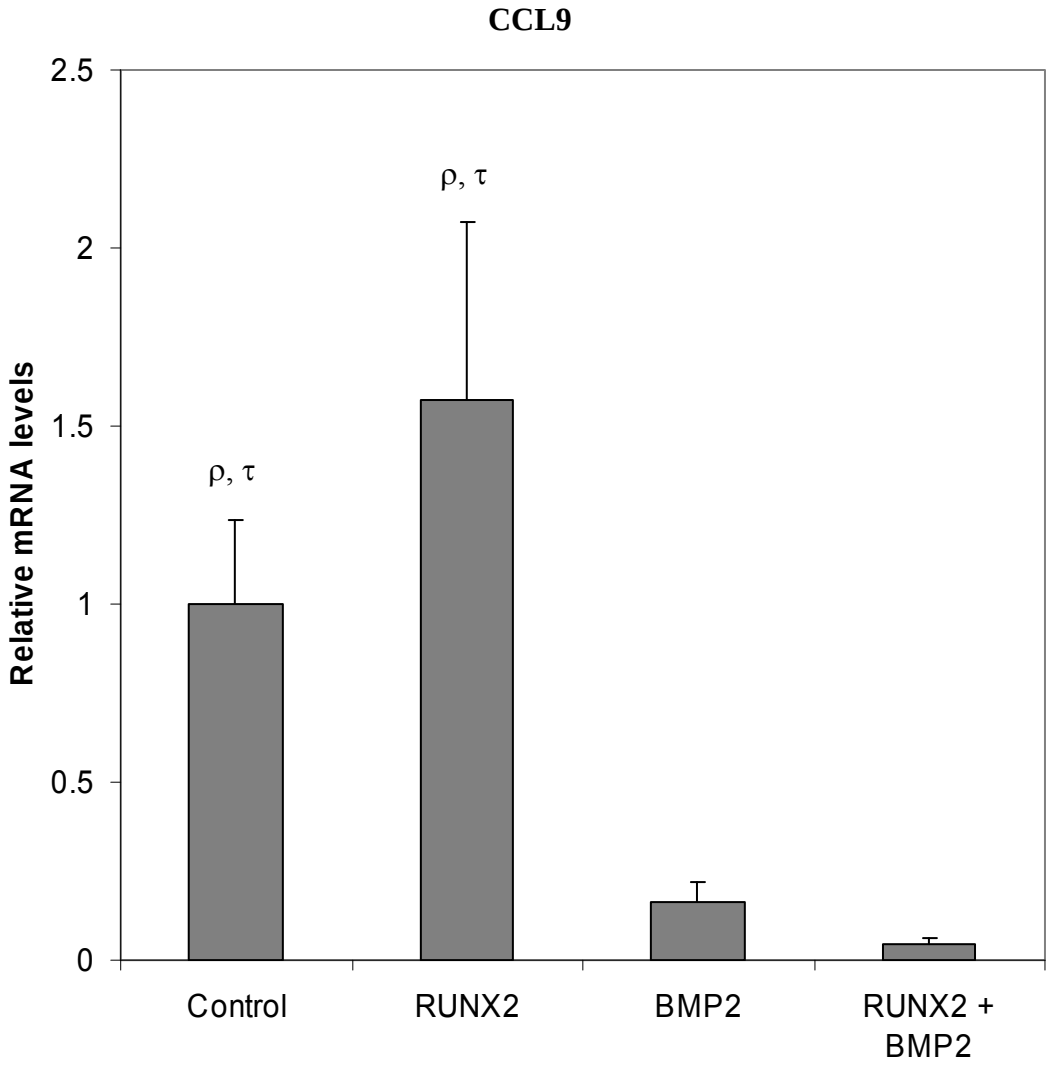

Figure 5.8: RT-PCR analysis of CCL9 mRNA levels in control and stably transfected cell lines. The overexpression of RUNX2 had no significant effect on CCL9 mRNA levels. However, in NIH3T3-BMP2 and NIH3T3-BMP2-RUNX2 cells CCL9 mRNA levels were significantly suppressed 6.1 and 22.8 fold respectively.

ρ = significantly greater than BMP2 ($p < 0.05$), τ = significantly greater than RUNX2 + BMP2 ($p < 0.05$).

5.4 Discussion

5.4.1 Identification of RUNX2 target genes

RUNX2 is a master organizer of gene transcription and acts as a transcriptional modulator by functioning as both a repressor and an activator. It regulates target genes by associating with numerous transcription factors and cofactors at specific nuclear matrix sites (Schroeder *et al*, 2005) and has been implemented in the regulation of many genes including osteocalcin, collagen α1(I), MMP-13, bone sialoprotein and osteopontin (Geoffory *et al*, 1995; Ducy *et al,* 1997; Jimenez *et al*, 1999). To identify potential novel RUNX2 gene targets, RUNX2 was stably overexpressed in NIH3T3 mouse embryonic fibroblasts. RT-PCR verified that RUNX2 was significantly overexpressed in the stably transfected cells (NIH3T3-RUNX2). Affymetrix microarray analysis of RNA derived from NIH3T3-RUNX2 and NIH3T3 cells was used to identify RUNX2 gene targets. Comparison of the gene expression profiles revealed that very few genes were differentially regulated at levels greater than background. The analysis confirmed that RUNX2 was significantly overexpressed in NIH3T3-RUNX2 cells. 6 differentially regulated genes further characterised via RT-PCR. The genes were N-MYC, SFRP2, MMP-13, OSC, IGF-II and SCYA11.

N-MYC is a member of the Myc family of oncogenes which have been demonstrated to participate in the transcriptional regulation of genes by functioning as activators and repressors. N-MYC participates in many diverse functions in the developing embryo and is expressed in subsets of undifferentiated cells which develop to

eventually form the lung, heart, central nervous system, peripheral nervous system, kidneys and eyes (Hurlin, 2005). Germline deletion of N-MYC is embryonic lethal and demonstrated the essential function of N-MYC during development (Charron *et al*, 1992). The microarray analysis revealed that N-MYC was upregulated 267 fold in NIH3T3-RUNX2 cells. RT-PCR analysis was used to confirm the microarray result. The RT-PCR investigation failed to show a significant induction of N-MYC mRNA in NIH3T3-RUNX2 cells and indicated that N-MYC was not significantly regulated by RUNX2. The analysis demonstrated that the microarray result was a false positive and that N-MYC was not regulated by RUNX2.

SFRP2 is a small secreted molecule that functions as an inhibitor of the WNT signaling pathway. SFRP2 is one of eight known members of the SFRP family which antagonize the WNT signaling pathway by binding directly to WNTs. The binding of SFRPs to WNTs alters the ability of WNTs to bind to the WNT receptor complex and thus inhibits signal transduction (Kawano and Kypta, 2003). The microarray analysis revealed SFRP2 was up-regulated 18.5 fold by RUNX2 and seemed to be a reasonable RUNX2 target gene candidate. The WNT signaling pathway is involved in osteogenesis and functions in osteoblasts by regulating proliferation, function and survival (Westendorf *et al*, 2004). In addition, Gaur *et al* (2005) demonstrated that the canonical WNT signaling pathway promoted osteogenesis by directly stimulating RUNX2. The possible up-regulation of SFRP2 by RUNX2 could have functioned as a negative feedback mechanism which would have ultimately suppressed the endogenous RUNX2 promoter. However, the RT-PCR results failed to confirm the microarray result and indicated that SFRP2 was modestly down-regulated rather than induced in NIH3T3-RUNX2 cells. The more reliable RT-PCR analysis indicated that

the microarray result was a false positive and demonstrated that SFRP2 was not actually induced by RUNX2.

The results from the microarray indicated that MMP-13 mRNA levels were induced 6.4 fold via RUNX2 overexpression. MMP-13 belongs to the family of structurally related endopeptidases that are responsible for the proteolytic degradation of extracellular matrix (Birkedal-Hansen *et al*., 1993). MMP-13 is expressed in cells that secrete extracellular matrix: the osteoblasts, osteocytes and hypertrophic chondrocytes (Borden *et al*., 1996; Johansson *et al*., 1997; Nakamura *et al*., 2004). MMP-13 is responsible for collagen degradation and thus participates in matrix remodeling which is necessary for growth plate cartilage development, endochondral ossification, bone remodeling and bone repair (Johansson *et al*., 1997; Yamagiwa *et al*., 1999; Inada *et al*., 2004). RUNX2 binding sites are present in the promoter of mouse MMP-13 and RUNX2 has been demonstrated to regulate MMP-13 expression in cooperation with other factors including SMADs and AP1 (Jimenez *et al*, 1999; Hess *et al*., 2001; D'Alonzo *et al*., 2002; Selvamurugan *et al*., 2004). RT-PCR analysis confirmed MMP-13 mRNA levels were significantly up-regulated in NIH3T3-RUNX2 cells showing an induction of 2.1 fold. The results confirmed that MMP-13 is a transcriptional target of RUNX2 and acted more as a positive control in the context of identifying novel target genes by indicating that RUNX2 was active.

Osteocalcin is another known RUNX2 target gene (Geoffroy *et al*, 1995) and also served as a positive control for the experiment. Osteocalcin is a small extracellular matrix protein synthesized by osteoblasts, odontoblasts and hypertrophic chondrocytes. Its precise function is not known however there is evidence to suggest

that it is involved in regulating bone formation as indicated by a knockout mouse model which presented with a higher bone mass phenotype (Ducy *et al*, 1996). The microarray analysis demonstrated that osteocalcin was induced 2.6 fold and was supported by the RT-PCR investigation which confirmed osteocalcin mRNA levels were significantly increased 2.5 fold.

IGF-II was determined to be down-regulated in the microarray and belongs to the family of insulin growth factors which participate in a myriad of activities during development and in adulthood. The activities include regulation of cellular growth, proliferation, differentiation, migration and protection against apoptosis which collectively participate in key biological functions relating to brain development, tissue formation and remodeling, energy metabolism and bone growth (Khandwala *et al*, 2000; Denley *et al*, 2005). Insulin like growth factors play an important role in bone formation and remodeling and IGF-II is the most abundant growth factor stored in bone (Mohan, 1993; Hayden *et al*, 1995; Hill *et al*, 1995; Zhang *et al*, 2002). IGFs function to stimulate the proliferation and differentiation of osteoblasts and chondrocytes (Langdahl *et al*, 1998; Olney *et al*, 2004). In addition to its mitogenic effects in osteoblasts, IGFs stimulate the production of collagen and other matrix proteins and also inhibit collagen degradation by limiting the production of collagenases (Rydziel *et al*, 1997; Langdahl *et al*, 1998). IGF-II was determined to be down-regulated 11 fold in NIH3T3-RUNX2 cells indicating that RUNX2 was suppressing IGF-II levels. The RT-PCR analysis confirmed the microarray result demonstrating that IGF-II mRNA levels were suppressed 27.6 fold by RUNX2. RUNX2 is expressed in both osteoblasts and chondrocytes where IGF-II is known to have stimulatory effects. If RUNX2 was to have the same suppressive effect on IGF-

II in osteoblasts or chondrocytes as it does in NIH3T3 cells, the significant suppression of IGF-II mRNA levels by RUNX2 could be explained as a regulatory mechanism which would serve to limit proliferation and differentiation in addition to decreasing the production of extracellular matrix proteins. Furthermore, IGF-II promotes apoptosis in osteoblast-like cells (Gronowicz *et al*, 2004) and thus the reduction in IGF-II mRNA levels by RUNX2 could serve the function of promoting the survival of the cells. However, the exact purpose for the suppression of IGF-II by RUNX2 is unclear and one might have actually expected an increase in IGF-II levels if RUNX2 was attempting to transform the NIH3T3 fibroblasts into osteoblast-like cells. Nonetheless, in the context of the NIH3T3 cellular environment, RUNX2 had the capacity to repress IGF-II mRNA levels.

SCYA11 also referred to as CCL11/eotaxin is an eosinophil specific chemoattractant protein that is involved in the regulation of allergen-induced eosinophilia and asthmatic responses (Garcia-Zepeda *et al*, 1996; Zimmermann *et al*, 2003; Pope *et al*, 2005). Eotaxin is up-regulated in the bronchial mucosa of patients with asthma and is responsible for inducing eosinophil migration, degranulation and differentiation from $CD34^+$ progenitor cells (Garcia-Zepeda *et al*, 1996; Ying *et al*, 1997; Fujisawa *et al*, 2000; Lamkhioued *et al*, 2003). The microarray revealed that SCYA11 was down-regulated 6.4 fold. The suppression of SCYA11 transcript levels was confirmed by the RT-PCR analysis which indicated SCYA11 mRNA levels were significantly decreased 10.1 fold. There is no literature to date to indicate that SCYA11 is involved in any aspect of bone biology and thus there are obvious reasons to explain why RUNX2 would suppress its expression. There are no RUNX binding sites in the 3kbp promoter of the mouse SCYA11 gene and thus there is no evidence to indicate that

RUNX2 or any of the other RUNX proteins could potentially directly regulate the promoter. Most likely, the regulation of SCYA11 by RUNX2 occurs via an indirect mechanism. Another member of the C-C chemokine family, CCL9/MIP1-γ is expressed by osteoclasts and participates in the formation, survival and activity of osteoclasts (Lean *et al*, 2002; Okamatsu *et al*, 2004). In addition, it was shown that human CCL2/MCP-1 was also important for osteoclast biology by promoting the fusion of human osteoclasts and inducing several osteoclast specific genes such as tartrate-resistant acid phosphatase and NFATc-1 (Kim *et al*, 2005; Kim *et al*, 2006). Based on the evidence linking other C-C chemokines and osteoclast biology, one could propose that SCYA11 might also be involved in similar actions. It could be possible that SCYA11 is expressed by osteoblasts and could carry out similar actions on osteoclast precursors as CCL9 in mouse or MCP-1 in humans. However, there is no data to indicate that SCYA11 is expressed in osteoblasts and the chemotactic ability of SCYA11 is limited to eosinophils and does not act on mononuclear cells from which osteoclasts are derived (Garcia-Zepeda *et al*, 1996).

5.4.2 Identification of genes cooperatively regulated by RUNX2 and BMP2

RUNX2 is an organizing centre for transcription and functions to regulate transcription by interacting with transcriptional co-repressors, co-activators and transcription factors at specific subcellular foci to cooperatively regulate target genes (Schroeder *et al*, 2005). SMADs are downstream signal transducers of the TGF-β superfamily and are known to interact with RUNX2 by binding to the SMAD interacting domain (SMID) which is embedded in the well defined nuclear matrix targeting signal (Afzal *et al*, 2004). A mutation resulting in the disruption of the SMID in RUNX2 was associated with CCD and severely decreased transactivation function. Furthermore, the mutant protein was incapable of inducing an osteoblast phenotype in C2C12 cells upon treatment with BMP2 (Zhang *et al*, 2000a). BMP2 belongs to the TGB-β superfamily and elicits its signals by binding to its receptors which in turn activate SMADs. During the process, SMADs are phosphorylated and translocated to the nucleus to regulate gene expression. SMADs 1, 5 and 8 respond to BMP signals and the functional cooperation between SMAD5 and RUNX2 was determined to be involved in the regulation of alkaline phosphatase in C2C12 cells (Lee *et al*, 2000; Cao and Chen, 2005). The results from such investigations indicated that the coordinated activity of RUNX2 and BMP2 was essential for osteoblast function and skeletal development.

To identify genes cooperatively regulated by RUNX2 and BMP2, stably transfected cell lines were created and microarray and RT-PCR gene expression analysis was

used to screen for candidate genes. RT-PCR and conventional PCR confirmed the overexpression of each factor (RUNX2 and BMP2) in the stably transfected cells. The search for cooperatively regulated genes was initiated via microarray analysis of RNA derived from NIH3T3 cells and NIH3T3-BMP2-RUNX2 cells using codelink gene chips. The expression profile of NIH3T3-BMP2-RUNX2 cells was compared to control NIH3T3 cells. Observation of the expression plot revealed there were many genes differentially regulated above background levels. To simplify the analysis, only genes differentially regulated greater than 4 fold (up-regulated or down-regulated) were analysed for the presence of legitimate and interesting gene targets. Four candidate genes were chosen to be further analysed via RT-PCR to determine if their regulation was dependent on RUNX2, BMP2 or both factors. The genes were EHOX, CSF2, CCL9 and OSF-1.

EHOX is a paired-like homeobox containing gene which participates in the early stages of embryonic stem (ES) cell differentiation (Jackson *et al*, 2002). Inhibition of EHOX using anti-sense mRNA resulted in the suppression of ES cell differentiation and prevented the expression of marker genes associated with hematopoietic, endothelial or cardiac differentiation. In contrast, overexpression of EHOX in ES cells accelerated the induction of the differentiation markers (Jackson *et al*, 2002). Subsequent experiments suggested a dual role for EHOX in (1) trophoblast stem cells and compartments of the developing placenta and (2) during the development of pharyngeal pouches (Jackson *et al*, 2003). However there is no literature to date to indicate that EHOX has a role(s) in osteoblasts, chondrocytes or in bone development. The microarray revealed EHOX was induced 52.5 fold in NIH3T3-BMP2-RUNX2 cells. RT-PCR analysis indicated that EHOX was not differentially

regulated in NIH3T3 cells stably transfected with either RUNX2 or BMP2. However, when both RUNX2 and BMP2 were simultaneously over-expressed, EHOX levels were significantly up-regulated 26.6 fold compared to control cells confirming the microarray result. The results indicated that EHOX was cooperatively regulated by RUNX2 and BMP2. The possible role of EHOX in relation to bone development is not known. It could potentially function in mesenchymal stem cells to promote the differentiation towards the osteoblastic lineage. However this is entirely speculative and its possible roles in bone development remain undefined.

CSF2 also known as GM-CSF was originally defined by its ability to promote the formation of granulocyte and macrophage colonies from bone marrow precursors (Fleetwood *et al*, 2005). CSF2 promotes the homeostasis of myeloid cells and governs the function of granulocytes and macrophages during immune responses (Fleetwood *et al*, 2005). The microarray indicated CSF2 mRNA levels were induced a modest 4.6 fold. The RT-PCR analysis confirmed that CSF2 was up-regulated in NIH3T3-BMP2-RUNX2 cells showing a 31.3 fold induction thus supporting the direction but not the actual magnitude of the microarray. The investigation of CSF2 mRNA levels in RUNX2 and BMP2 stable transfectants indicated it was significantly up-regulated in both cell lines. However, the greatest induction of CSF2 mRNA was observed when both factors were simultaneously overexpressed providing evidence to suggest that CSF2 was cooperatively regulated by RUNX2 and BMP2. A RUNX binding site is present in the CSF2 promoter and both RUNX1 and RUNX2 are able to activate the CSF2 promoter (Otto *et al,* 2003; Liu *et al*, 2004). The experiment provided support for the ability of RUNX2 to transactivate the CSF2 promoter.

The RT-PCR analysis provided strong support to indicate that BMP2 and RUNX2 cooperatively induced CSF2. Based on that data one could imagine that RUNX2 and BMP2 could also induce CSF2 in osteoblasts. The secretion of CSF2 by osteoblasts could function to regulate osteoclast activity. CSF2 was shown to completely inhibit M-CSF and sRANKL induced osteoclastogenesis in mouse cells (Miyamoto *et al*, 2001). Similar results were observed during the differentiation of human CFU-GM cells into osteoclasts. The study demonstrated that exposure of CFU-GM cells to CSF2 for prolonged periods of time potently inhibited osteoclast formation. However, the study also reported that short term treatment (2-48 hours) with CSF2 at the initial stages of osteoclast differentiation stimulated proliferation resulting in enhanced osteoclast formation suggesting the effect of CSF2 on osteoclastogenesis was biphasic (Hodge *et al*, 2004). One could propose that the expression of CSF2 in osteoblasts could modulate osteoclast differentiation. This would create another avenue via which osteoblasts could regulate osteoclast differentiation in addition to the already well characterized RANK/RANKL/OPG pathway. Furthermore, CSF2 was shown to be expressed in human osteoblastic (hOB) cells and CSF2 acted in an autocrine manner to promote hOB proliferation (Modrowski *et al*, 1997). As an alternative mechanism, the induction of CSF2 via the cooperative actions of RUNX2 and BMP2 could act directly on osteoblasts to regulate osteoblast differentiation.

OSF-1, also referred to as pleiotrophin is a 136 amino acid secreted heparin-binding cytokine that participates in the signaling of diverse functions such as neurite outgrowth, lineage specific differentiation of glial cells and angiogenesis (Deuel *et al*, 2002). OSF-1 is widely expressed during development and its expression is increased in cells which adopt a differentiation phenotype during wound repair

(Deuel *et al*, 2002). The expression of OSF-1 during embryonic development is associated with epithelial-mesenchymal interactions (Mitsiadis *et al*, 1995) and OSF-1 participates in a myriad of actions relating to mitogenic, apoptotic, oncogenic, angiogenic and differentiation activities (Deuel *et al*, 2002). The microarray revealed that OSF-1 was potently suppressed in NIH3T3-BMP2-RUNX2 cells. The suppression was confirmed via RT-PCR which demonstrated that OSF-1 mRNA levels were significantly decreased 308 fold in NIH3T3-BMP2-RUNX2 cells. A trend for a decrease in OSF-1 levels was observed in cells stably transfected with RUNX2 and OSF-1 mRNA was significantly repressed 48 fold in NIH3T3-BMP2 cells. Collectively, the RT-PCR analyses provided strong evidence to indicate that OSF-1 was powerfully suppressed by BMP2 with the greatest suppressive effect seen in NIH3T3-BMP2-RUNX2 cells suggesting synergism between RUNX2 and BMP2.

OSF-1 is involved in bone biology and is synthesized by osteoblasts during the early stages of osteogenic differentiation and is stored in the matrix of new bone (Tare *et al*, 2002). The addition of low concentrations of OSF-1 was shown to stimulate osteogenic differentiation of bone marrow cells (Tare *et al*, 2002). In contrast to the stimulatory effects of OSF-1 in bone marrow stromal cells, OSF-1 inhibited the BMP2-mediated osteoinduction of C2C12 cells when added to the culture media at the same time as BMP2. However, OSF-1 enhanced BMP2 osteogenic differentiation of C2C12 cells when supplemented to the media after osteoinduction had occurred suggesting temporal specific effects (Tare *et al*, 2002). Furthermore, a study by Yang *et al* (2003) demonstrated that OSF-1 promoted the adhesion, migration, proliferation and differentiation of human osteoprogenitor cells firmly establishing the role of OSF-1 in bone biology. Our data indicated that BMP2 was capable of decreasing

OSF-1 expression in fibroblasts. Assuming BMP2 was also capable of suppressing OSF-1 mRNA levels in osteoblasts, the significant decrease in OSF-1 levels caused by BMP2 could function as a mechanism to regulate osteoblast differentiation.

CCL9/MIP1-γ belongs to the family of CC chemokines and is one of four members of the MIP1 subfamily (MIP-1α, β, γ, δ). The closely related ligands function by binding to G-protein-coupled cell surface receptors (CCR1, 3 and 5). MIP1 proteins modulate inflammatory responses and participate in the homeostasis of various tissues (Maurer & von Stebut, 2004). The microarray showed that CCL9 mRNA levels were decreased in NIH3T3-BMP2-RUNX2 cells. RT-PCR analysis indicated that CCL9 mRNA levels were unchanged in NIH3T3-RUNX2 cells. However CCL9 levels were significantly lowered in NIH3T3-BMP2 and NIH3T3-BMP2-RUNX2 cells and thus confirmed the microarray result. The simultaneous overexpression of RUNX2 and BMP2 had a more potent suppressive effect on CCL9 levels compared to BMP2 alone but the difference did not reach statistical significance. Collectively, the RT-PCR data suggested that BMP2 was primarily responsible for down-regulating CCL9. The significant suppression of CCL9 by BMP2 could function to negatively regulate osteoclast formation. CCL9 has been implicated in mouse osteoclastogenesis and it was demonstrated that CCL9 and its receptor CCR1 were the predominant chemokine ligand/receptor species expressed on osteoclasts (Lean *et al*, 2002). CCL9 was shown to promote RANKL induced osteoclast formation and survival (Okamatsu *et al*, 2004). If BMP2 was to suppress CCL9 expression in osteoblasts or even in osteoclasts it could potentially function to inhibit osteoclast formation and function.

Chapter 6

The effect of RUNX2 and BMP2 in the ascorbic acid (AA) mediated induction of MMP-13 mRNA

6.1 Introduction

MMP-13 (collagense-3) belongs to the family of structurally related endopeptidases (matrix metalloproteinases) that are responsible for the proteolytic degradation of proteins that form the extracellular matrix (Birkedal-Hansen *et al*, 1993). In skeletal tissue, MMP-13 is expressed in cells that secrete extracellular matrix; the osteoblasts, osteocytes and hypertrophic chondrocytes (Borden *et al*, 1996; Johansson *et al*, 1997; Nakamura *et al*, 2004). MMP-13 is responsible for collagen degradation and thus participates in matrix remodeling which is necessary for growth plate cartilage development, endochondral ossification, bone remodeling and bone repair (Johansson *et al*, 1997; Yamagiwa *et al*, 1999; Inada *et al*, 2004). MMP-13 expression is regulated by a number of factors including parathyroid hormone (PTH) and TGF-β1. PTH induction of MMP-13 requires intact AP1 and RD sites and the physical interaction between AP1 proteins and RUNX2 is responsible for PTH activation of the MMP-13 promoter (Hess *et al*, 2001; D'Alonzo *et al*, 2002). TGF-β1 has been shown to stimulate MMP-13 expression in the rat osteoblastic cell line UMR106. The regulation of MMP-13 by TGF-β1 is facilitated by the interaction between SMADs and RUNX2 which cooperatively stimulate MMP-13 expression (Selvamurugan *et al*, 2004).

A common feature of both regulatory pathways is the RUNX2 transcription factor. RUNX2 is essential for skeletal development and cartilage formation and transactivates genes by binding to the consensus sequence AACCACA (OSE2) (Ducy *et al*, 1997; Komori *et al*, 1997; Otto *et al*, 1997; Enomoto *et al*, 2000). This same sequence is present in murine and rat MMP-13 promoters and mutation of the

proximal OSE2 site in the rat promoter significantly decreased PTH induction of MMP-13 in UMR106 cells (Hess *et al*, 2001). Interestingly, BMP2, a member of the TGF-β superfamily has been shown to suppress MMP-13 promoter activity via a RUNT domain (RD) site in osteoblasts. BMP2 reduced MMP-13 promoter activity in a time and dose dependent manner in rat fetal osteoblasts. However, in the presence of a mutated RD site, BMP2 failed to suppress MMP-13 promoter activity in the rat foetal osteoblasts (Varghese *et al*, 2005)

Ascorbic acid (AA) can also regulate MMP-13 expression. AA is required for normal bone formation and is necessary for *in vitro* osteoblast proliferation and differentiation. AA is responsible for stimulating the hydroxylation, cleavage and processing of type 1 collagen propeptides into mature alpha 1(I) and alpha 2(I) collagen components (Harada *et al*, 1991; Franceschi *et al*, 1994; Togari *et al*, 1995). The accumulation of a collagen rich extracellular matrix stimulated by AA is required for the expression of osteoblast specific genes such as osteocalcin, alkaline phosphatase and bone sialoprotein (Franceschi and Iyer, 1992). The expression of MMP-13 was found to be dependent on AA during the ascorbate induced osteoblast differentiation of MC3T3-E1 cells. The expression of MMP-13 was reduced in the presence of the collagen synthesis inhibitor 3,4-dehydroproline demonstrating the requisite role of collagen in the regulation of MMP-13 (D'Alonzo *et al*, 2002). In this study, we demonstrated that RUNX2 is required for the AA mediated induction of MMP-13 mRNA in NIH3T3 cells. Additionally, BMP2 acts synergistically with RUNX2 to up-regulate MMP-13 mRNA in the presence of AA.

6.2 Methods

6.2.1 Plasmids, cell lines, RNA extraction, cDNA synthesis, quantitative RT-PCR and statistical analysis

For methods on plasmids, cell lines, RNA extraction, cDNA synthesis, quantitative RT-PCR and statistical analysis, please refer to sections 5.2.1, 5.2.3, 5.2.4, 5.2.5, 5.2.7 and 5.2.10 respectively in chapter 5.0.

6.2.2 Tissue culture

All cell lines were maintained in DMEM (GIBCO) supplemented with 10% FBS (v/v) (GIBCO), 1% Penicillin-Streptomycin (v/v) (GIBCO) in a 5% CO_2 humidified atmosphere at 37˚C with appropriate selecting antibiotics. The effect of AA on MMP-13 expression was investigated by culturing cells to confluence and maintaining them for a further 12 days in standard media or media supplemented with 50 µg/ml AA (Sigma). The media was changed every three days.

6.2.3 Primer list

Refer to section 5.2.6 in chapter 5.0 for RT-PCR primer design. Table 6.1 lists the PCR primers used in the study. 18s, BMP2 and RUNX2 primers were based on human templates whereas MMP-13 was from mouse origin.

Table 6.1: Real-time PCR primers for MMP-13, RUNX2, BMP2 and 18s ribosomal RNA and their cDNA product sizes.

Gene	Forward 5'-3'	Reverse 5'-3'	cDNA product (bp)
MMP-13	GTTGGTCATTACTCAAGGCTATGCA	GGCTTGCTGTGTCTTAGCTGGATC	330
RUNX2	CAGTCACCTCAGGCATGTC	GCGTGCTGCCATTCGAG	237
BMP2	ATGCGGTGGACTGCACAGGGACAC	GACCAACGTCTGAACAATGGCATG	409
18s	CTTAGAGGGACAAGTGGCG	ACGCTGAGCCAGTCAGTGTA	106

6.3 Results

6.3.1 AA is not sufficient to induce MMP-13 mRNA expression in NIH3T3 mouse embryonic fibroblasts

The effect of ascorbic acid on MMP-13 mRNA expression was investigated in mouse embryonic fibroblasts. NIH3T3 cells were grown to confluence and were either cultured in AA free media (control) or in media containing 50 μg/ml AA (AA) for 12 days. The relative amounts of MMP-13 mRNA were 1.0 ± 0.17 and 0.95 ± 0.11 for control and AA cells respectively (figure 6.1). MMP-13 mRNA levels were not significantly different ($p = 0.837$) between control cells and those exposed to AA indicating that AA did not induce MMP-13 mRNA expression in NIH3T3 cells.

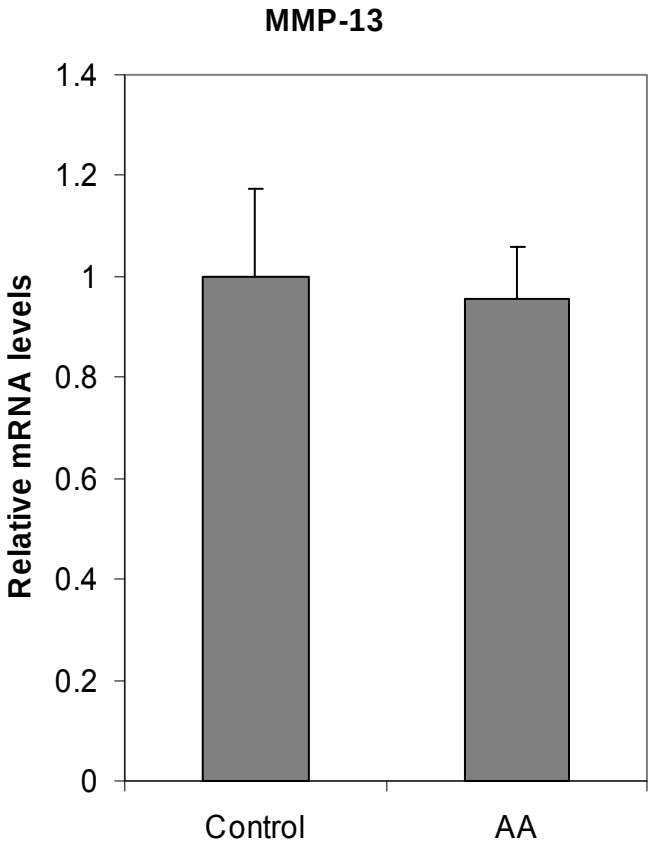

Figure 6.1: Relative amounts of MMP-13 transcripts between control cells and AA treated cells. There was no significant difference in MMP-13 mRNA levels ($p = 0.837$).

6.3.2 Induction of MMP-13 mRNA by AA is facilitated by RUNX2

The ability of RUNX2 to increase MMP-13 mRNA levels was investigated by creating a stably transfected cell line overexpressing human RUNX2-I. pBABE-RUNX2 was transfected in NIH3T3 cells and stable transfectants were selected using puromycin. NIH3T3-RUNX2 cells (stable transfectants) were grown to confluence and cultured in AA free media for 12 days. NIH3T3-RUNX2 had significantly increased levels of RUNX2 mRNA ($p = 2.7E-08$) displaying a 28 fold increase compared to NIH3T3 cells (figure 5.1, chapter 5.0). MMP-13 mRNA levels were investigated in NIH3T3-RUNX2 cells (Figure 6.2). The presence of RUNX2 significantly increased MMP-13 transcripts 85 fold ($p = 8.4E-05$). The data suggested that RUNX2 was a key factor in regulating MMP-13 mRNA levels. The effect of AA on MMP-13 mRNA levels in the presence of RUNX2 was investigated by culturing confluent NIH3T3-RUNX2 cells in media supplemented with AA for 12 days. Relative MMP-13 mRNA levels in RUNX2 + AA treated cells were compared to control, AA and RUNX2 treated cells (figure 6.2). The combination of RUNX2 and AA had a dramatic effect on MMP-13 mRNA expression with mRNA levels up-regulated 254 fold compared to control cells ($p = 3.9E-09$) and induced 3 fold in comparison to NIH3T3-RUNX2 cells ($p = 2.5E-04$).

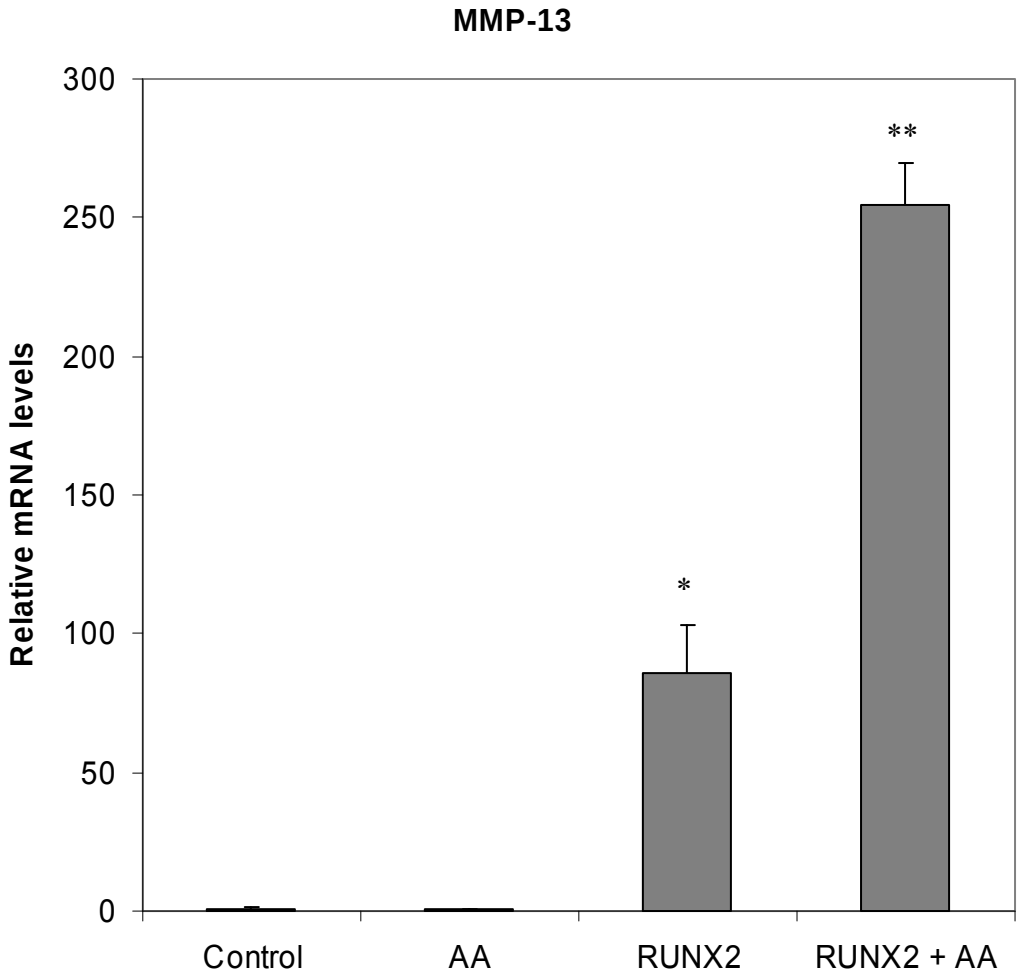

* Significantly different compared to control and AA (p = < 0.05)

** Significantly different compared to control, AA and RUNX2 (p = < 0.05)

Figure 6.2: Relative MMP-13 mRNA levels in control, AA, RUNX2 and RUNX2 + AA cells. AA in the presence of RUNX2 overexpression induced MMP-13 mRNA expression 254 fold compared to control cells.

6.3.3 RUNX2 and BMP2 synergize to induce MMP-13 mRNA expression

The effect of BMP2 on MMP-13 mRNA expression when cultured with AA or in the presence of RUNX2 + AA was investigated by creating stable transfectants overexpressing BMP2. NIH3T3 and NIH3T3-RUNX2 cells were transfected with pCMV-BMP2 and stable transfectants were selected with G418. The expression of BMP2 was analysed by conventional PCR and RT-PCR (figure 6.3). Conventional PCR revealed human BMP2 was only detectable in cell lines stably transfected with BMP2. RT-PCR showed that there was no significant difference in BMP2 mRNA levels between NIH3T3-BMP2 and NIH3T3-RUNX2-BMP2 overexpressing cells ($p = 0.844$).

The expression of MMP-13 mRNA was investigated in the stably transfected cell lines. Figure 6.4 shows that BMP2 had a moderate effect on MMP-13 levels when cultured in media supplemented with AA, inducing mRNA levels 3.8 fold compared to AA ($p = 2.7E-03$). However a spectacular effect was seen when both RUNX2 and BMP2 were overexpressed. The combined overexpression resulted in a massive 4026 fold induction of MMP-13 transcripts compared to AA ($p = 2.7 \times 10^{-7}$) and a 16 fold increase compared to RUNX2 + AA ($p = 1.7 \times 10^{-5}$, figure 6.5).

6.3A

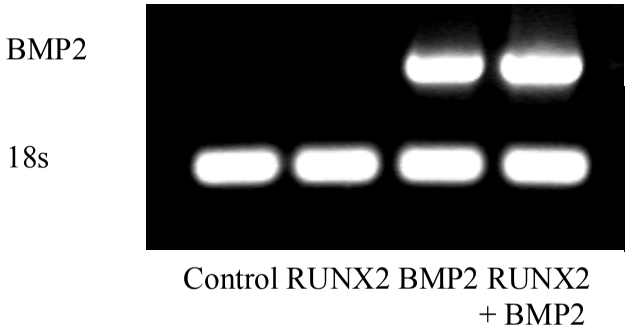

6.3B

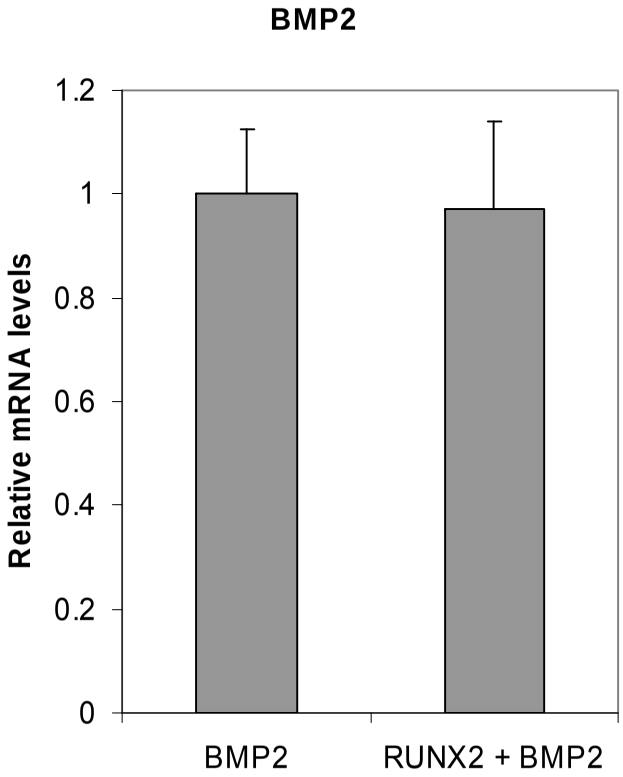

Figure 6.3: (A): Conventional PCR of BMP2 in control, RUNX2, BMP2 and RUNX2 + BMP2 cells. Only NIH3T3-BMP2 and NIH3T3-BMP2-RUNX2 cells had detectable levels of human BMP2. (B): There was no significant difference in the relative BMP2 mRNA levels between NIH3T3-BMP2 and NIH3T3-BMP2-RUNX2 cells.

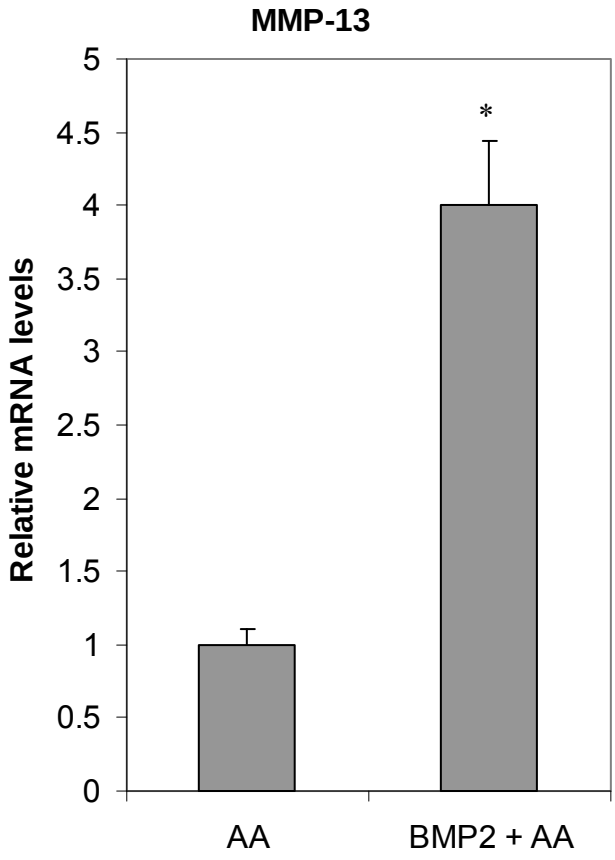

* Significantly different to AA (p = < 0.05)

Figure 6.4: Relative levels of MMP-13 as measured by quantitative RT-PCR in AA and BMP2 + AA treated cells. The overexpression of BMP2 resulted in a modest 4 fold increase in MMP-13 mRNA levels.

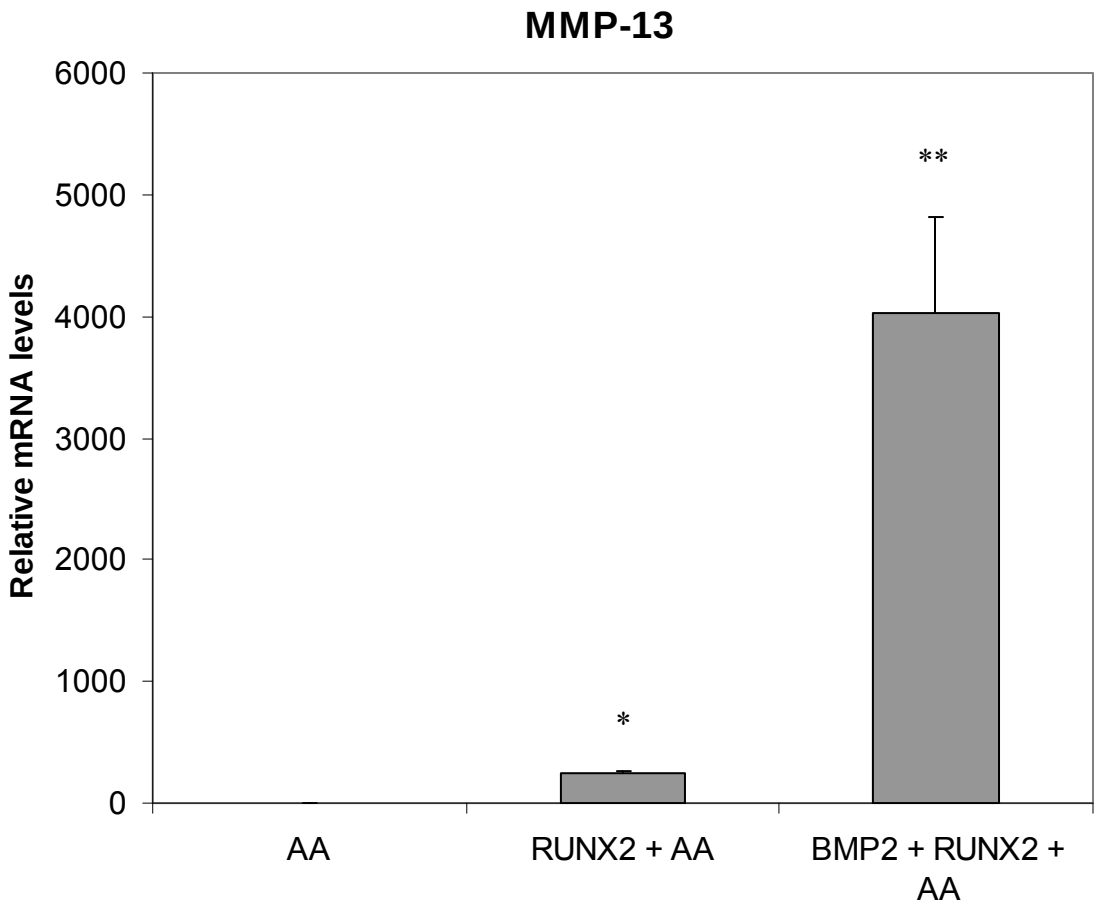

* Significantly different to AA (p = < 0.05)

** Significantly different to AA and RUNX2 + AA (p = < 0.05)

Figure 6.5: Relative levels of MMP-13 mRNA in AA, RUNX2 + AA and RUNX2 + BMP2 + AA treated cells. The functional cooperation of RUNX2 and BMP2 in the presence of AA resulted in a potent increase in MMP-13 mRNA levels.

6.4 Discussion

When pre-osteoblastic MC3T3-E1 cells are treated with ascorbic acid and β-glycerophosphate they undergo osteogenic differentiation and eventually form bone nodules when cultured in vitro (Quarles *et al,* 1992). During this process MMP-13 is highly expressed and its expression was found to be dependent on AA (D'Alonzo *et al,* 2002). The ability of AA to induce MMP-13 mRNA in non-osteoblastic NIH3T3 cells was investigated. The levels of MMP-13 mRNA were not significantly different between NIH3T3 cells cultured in media supplemented with AA and those cultured under standard conditions (control). This indicated that AA was not sufficient for inducing MMP-13 mRNA levels in NIH3T3 cells.

A key difference between MC3T3-E1 pre-osteoblastic cells and NIH3T3 fibroblasts is the expression of the osteoblast specific transcription factor RUNX2 which is expressed at high levels in osteoblasts but at low levels in fibroblasts (Ducy *et al,* 2000). To investigate the potential role of RUNX2 in facilitating AA mediated induction of MMP-13 mRNA, a stably transfected NIH3T3 cell line overexpressing RUNX2 was created. The stable cell line had significantly increased levels RUNX2 mRNA and produced 85 times more MMP-13 mRNA transcripts compared to control cells when grown in standard conditions. The result indicated that RUNX2 was sufficient for directly up-regulating MMP-13 in the absence of AA supplementation by either directly transactivating the MMP-13 promoter or via other pathways such as associating with AP1/SMADs to stimulate MMP-13 mRNA expression through already characterized regulatory mechanisms.

The effect of AA on MMP-13 mRNA expression in the presence RUNX2 over-expression was investigated. The addition of AA in combination with RUNX2 overexpression had a dramatic effect of MMP-13 mRNA levels resulting in a 254 fold increase compared to control cells and a 3 fold induction in relation to NIH3T3-RUNX2 cells not exposed to AA. The result indicated that the AA mediated induction of MMP-13 mRNA was facilitated by RUNX2 as only in the presence of RUNX2 over-expression did AA induce MMP-13 mRNA. Overall, the results revealed that AA had a modest effect MMP-13 mRNA expression by potentiating RUNX2 upregulation and suggested that RUNX2 was primarily responsible for up-regulating MMP-13 mRNA expression.

BMP2 is a powerful osteogenic factor that belongs to the transforming growth factor superfamily. It acts by binding to its receptors and elicits cellular responses by activating SMADs which subsequently associate with downstream factors to regulate cellular function (Wang *et al*, 1990; Riley *et al,* 1996; Ducy and Karsenty 2000). BMP2 is capable of inducing differentiation of C2C12 and stromal cells towards the osteoblast lineage and directs the synthesis of several osteoblast specific genes such as alkaline phosphatase and type I collagen (Katagiri *et al*, 1994; Takuwa *et al*, 1991; Thies *et al*, 1992). The effect of BMP2 on MMP-13 expression was investigated by creating stably transfected cell lines overexpressing BMP2. In the presence of AA, BMP2 had a modest effect on MMP-13 mRNA expression up-regulating transcript levels 3.8 fold. It is possible to suggest that the increased MMP-13 levels observed in BMP2 stably transfected cells could have been directly attributed to the upregulation of RUNX2 caused by BMP2. BMP2 is capable of inducing RUNX2 expression (Lee *et al*, 2003) and the modest 1.7 fold increase in RUNX2 mRNA in cells stably

transfected with BMP2 (data not shown) could have been responsible for the increased MMP-13 mRNA levels.

Varghese *et al* (2005) investigated the effect of BMP2 on MMP-13 promoter activity. The study showed that BMP2 was able to suppress MMP-13 promoter activity in a dose and time dependent manner in rat osteoblasts. A Runt Domain (RD) site was determined to be essential for the suppressive effect. In contrast to the results obtained by Varghese and colleagues, our data indicated that MMP-13 mRNA levels were significantly increased when BMP2 was over-expressed in the NIH3T3 cells suggesting a cell specific effect.

The outcome of combined BMP2 and RUNX2 over-expression on MMP-13 levels in the presence of AA was investigated. Simultaneous over-expression of both osteogenic factors had a spectacular effect on MMP-13 expression up-regulating mRNA levels a massive 4026 fold compared to control cells and 16 fold compared RUNX2 + AA cells. The result indicated that RUNX2 and BMP2 signals synergized to regulate MMP-13 mRNA and this functional cooperation was responsible for inducing enormous amounts of MMP-13 transcripts.

The synergy between RUNX2 and BMP2 in the transcriptional regulation of MMP-13 is most likely a consequence of SMAD-RUNX2 interaction. SMADs are signal transducers of the TGF-β superfamily and have been shown to physically associate with RUNX proteins in vitro (Zhang *et al*, 2000a; Afzal *et al*, 2005). RUNX2 and SMAD3 have been shown to cooperatively stimulate the germ line Ig Cα promoter when exposed to TGF-β indicating synergism between RUNX2 and BMP2 signal

transducers in gene regulation (Hanai *et al*, 1999 & Zhang *et al*, 2000a). Although we do not show evidence of direct physical association between RUNX2 and SMADs in regulating MMP-13 transcription, our study provides strong support for such a theory.

Chapter 7

Conclusions

RUNX2 belongs to the family of RUNT domain transcription factors which are key regulators of metazoan development (Coffman *et al*, 2003). RUNX2 participates in the regulation of a myriad of activities pertaining to the control of osteoblast differentiation, osteoblast function and skeletogenesis. RUNX2 acts as a scaffold for the integration, organization and assembly of regulatory factors at specific subcellular foci within the context of the three-dimensional nuclear structural design to regulate the complex pathways required for bone formation and turnover (Lian and Stein, 2003; Stein *et al*, 2004). Investigation of mutations and polymorphisms within the RUNX2 promoter and coding regions revealed mutations were associated with changes in BMD and indicated that RUNX2 also contributed to bone mass (Vaughan *et al*, 2002; Vaughan *et al*, 2004; Doecke *et al*, 2006). Four aims were addressed to further characterize the role of RUNX2 in skeletogenesis. The first aim was to screen the Southeast Queensland bone DNA cohort for gross variations of the RUNX2 Q/A domain and re-test the effect of the 11Ala allele on fracture. Secondly, the influence of rare RUNX2 Q/A repeat mutations on fracture and measures of bone density was investigated. The transactivation function of rare glutamine repeat mutations and the 11Ala allele was also assessed using a luciferase RUNX2 reporter gene assay. The third aim was to identify genes directly regulated by RUNX2 and genes regulated by the coordinated activities of BMP2 and RUNX2. The fourth aim was to investigate the role of RUNX2 and BMP2 in the ascorbic acid mediated induction of MMP-13 mRNA.

Genotyping the Southeast Queensland bone study served the purpose of identifying additional gross variations of the poly Q/A domain of RUNX2 in an attempt to enrich the population of already identified Q/A variants derived from previous genotyping

studies. Additionally, genotyping of the Southeast Queensland bone study provided an opportunity to re-test the effect of the common 11Ala allele on fracture which was previously shown to be overrepresented in fracture cases in the GOS. In the Southeast Queensland bone study, the 11Ala allele had no significant effects on anthropomorphic measures. However, analysis of fracture status revealed that individuals which carried at least one copy of the 11Ala allele had an increased frequency of fracture compared to non-carriers. The distribution of RUNX2 genotypes (WT and 11Ala allele) was investigated using chi-square analysis. The genotyped cohort was composed of singletons and families and the correlation between biologically related individuals was accounted for by selecting only one representative member from each family to contribute towards the analysis. Collectively, chi-square analyses revealed the 11Ala allele was enriched in individuals with fracture with an average OR of 1.712. Combining the results from the GOS fracture investigation and the Southeast Queensland bone study using Monte-Carlo simulations demonstrated that the maximum probability of obtaining both study results by chance was less than 5 times in two hundred and indicated that the 11Ala allele of RUNX2 was associated with an increased risk of fracture.

Analysis of rare RUNX2 Q/A variants identified from four epidemiological studies of bone suggested that glutamine repeat variants were associated with an increased risk of fracture. Glutamine repeat variants were more than twice as likely to have sustained incident fracture during a five year observation period compared to non-carriers in the CAIFOS. We have to keep in mind that only a small sample of Q-repeat variants were identified in the CAIFOS (n = 8) and the effect on fracture has to be interpreted as preliminary data. A larger collection of Q-variants would provide a

more accurate indication of the effect of Q-variants on fracture. Investigation of bone density as measured by quantitative ultrasound at the calcaneus and by DEXA at the femoral neck revealed that rare RUNX2 Q/A variants were associated with significantly decreased bone density. The average genetic effect was approximately a 0.70 SD reduction in bone density and one could expect the effect to double to -1.40 SD in homozygotes if the effect were additive. The significantly lower bone density in Q/A variants provided an avenue to explain the increased rate of fracture observed in Q-variants. Based on the evidence linking rare Q/A variants with fracture and significantly lower bone density, the investigations suggested that the Q/A domain of RUNX2 is functionally important.

Quantitative promoter activation analysis of rare glutamine mutations and of the 11Ala allele was conducted to elucidate the mechanism via which the Q/A repeat variants were significantly altering bone parameters. The analysis revealed that the 16Q and 30Q RUNX2 mutants had significantly lower transcriptional activity compared to WT RUNX2. Although the activation analysis demonstrated changes in RUNX2 function due to the Q-repeat mutations, it is hard to extrapolate the data towards a more global view in terms of the genes RUNX2 regulates due to the nature in which RUNX2 governs gene transcription. RUNX2 acts as a scaffold recruiting co-factors and transcription factors to specific nuclear matrix sites to regulate genes and thus RUNX2 has multiple methods of regulating target gene promoter activity depending on the factors it associates with. To fully understand the functional importance of Q-repeat mutations one would have to address the effect of the mutations on a larger collection of genes known to be regulated by RUNX2.

In contrast to the Q-repeat mutations, the 11Ala allele had no material effect on the transactivation function of RUNX2 and shed no light on its possible mechanism of action in contributing to an increased risk of fracture and lowered serum OC. The lack of an effect of the 11Ala allele on RUNX2 transactivation function is consistent with a previous report from Thirunavukkarasu *et al* (1998) which suggested the alanine tract did not participate in the transactivation ability of the Q/A domain. One could raise the argument that the deletion polymorphism could be linked to a nearby polymorphic intronic sequence which could disrupt mRNA processing and ultimately protein function as a possible explanation for the detrimental effects of the 11Ala allele. Alternatively the deletion could alter/limit the interaction between RUNX2 and accessory proteins required for skeletal development.

The establishment of cell lines overexpressing RUNX2 and BMP2 and subsequent gene expression analysis via microarrays and RT-PCR successfully identified downstream RUNX2 gene targets. Affymetrix microarrays were used to identify genes regulated by RUNX2. The significant increase in MMP-13 and osteocalcin mRNA levels provided evidence to suggest that the overexpressed human RUNX2 was functional and was transactivating target promoters. However, examination of the microarray gene expression analysis revealed that very few genes were differentially regulated between control cells and cells stably transfected with RUNX2. This suggested that RUNX2 was insufficient for optimal gene expression and indicated that RUNX2 required other factors to successfully regulate target genes.

The simultaneous overexpression of RUNX2 and BMP2 was used as a model to identify genes synergistically regulated by the two factors. Microarray analysis via

codelink gene chips provided an insight into possible genes regulated by the coordinated activity of RUNX2 and BMP2. Examination of the expression plot revealed a large number of differentially regulated genes between control cells and NIH3T3-RUNX2-BMP2 cells. CSF2, EHOX, CCL9 and OSF-1 were chosen to be further characterised by RT-PCR analysis. Quantitative RT-PCR revealed that CSF2 was significantly induced by both RUNX2 and BMP2 individually. The greatest induction of CSF2 was observed when both RUNX2 and BMP2 were simultaneously overexpressed suggesting a synergistic effect. EHOX was not significantly regulated when RUNX2 or BMP2 were expressed alone. In contrast, EHOX was highly induced when both RUNX2 and BMP2 were concurrently expressed. The data indicated that EHOX was cooperatively regulated by RUNX2 and BMP2. CCL9 was determined to be suppressed in the microarray. The result was confirmed by the RT-PCR analysis and indicated the effect was dependent on BMP2. OSF-1 mRNA levels were decreased in the microarray analysis. The investigation of gene expression via RT-PCR indicated a trend for decreased OSF-1 in NIH3T3-RUNX2 cells. The most potent inhibition of OSF-1 mRNA levels were observed in cells stably transfected with BMP2 and both BMP2 and RUNX2. The concurrent expression of both RUNX2 and BMP2 resulted in a massive 308 fold reduction in OSF-1 compared to control cells.

Collectively, the combined use of microarray and RT-PCR analyses to quantitate gene expression in cells stably transfected with RUNX2, BMP2 and both RUNX2 and BMP2 served as a successful model for the identification of genes cooperatively regulated by the two factors. The analysis revealed gene targets synergistically

regulated by RUNX2 and BMP2 (CSF2 and EHOX) in addition to identifying genes suppressed by BMP2 (CCL9 and OSF-1).

The role of RUNX2 during the AA mediated induction of MMP-13 mRNA was investigated in the fourth part of the research. The investigation revealed that AA was not sufficient for inducing MMP-13 mRNA in NIH3T3 cells. The experiment revealed that RUNX2 was able to induce MMP-13 mRNA levels in the absence of AA and that only in the presence of RUNX2 was AA able to induce MMP-13 mRNA levels. The result indicated that RUNX2 was essential for the AA mediated induction of MMP-13. BMP2 modestly induced MMP-13 mRNA in the presence of AA. When both RUNX2 and BMP2 were overexpressed in the presence of AA, MMP-13 mRNA levels were induced a massive 4026 fold compared to control cells indicating that RUNX2 and BMP2 cooperatively regulated MMP-13.

In summary, the experiments presented in this thesis served to characterise the RUNX2 transcription factor to provide a greater understanding of the complex pathways and mechanisms RUNX2 contributes to and regulates. The studies identified genetic variations within the trinucleotide repeat tract encoding the poly Q/A domain of RUNX2 and these mutations were used as a tool to extract information on the transcription factor. The genetic analyses conducted in chapters 3 and 4 established RUNX2 as a regulator of BMD and fracture and although the effect sizes could be construed a modest they should viewed as highly significant findings considering the polygenic and multifactorial nature of these traits. Future genetic analyses could be performed to confirm the findings. In relation to chapter 3, repeating the genotyping of the 11Ala allele in a larger population which has data on

radiologically confirmed fractures in addition to BMD and data on factors that could influence BMD and fracture such as diet, nutrition, smoking, exercise and medication would provide an opportunity to confirm the study results. This would be an extensive study however it would provide a great test of the original hypothesis and would also allow the determination of the effect of the 11Ala allele on fracture while adjusting for environmental influences which was perhaps a constraint of chapter 3. Chapter 4 was limited by the small sample of Q/A repeat variants observed. Not taking anything away from the significant results obtained, the small population of Q/A repeat variants made it difficult to estimate the true effects of the mutants on BMD and in particular fracture. A future study should be implemented to genotype a much larger population to further study the effects of the variations on bone phenotype. If a population of 10,000 DNA samples were genotyped for rare Q/A repeat variants, one would expect to observe approximately 50 mutants based on a frequency of 0.5%. An additional 50 mutants would provide substantially more power to subsequent analyses further defining the results.

Chapters 5 and 6 used molecular and cell biology to study RUNX2. The experiments were conducted to broaden our understanding of RUNX2 function at the molecular level by studying its role in regulating gene expression. Chapter 5 provided potent results in relation to the functional cooperation between RUNX2 and BMP2 in regulating target genes. The results also demonstrated that RUNX2 on its own is not optimal for regulating gene expression and requires additional factors to elicit maximal effects. Future experiments should be carried out to further define the mechanism(s) via which RUNX2 and BMP2 unite to regulate genes. This work would be molecular biology in nature and would study whether the cooperation was due

SMAD-RUNX interactions or whether an alternative pathway is involved. Chapter 6 provided an insight into the involvement of RUNX2 in the AA mediated induction of MMP-13 mRNA. The results demonstrated that RUNX2 was essential for MMP-13 upregulation in response to AA. However, the chapter was limited in a sense that it was unable to provide the mechanism via which RUNX2 and AA interact to regulate the MMP-13 promoter. Future experiments would cater for such an explanation and would also be based on molecular biology.

In conclusion, four experimental aims were addressed and presented in this thesis. The research demonstrated that a common allele of RUNX2, the 11Ala allele, was associated with an increased fracture risk. Rare poly Q/A mutations in RUNX2 were determined to be associated with significantly lower measures of bone density and also an increased risk of fracture. Chapter 5 demonstrated that RUNX2 and the powerful bone promoting factor BMP2 interacted to synergistically regulate genes and RUNX2 was determined to be an integral component in the ascorbic acid mediated induction of MMP-13 in chapter 6. Collectively the experiments have provided novel findings in relation to the RUNX2 transcription factor at the genetic level and at the molecular level. The results should be incorporated into our current understanding of RUNX2 to further increase our knowledge of RUNX2 and bone biology.

Appendix A1

Analysis of RUNX2 genotype distributions within fracture and non-fracture groups via chi-square

Dataset 1

Case Processing Summary

	Cases					
	Valid		Missing		Total	
	N	Percent	N	Percent	N	Percent
MIN_Y_N * ALA_Y_N	474	100.0%	0	.0%	474	100.0%

MIN_Y_N * ALA_Y_N Crosstabulation

			ALA_Y_N		
			wt	11Ala	Total
MIN_Y_N	no	Count	361	40	401
		Expected Count	357.0	44.0	401.0
	yes	Count	61	12	73
		Expected Count	65.0	8.0	73.0
Total		Count	422	52	474
		Expected Count	422.0	52.0	474.0

Chi-Square Tests

	Value	df	Asymp. Sig. (2-sided)	Exact Sig. (2-sided)	Exact Sig. (1-sided)
Pearson Chi-Square	2.641[b]	1	.104		
Continuity Correction[a]	2.021	1	.155		
Likelihood Ratio	2.391	1	.122		
Fisher's Exact Test				.107	.082
Linear-by-Linear Association	2.636	1	.104		
N of Valid Cases	474				

a. Computed only for a 2x2 table

b. 0 cells (.0%) have expected count less than 5. The minimum expected count is 8.01.

Risk Estimate

	Value	95% Confidence Interval	
		Lower	Upper
Odds Ratio for MIN_Y_N (no / yes)	1.775	.882	3.575
For cohort ALA_Y_N = wt	1.077	.968	1.199
For cohort ALA_Y_N = 11Ala	.607	.335	1.100
N of Valid Cases	474		

Dataset 2

Case Processing Summary

	Cases					
	Valid		Missing		Total	
	N	Percent	N	Percent	N	Percent
MIN_Y_N * ALA_Y_N	474	100.0%	0	.0%	474	100.0%

MIN_Y_N * ALA_Y_N Crosstabulation

			ALA_Y_N		
			wt	11Ala	Total
MIN_Y_N	no	Count	355	39	394
		Expected Count	351.6	42.4	394.0
	yes	Count	68	12	80
		Expected Count	71.4	8.6	80.0
Total		Count	423	51	474
		Expected Count	423.0	51.0	474.0

Chi-Square Tests

	Value	df	Asymp. Sig. (2-sided)	Exact Sig. (2-sided)	Exact Sig. (1-sided)
Pearson Chi-Square	1.802[b]	1	.179		
Continuity Correction[a]	1.310	1	.252		
Likelihood Ratio	1.665	1	.197		
Fisher's Exact Test				.233	.128
Linear-by-Linear Association	1.799	1	.180		
N of Valid Cases	474				

a. Computed only for a 2x2 table

b. 0 cells (.0%) have expected count less than 5. The minimum expected count is 8.61.

Risk Estimate

	Value	95% Confidence Interval	
		Lower	Upper
Odds Ratio for MIN_Y_N (no / yes)	1.606	.800	3.225
For cohort ALA_Y_N = wt	1.060	.961	1.169
For cohort ALA_Y_N = 11Ala	.660	.362	1.203
N of Valid Cases	474		

Dataset 3

Case Processing Summary

	Cases					
	Valid		Missing		Total	
	N	Percent	N	Percent	N	Percent
MIN_Y_N * ALA_Y_N	474	100.0%	0	.0%	474	100.0%

MIN_Y_N * ALA_Y_N Crosstabulation

			ALA_Y_N		
			wt	11Ala	Total
MIN_Y_N	no	Count	354	39	393
		Expected Count	351.5	41.5	393.0
	yes	Count	70	11	81
		Expected Count	72.5	8.5	81.0
Total		Count	424	50	474
		Expected Count	424.0	50.0	474.0

Chi-Square Tests

	Value	df	Asymp. Sig. (2-sided)	Exact Sig. (2-sided)	Exact Sig. (1-sided)
Pearson Chi-Square	.952[b]	1	.329		
Continuity Correction[a]	.604	1	.437		
Likelihood Ratio	.896	1	.344		
Fisher's Exact Test				.324	.215
Linear-by-Linear Association	.950	1	.330		
N of Valid Cases	474				

a. Computed only for a 2x2 table

b. 0 cells (.0%) have expected count less than 5. The minimum expected count is 8.54.

Risk Estimate

	Value	95% Confidence Interval	
		Lower	Upper
Odds Ratio for MIN_Y_N (no / yes)	1.426	.697	2.920
For cohort ALA_Y_N = wt	1.042	.950	1.143
For cohort ALA_Y_N = 11Ala	.731	.391	1.365
N of Valid Cases	474		

Dataset 4

Case Processing Summary

	Cases					
	Valid		Missing		Total	
	N	Percent	N	Percent	N	Percent
MIN_Y_N * ALA_Y_N	474	100.0%	0	.0%	474	100.0%

MIN_Y_N * ALA_Y_N Crosstabulation

			ALA_Y_N		
			wt	11Ala	Total
MIN_Y_N	no	Count	362	38	400
		Expected Count	357.8	42.2	400.0
	yes	Count	62	12	74
		Expected Count	66.2	7.8	74.0
Total		Count	424	50	474
		Expected Count	424.0	50.0	474.0

Chi-Square Tests

	Value	df	Asymp. Sig. (2-sided)	Exact Sig. (2-sided)	Exact Sig. (1-sided)
Pearson Chi-Square	2.985[b]	1	.084		
Continuity Correction[a]	2.316	1	.128		
Likelihood Ratio	2.684	1	.101		
Fisher's Exact Test				.098	.069
Linear-by-Linear Association	2.979	1	.084		
N of Valid Cases	474				

a. Computed only for a 2x2 table

b. 0 cells (.0%) have expected count less than 5. The minimum expected count is 7.81.

Risk Estimate

	Value	95% Confidence Interval	
		Lower	Upper
Odds Ratio for MIN_Y_N (no / yes)	1.844	.913	3.723
For cohort ALA_Y_N = wt	1.080	.972	1.200
For cohort ALA_Y_N = 11Ala	.586	.322	1.067
N of Valid Cases	474		

Dataset 5

Case Processing Summary

	Cases					
	Valid		Missing		Total	
	N	Percent	N	Percent	N	Percent
MIN_Y_N * ALA_Y_N	474	100.0%	0	.0%	474	100.0%

MIN_Y_N * ALA_Y_N Crosstabulation

			ALA_Y_N		
			wt	11Ala	Total
MIN_Y_N	no	Count	357	36	393
		Expected Count	353.2	39.8	393.0
	yes	Count	69	12	81
		Expected Count	72.8	8.2	81.0
Total		Count	426	48	474
		Expected Count	426.0	48.0	474.0

Chi-Square Tests

	Value	df	Asymp. Sig. (2-sided)	Exact Sig. (2-sided)	Exact Sig. (1-sided)
Pearson Chi-Square	2.359[b]	1	.125		
Continuity Correction[a]	1.779	1	.182		
Likelihood Ratio	2.153	1	.142		
Fisher's Exact Test				.154	.095
Linear-by-Linear Association	2.354	1	.125		
N of Valid Cases	474				

a. Computed only for a 2x2 table

b. 0 cells (.0%) have expected count less than 5. The minimum expected count is 8.20.

Risk Estimate

	Value	95% Confidence Interval	
		Lower	Upper
Odds Ratio for MIN_Y_N (no / yes)	1.725	.854	3.481
For cohort ALA_Y_N = wt	1.066	.969	1.174
For cohort ALA_Y_N = 11Ala	.618	.337	1.136
N of Valid Cases	474		

Dataset 6

Case Processing Summary

	Cases					
	Valid		Missing		Total	
	N	Percent	N	Percent	N	Percent
MIN_Y_N * ALA_Y_N	474	100.0%	0	.0%	474	100.0%

MIN_Y_N * ALA_Y_N Crosstabulation

			ALA_Y_N		
			wt	11Ala	Total
MIN_Y_N	no	Count	358	37	395
		Expected Count	354.2	40.8	395.0
	yes	Count	67	12	79
		Expected Count	70.8	8.2	79.0
Total		Count	425	49	474
		Expected Count	425.0	49.0	474.0

Chi-Square Tests

	Value	df	Asymp. Sig. (2-sided)	Exact Sig. (2-sided)	Exact Sig. (1-sided)
Pearson Chi-Square	2.408[b]	1	.121		
Continuity Correction[a]	1.821	1	.177		
Likelihood Ratio	2.194	1	.139		
Fisher's Exact Test				.154	.092
Linear-by-Linear Association	2.403	1	.121		
N of Valid Cases	474				

a. Computed only for a 2x2 table

b. 0 cells (.0%) have expected count less than 5. The minimum expected count is 8.17.

Risk Estimate

	Value	95% Confidence Interval	
		Lower	Upper
Odds Ratio for MIN_Y_N (no / yes)	1.733	.859	3.495
For cohort ALA_Y_N = wt	1.069	.968	1.179
For cohort ALA_Y_N = 11Ala	.617	.337	1.129
N of Valid Cases	474		

Dataset 7

Case Processing Summary

	Cases					
	Valid		Missing		Total	
	N	Percent	N	Percent	N	Percent
MIN_Y_N * ALA_Y_N	474	100.0%	0	.0%	474	100.0%

MIN_Y_N * ALA_Y_N Crosstabulation

			ALA_Y_N		Total
			wt	11Ala	
MIN_Y_N	no	Count	357	40	397
		Expected Count	354.3	42.7	397.0
	yes	Count	66	11	77
		Expected Count	68.7	8.3	77.0
Total		Count	423	51	474
		Expected Count	423.0	51.0	474.0

Chi-Square Tests

	Value	df	Asymp. Sig. (2-sided)	Exact Sig. (2-sided)	Exact Sig. (1-sided)
Pearson Chi-Square	1.191[b]	1	.275		
Continuity Correction[a]	.792	1	.373		
Likelihood Ratio	1.112	1	.292		
Fisher's Exact Test				.313	.184
Linear-by-Linear Association	1.188	1	.276		
N of Valid Cases	474				

a. Computed only for a 2x2 table

b. 0 cells (.0%) have expected count less than 5. The minimum expected count is 8.28.

Risk Estimate

	Value	95% Confidence Interval	
		Lower	Upper
Odds Ratio for MIN_Y_N (no / yes)	1.488	.726	3.047
For cohort ALA_Y_N = wt	1.049	.952	1.156
For cohort ALA_Y_N = 11Ala	.705	.379	1.312
N of Valid Cases	474		

Dataset 8

Case Processing Summary

	Cases					
	Valid		Missing		Total	
	N	Percent	N	Percent	N	Percent
MIN_Y_N * ALA_Y_N	474	100.0%	0	.0%	474	100.0%

MIN_Y_N * ALA_Y_N Crosstabulation

			ALA_Y_N		
			wt	11Ala	Total
MIN_Y_N	no	Count	362	36	398
		Expected Count	358.5	39.5	398.0
	yes	Count	65	11	76
		Expected Count	68.5	7.5	76.0
Total		Count	427	47	474
		Expected Count	427.0	47.0	474.0

Chi-Square Tests

	Value	df	Asymp. Sig. (2-sided)	Exact Sig. (2-sided)	Exact Sig. (1-sided)
Pearson Chi-Square	2.105[b]	1	.147		
Continuity Correction[a]	1.541	1	.214		
Likelihood Ratio	1.918	1	.166		
Fisher's Exact Test				.147	.110
Linear-by-Linear Association	2.101	1	.147		
N of Valid Cases	474				

a. Computed only for a 2x2 table

b. 0 cells (.0%) have expected count less than 5. The minimum expected count is 7.54.

Risk Estimate

	Value	95% Confidence Interval	
		Lower	Upper
Odds Ratio for MIN_Y_N (no / yes)	1.702	.824	3.514
For cohort ALA_Y_N = wt	1.063	.965	1.172
For cohort ALA_Y_N = 11Ala	.625	.333	1.172
N of Valid Cases	474		

Dataset 9

Case Processing Summary

	Cases					
	Valid		Missing		Total	
	N	Percent	N	Percent	N	Percent
MIN_Y_N * ALA_Y_N	474	100.0%	0	.0%	474	100.0%

MIN_Y_N * ALA_Y_N Crosstabulation

			ALA_Y_N		
			wt	11Ala	Total
MIN_Y_N	no	Count	350	39	389
		Expected Count	348.0	41.0	389.0
	yes	Count	74	11	85
		Expected Count	76.0	9.0	85.0
Total		Count	424	50	474
		Expected Count	424.0	50.0	474.0

Chi-Square Tests

	Value	df	Asymp. Sig. (2-sided)	Exact Sig. (2-sided)	Exact Sig. (1-sided)
Pearson Chi-Square	.628[b]	1	.428		
Continuity Correction[a]	.357	1	.550		
Likelihood Ratio	.599	1	.439		
Fisher's Exact Test				.437	.268
Linear-by-Linear Association	.627	1	.428		
N of Valid Cases	474				

a. Computed only for a 2x2 table

b. 0 cells (.0%) have expected count less than 5. The minimum expected count is 8.97.

Risk Estimate

	Value	95% Confidence Interval	
		Lower	Upper
Odds Ratio for MIN_Y_N (no / yes)	1.334	.653	2.726
For cohort ALA_Y_N = wt	1.033	.946	1.129
For cohort ALA_Y_N = 11Ala	.775	.414	1.450
N of Valid Cases	474		

Dataset 10

Case Processing Summary

	Cases					
	Valid		Missing		Total	
	N	Percent	N	Percent	N	Percent
MIN_Y_N * ALA_Y_N	474	100.0%	0	.0%	474	100.0%

MIN_Y_N * ALA_Y_N Crosstabulation

			ALA_Y_N		
			wt	11Ala	Total
MIN_Y_N	no	Count	362	37	399
		Expected Count	357.8	41.2	399.0
	yes	Count	63	12	75
		Expected Count	67.2	7.8	75.0
Total		Count	425	49	474
		Expected Count	425.0	49.0	474.0

Chi-Square Tests

	Value	df	Asymp. Sig. (2-sided)	Exact Sig. (2-sided)	Exact Sig. (1-sided)
Pearson Chi-Square	3.082[b]	1	.079		
Continuity Correction[a]	2.399	1	.121		
Likelihood Ratio	2.767	1	.096		
Fisher's Exact Test				.096	.066
Linear-by-Linear Association	3.076	1	.079		
N of Valid Cases	474				

a. Computed only for a 2x2 table

b. 0 cells (.0%) have expected count less than 5. The minimum expected count is 7.75.

Risk Estimate

	Value	95% Confidence Interval	
		Lower	Upper
Odds Ratio for MIN_Y_N (no / yes)	1.864	.922	3.768
For cohort ALA_Y_N = wt	1.080	.974	1.198
For cohort ALA_Y_N = 11Ala	.580	.317	1.059
N of Valid Cases	474		

Dataset 11

Case Processing Summary

	Cases					
	Valid		Missing		Total	
	N	Percent	N	Percent	N	Percent
MIN_Y_N * ALA_Y_N	474	100.0%	0	.0%	474	100.0%

MIN_Y_N * ALA_Y_N Crosstabulation

			ALA_Y_N		Total
			wt	11Ala	
MIN_Y_N	no	Count	362	35	397
		Expected Count	356.8	40.2	397.0
	yes	Count	64	13	77
		Expected Count	69.2	7.8	77.0
Total		Count	426	48	474
		Expected Count	426.0	48.0	474.0

Chi-Square Tests

	Value	df	Asymp. Sig. (2-sided)	Exact Sig. (2-sided)	Exact Sig. (1-sided)
Pearson Chi-Square	4.611[b]	1	.032		
Continuity Correction[a]	3.768	1	.052		
Likelihood Ratio	4.066	1	.044		
Fisher's Exact Test				.039	.031
Linear-by-Linear Association	4.602	1	.032		
N of Valid Cases	474				

a. Computed only for a 2x2 table

b. 0 cells (.0%) have expected count less than 5. The minimum expected count is 7.80.

Risk Estimate

	Value	95% Confidence Interval	
		Lower	Upper
Odds Ratio for MIN_Y_N (no / yes)	2.101	1.054	4.188
For cohort ALA_Y_N = wt	1.097	.987	1.219
For cohort ALA_Y_N = 11Ala	.522	.290	.940
N of Valid Cases	474		

Dataset 12

Case Processing Summary

	Cases					
	Valid		Missing		Total	
	N	Percent	N	Percent	N	Percent
MIN_Y_N * ALA_Y_N	474	100.0%	0	.0%	474	100.0%

MIN_Y_N * ALA_Y_N Crosstabulation

			ALA_Y_N		
			wt	11Ala	Total
MIN_Y_N	no	Count	356	38	394
		Expected Count	351.6	42.4	394.0
	yes	Count	67	13	80
		Expected Count	71.4	8.6	80.0
Total		Count	423	51	474
		Expected Count	423.0	51.0	474.0

Chi-Square Tests

	Value	df	Asymp. Sig. (2-sided)	Exact Sig. (2-sided)	Exact Sig. (1-sided)
Pearson Chi-Square	3.022[b]	1	.082		
Continuity Correction[a]	2.373	1	.123		
Likelihood Ratio	2.737	1	.098		
Fisher's Exact Test				.111	.066
Linear-by-Linear Association	3.015	1	.082		
N of Valid Cases	474				

a. Computed only for a 2x2 table

b. 0 cells (.0%) have expected count less than 5. The minimum expected count is 8.61.

Risk Estimate

	Value	95% Confidence Interval	
		Lower	Upper
Odds Ratio for MIN_Y_N (no / yes)	1.818	.919	3.594
For cohort ALA_Y_N = wt	1.079	.974	1.194
For cohort ALA_Y_N = 11Ala	.594	.332	1.062
N of Valid Cases	474		

Dataset 13

Case Processing Summary

	Cases					
	Valid		Missing		Total	
	N	Percent	N	Percent	N	Percent
MIN_Y_N * ALA_Y_N	474	100.0%	0	.0%	474	100.0%

MIN_Y_N * ALA_Y_N Crosstabulation

			ALA_Y_N		Total
			wt	11Ala	
MIN_Y_N	no	Count	354	39	393
		Expected Count	350.7	42.3	393.0
	yes	Count	69	12	81
		Expected Count	72.3	8.7	81.0
Total		Count	423	51	474
		Expected Count	423.0	51.0	474.0

Chi-Square Tests

	Value	df	Asymp. Sig. (2-sided)	Exact Sig. (2-sided)	Exact Sig. (1-sided)
Pearson Chi-Square	1.673[b]	1	.196		
Continuity Correction[a]	1.203	1	.273		
Likelihood Ratio	1.551	1	.213		
Fisher's Exact Test				.235	.137
Linear-by-Linear Association	1.670	1	.196		
N of Valid Cases	474				

a. Computed only for a 2x2 table

b. 0 cells (.0%) have expected count less than 5. The minimum expected count is 8.72.

Risk Estimate

	Value	95% Confidence Interval	
		Lower	Upper
Odds Ratio for MIN_Y_N (no / yes)	1.579	.787	3.168
For cohort ALA_Y_N = wt	1.057	.960	1.165
For cohort ALA_Y_N = 11Ala	.670	.367	1.222
N of Valid Cases	474		

Dataset 14

Case Processing Summary

	Cases					
	Valid		Missing		Total	
	N	Percent	N	Percent	N	Percent
MIN_Y_N * ALA_Y_N	474	100.0%	0	.0%	474	100.0%

MIN_Y_N * ALA_Y_N Crosstabulation

			ALA_Y_N		
			wt	11Ala	Total
MIN_Y_N	no	Count	363	33	396
		Expected Count	357.6	38.4	396.0
	yes	Count	65	13	78
		Expected Count	70.4	7.6	78.0
Total		Count	428	46	474
		Expected Count	428.0	46.0	474.0

Chi-Square Tests

	Value	df	Asymp. Sig. (2-sided)	Exact Sig. (2-sided)	Exact Sig. (1-sided)
Pearson Chi-Square	5.164[b]	1	.023		
Continuity Correction[a]	4.257	1	.039		
Likelihood Ratio	4.518	1	.034		
Fisher's Exact Test				.034	.024
Linear-by-Linear Association	5.153	1	.023		
N of Valid Cases	474				

a. Computed only for a 2x2 table

b. 0 cells (.0%) have expected count less than 5. The minimum expected count is 7.57.

Risk Estimate

	Value	95% Confidence Interval	
		Lower	Upper
Odds Ratio for MIN_Y_N (no / yes)	2.200	1.099	4.404
For cohort ALA_Y_N = wt	1.100	.992	1.220
For cohort ALA_Y_N = 11Ala	.500	.276	.906
N of Valid Cases	474		

Dataset 15

Case Processing Summary

	Cases					
	Valid		Missing		Total	
	N	Percent	N	Percent	N	Percent
MIN_Y_N * ALA_Y_N	474	100.0%	0	.0%	474	100.0%

MIN_Y_N * ALA_Y_N Crosstabulation

			ALA_Y_N		
			wt	11Ala	Total
MIN_Y_N	no	Count	356	42	398
		Expected Count	352.7	45.3	398.0
	yes	Count	64	12	76
		Expected Count	67.3	8.7	76.0
Total		Count	420	54	474
		Expected Count	420.0	54.0	474.0

Chi-Square Tests

	Value	df	Asymp. Sig. (2-sided)	Exact Sig. (2-sided)	Exact Sig. (1-sided)
Pearson Chi-Square	1.734[b]	1	.188		
Continuity Correction[a]	1.254	1	.263		
Likelihood Ratio	1.603	1	.206		
Fisher's Exact Test				.235	.133
Linear-by-Linear Association	1.730	1	.188		
N of Valid Cases	474				

a. Computed only for a 2x2 table

b. 0 cells (.0%) have expected count less than 5. The minimum expected count is 8.66.

Risk Estimate

	Value	95% Confidence Interval	
		Lower	Upper
Odds Ratio for MIN_Y_N (no / yes)	1.589	.794	3.183
For cohort ALA_Y_N = wt	1.062	.958	1.177
For cohort ALA_Y_N = 11Ala	.668	.369	1.209
N of Valid Cases	474		

Dataset 16

Case Processing Summary

	Cases					
	Valid		Missing		Total	
	N	Percent	N	Percent	N	Percent
MIN_Y_N * ALA_Y_N	474	100.0%	0	.0%	474	100.0%

MIN_Y_N * ALA_Y_N Crosstabulation

			ALA_Y_N		
			wt	11Ala	Total
MIN_Y_N	no	Count	356	39	395
		Expected Count	351.7	43.3	395.0
	yes	Count	66	13	79
		Expected Count	70.3	8.7	79.0
Total		Count	422	52	474
		Expected Count	422.0	52.0	474.0

Chi-Square Tests

	Value	df	Asymp. Sig. (2-sided)	Exact Sig. (2-sided)	Exact Sig. (1-sided)
Pearson Chi-Square	2.920[b]	1	.087		
Continuity Correction[a]	2.285	1	.131		
Likelihood Ratio	2.650	1	.104		
Fisher's Exact Test				.112	.070
Linear-by-Linear Association	2.914	1	.088		
N of Valid Cases	474				

a. Computed only for a 2x2 table

b. 0 cells (.0%) have expected count less than 5. The minimum expected count is 8.67.

Risk Estimate

	Value	95% Confidence Interval	
		Lower	Upper
Odds Ratio for MIN_Y_N (no / yes)	1.798	.910	3.551
For cohort ALA_Y_N = wt	1.079	.973	1.196
For cohort ALA_Y_N = 11Ala	.600	.336	1.071
N of Valid Cases	474		

Dataset 17

Case Processing Summary

	Cases					
	Valid		Missing		Total	
	N	Percent	N	Percent	N	Percent
MIN_Y_N * ALA_Y_N	474	100.0%	0	.0%	474	100.0%

MIN_Y_N * ALA_Y_N Crosstabulation

			ALA_Y_N		
			wt	11Ala	Total
MIN_Y_N	no	Count	359	37	396
		Expected Count	355.9	40.1	396.0
	yes	Count	67	11	78
		Expected Count	70.1	7.9	78.0
Total		Count	426	48	474
		Expected Count	426.0	48.0	474.0

Chi-Square Tests

	Value	df	Asymp. Sig. (2-sided)	Exact Sig. (2-sided)	Exact Sig. (1-sided)
Pearson Chi-Square	1.622[b]	1	.203		
Continuity Correction[a]	1.141	1	.285		
Likelihood Ratio	1.496	1	.221		
Fisher's Exact Test				.218	.143
Linear-by-Linear Association	1.618	1	.203		
N of Valid Cases	474				

a. Computed only for a 2x2 table

b. 0 cells (.0%) have expected count less than 5. The minimum expected count is 7.90.

Risk Estimate

	Value	95% Confidence Interval	
		Lower	Upper
Odds Ratio for MIN_Y_N (no / yes)	1.593	.774	3.279
For cohort ALA_Y_N = wt	1.055	.959	1.161
For cohort ALA_Y_N = 11Ala	.663	.354	1.241
N of Valid Cases	474		

Dataset 18

Case Processing Summary

	Cases					
	Valid		Missing		Total	
	N	Percent	N	Percent	N	Percent
MIN_Y_N * ALA_Y_N	474	100.0%	0	.0%	474	100.0%

MIN_Y_N * ALA_Y_N Crosstabulation

			ALA_Y_N		Total
			wt	11Ala	
MIN_Y_N	no	Count	352	40	392
		Expected Count	349.0	43.0	392.0
	yes	Count	70	12	82
		Expected Count	73.0	9.0	82.0
Total		Count	422	52	474
		Expected Count	422.0	52.0	474.0

Chi-Square Tests

	Value	df	Asymp. Sig. (2-sided)	Exact Sig. (2-sided)	Exact Sig. (1-sided)
Pearson Chi-Square	1.363[b]	1	.243		
Continuity Correction[a]	.947	1	.331		
Likelihood Ratio	1.273	1	.259		
Fisher's Exact Test				.246	.164
Linear-by-Linear Association	1.360	1	.244		
N of Valid Cases	474				

a. Computed only for a 2x2 table

b. 0 cells (.0%) have expected count less than 5. The minimum expected count is 9.00.

Risk Estimate

	Value	95% Confidence Interval	
		Lower	Upper
Odds Ratio for MIN_Y_N (no / yes)	1.509	.753	3.020
For cohort ALA_Y_N = wt	1.052	.956	1.157
For cohort ALA_Y_N = 11Ala	.697	.383	1.270
N of Valid Cases	474		

Dataset 19

Case Processing Summary

	Cases					
	Valid		Missing		Total	
	N	Percent	N	Percent	N	Percent
MIN_Y_N * ALA_Y_N	474	100.0%	0	.0%	474	100.0%

MIN_Y_N * ALA_Y_N Crosstabulation

			ALA_Y_N		
			wt	11Ala	Total
MIN_Y_N	no	Count	360	34	394
		Expected Count	354.9	39.1	394.0
	yes	Count	67	13	80
		Expected Count	72.1	7.9	80.0
Total		Count	427	47	474
		Expected Count	427.0	47.0	474.0

Chi-Square Tests

	Value	df	Asymp. Sig. (2-sided)	Exact Sig. (2-sided)	Exact Sig. (1-sided)
Pearson Chi-Square	4.323[b]	1	.038		
Continuity Correction[a]	3.512	1	.061		
Likelihood Ratio	3.833	1	.050		
Fisher's Exact Test				.062	.036
Linear-by-Linear Association	4.314	1	.038		
N of Valid Cases	474				

a. Computed only for a 2x2 table

b. 0 cells (.0%) have expected count less than 5. The minimum expected count is 7.93.

Risk Estimate

	Value	95% Confidence Interval	
		Lower	Upper
Odds Ratio for MIN_Y_N (no / yes)	2.054	1.030	4.097
For cohort ALA_Y_N = wt	1.091	.986	1.207
For cohort ALA_Y_N = 11Ala	.531	.294	.960
N of Valid Cases	474		

Dataset 20

Case Processing Summary

	Cases					
	Valid		Missing		Total	
	N	Percent	N	Percent	N	Percent
MIN_Y_N * ALA_Y_N	474	100.0%	0	.0%	474	100.0%

MIN_Y_N * ALA_Y_N Crosstabulation

			ALA_Y_N		Total
			wt	11Ala	
MIN_Y_N	no	Count	352	40	392
		Expected Count	349.0	43.0	392.0
	yes	Count	70	12	82
		Expected Count	73.0	9.0	82.0
Total		Count	422	52	474
		Expected Count	422.0	52.0	474.0

Chi-Square Tests

	Value	df	Asymp. Sig. (2-sided)	Exact Sig. (2-sided)	Exact Sig. (1-sided)
Pearson Chi-Square	1.363[b]	1	.243		
Continuity Correction[a]	.947	1	.331		
Likelihood Ratio	1.273	1	.259		
Fisher's Exact Test				.246	.164
Linear-by-Linear Association	1.360	1	.244		
N of Valid Cases	474				

a. Computed only for a 2x2 table

b. 0 cells (.0%) have expected count less than 5. The minimum expected count is 9.00.

Risk Estimate

	Value	95% Confidence Interval	
		Lower	Upper
Odds Ratio for MIN_Y_N (no / yes)	1.509	.753	3.020
For cohort ALA_Y_N = wt	1.052	.956	1.157
For cohort ALA_Y_N = 11Ala	.697	.383	1.270
N of Valid Cases	474		

References

Alliston, T., Choy, L., Ducy, P., Karsenty, G. and Derynck, R. (2001). TGF-β-induced repression of CBFA1 by Smad3 decreases cbfa1 and osteocalcin expression and inhibits osteoblast differentiation. *EMBO J* **20**: 2254–2272.

Andrew, T. and Macgregor, A.J. (2005). Genes and osteoporosis. *Curr Osteoporos Rep* **2:**79-89.

Afzal, F., Pratap, J., Ito, K., Ito, Y., Stein, J.L., van Wijnen, A.J., Stein, G.S., Lian, J.B. and Javed, A. (2005). Smad function and intranuclear targeting share a Runx2 motif required for osteogenic lineage induction and BMP2 responsive transcription. *J Cell Physiol* **204:**63-72.

Ammann, P. and Rizzoli, R. (2003). Bone strength and its determinants. *Osteoporos Int* **14 Suppl 3:** S13-18.

Archer, C.W. and Francis-West, P. (2003). The chondrocyte. *Int J Biochem Cell Biol* **35**:401-404.

Aronson, B.D., Fisher, A.L., Blechman, K., Caudy, M., and Gergen, J.P. (1997). Groucho-dependent and -independent repression activities of Runt domain proteins. *Mol Cell Biol* **17**:5581-5587.

Atik, O.S., Gunal, I. and Korkusuz, F. (2006). Burden of Osteoporosis. *Clin Orthop Relat Res* **443:**19-24.

Banerjee, C., Javed, A., Choi, J.Y., Green, J., Rosen, V., van Wijnen, A.J., Stein, J.L., Lian, J.B. and Stein, G.S. (2001). *Endocrinology* **142**:4026-4039.

Banerjee, C., Javed, A., Choi, J.Y., Green, J., Rosen, V., van Wijnen, A.J., Stein, J.L., Lian, J.B., Stein, G.S. (2001). Differential regulation of the two principal Runx2/Cbfa1 n-terminal isoforms in response to bone morphogenetic protein-2 during development of the osteoblast phenotype. *Endocrinology* **142**: 4026-4039.

Birkedal-Hansen, H., Moore, W.G., Bodden, M.K., Windsor, L.J., Birkedal-Hansen, B., DeCarlo, A. and Engler, J.A. (1993). Matrix metalloproteinases: a review. *Crit Rev Oral Biol Med* **4:**197-250.

Borden, P., Solymar, D., Sucharczuk, A., Lindman, B., Cannon, P. and Heller, R.A. (1996). Cytokine control of interstitial collagenase and collagenase-3 gene expression in human chondrocytes. *J Biol Chem* **271:**23577-23581.

Cao, X. and Chen, D. (2005). The BMP signaling and in vivo bone formation. *Gene* **357:**1-8.

Charron, J., Malynn. B.A., Fisher, P., Stewart, V., Jeannotte, L., Goff, S.P., Robertson, E.J. and Alt, F.W. (1992). Embryonic lethality in mice homozygous for a targeted disruption of the N-myc gene. *Genes Dev* **6:**2248-22457.

Chen, D., Zhao, M. and Mundy, G.R. (2004). Bone morphogenetic proteins. *Growth Factors* **22:**233-241.

Coffman, J.A. (2003). Runx transcription factors and the developmental balance between cell proliferation and differentiation. *Cell Biol Int* **27:**315-324.

Cummings, C.J. and Zoghbi, H.Y. (2000) Fourteen and counting: unraveling trinucleotide repeat diseases. *Hum Mol Genet* **9**:909-916.

D'Alonzo, R.C., Kowalski, A.J., Denhardt, D.T., Nickols, G.A. and Partridge, N.C. (2002). Regulation of collagenase-3 and osteocalcin gene expression by collagen and osteopontin in differentiating MC3T3-E1 cells. *J Biol Chem* **277:**24788-24798.

Deng, H.W., Xu, F.H., Huang, Q.Y., Shen, H., Deng, H., Conway, T., Liu, Y.J., Liu, Y.Z., Li, J.L., Zhang, H.T., Davies, K.M. and Recker, R.R. (2002). A whole-genome linkage scan suggests several genomic regions potentially containing quantitative trait loci for osteoporosis. *J Clin Endocrinol Metab* **87:**5151-5159.

Denley, A., Cosgrove, L.J., Booker, G.W., Wallace, J.C. and Forbes, B.E. (2005). Molecular interactions of the IGF system. *Cytokine Growth Factor Rev* **16:**421-439.

Deuel, T.F., Zhang, N., Yeh, H.J., Silos-Santiago, I. and Wang, Z.Y. (2002). Pleiotrophin: a cytokine with diverse functions and a novel signaling pathway. *Arch Biochem Biophys* **397:**162-171.

Di Prospero, N.A. and Fischbeck, F.H. (2005) Therapeutics development for triplet repeat expansion diseases. *Nat Rev Genet* **6**:729-742.

Dick, I. M., Devine, A., Marangou, A., Dhaliwal, S. S., Laws, S., Martins, R. N. and Prince, R. L. (2002) Apolipoprotein E4 is associated with reduced calcaneal quantitative ultrasound measurements and bone mineral density in elderly women. *Bone* **31:** 497-502.

Doecke, J.D., Day, C.J., Stephens, A.S., Carter, S.L., van Daal, A., Kotowicz, M.A., Nicholson, G.C. and Morrison, N.A. (2006). Association of Functionally Different RUNX2 P2 Promoter Alleles With BMD. *J Bone Miner Res* **21:**265-273.

Drissi, H., Luc, Q., Shakoori, R., Chuva, De Sousa Lopes S., Choi, J.Y., Terry, A., Hu, M., Jones, S., Neil, J.C., Lian, J.B., Stein, J.L., Van Wijnen, A.J. and Stein, G.S. (2000). Transcriptional autoregulation of the bone related CBFA1/RUNX2 gene. *J Cell Physiol* **184**: 341-350.

Drissi, H., Pouliot, A., Koolloos, C., Stein, J.L., Lian, J.B., Stein, G.S. and van Wijnen, A.J. (2002). 1,25-(OH)2-vitamin D3 suppresses the bone-related Runx2/Cbfa1 gene promoter. *Exp Cell Res* **274**: 323-333.

Dyer, B.W., Ferrer, F.A., Klinedinst, D.K. and Rodriguez, R. (2000) A noncommercial dual luciferase enzyme assay system for reporter gene analysis. *Anal Biochem* **282** :158-161.

Ducy, P. and Karsenty, G. (1995). Two distinct osteoblast-specific cis-acting elements control expression of a mouse osteocalcin gene. *Mol Cell Biol* **15**:1858-1869.

Ducy, P., Geoffroy, V. and Karsenty, G. (1996). Study of osteoblast-specific expression of one mouse osteocalcin gene: characterization of the factor binding to OSE2. *Connect Tissue Res* **35**:7-14.

Ducy, P., Desbois, C., Boyce, B., Pinero, G., Story, B., Dunstan, C., Smith, E., Bonadio, J., Goldstein, S., Gundberg, C., Bradley, A. and Karsenty, G. (1996). Increased bone formation in osteocalcin-deficient mice. *Nature* **382:**448-452.

Ducy, P., Zhang, R., Geoffroy, V., Ridall, A.L. and Karsenty, G. (1997). Osf2/Cbfa1: a transcriptional activator of osteoblast differentiation. *Cell* **89**:747-754.

Ducy, P. and Karsenty, G. (1998). Genetic control of cell differentiation in the skeleton. *Curr Opin Cell Biol* **10**:614-619.

Ducy, P. and Karsenty, G. (2000). The family of bone morphogenetic proteins. *Kidney Int* **57:**2207-2214.

Ducy, P., Schinke, T. and Karsenty, G. (2000). The osteoblast: a sophisticated fibroblast under central surveillance. *Science* **289:**1501-1504.

Durst, K.L. and Hiebert, S.W. (2004) Role of RUNX family members in transcriptional repression and gene silencing. *Oncogene* **23:**4220-4224.

Enomoto, H., Enomoto-Iwamoto, M., Iwamoto, M., Nomura, S., Himeno, M., Kitamura, Y., Kishimoto, T. and Komori, T. (2000). Cbfa1 is a positive regulatory factor in chondrocyte maturation. *J Biol Chem* **275**:8695-8702.

Fleetwood, A.J., Cook, A.D. and Hamilton, J.A. (2005). Functions of granulocyte-macrophage colony-stimulating factor. *Crit Rev Immunol* **25:**405-428.

Franceschi, R.T., Iyer, B.S. and Cui, Y. (1994). Effects of ascorbic acid on collagen matrix formation and osteoblast differentiation in murine MC3T3-E1 cells. *J Bone Miner Res* **9:**843-854.

Franceschi, R.T. and Iyer, B.S. (1992). Relationship between collagen synthesis and expression of the osteoblast phenotype in MC3T3-E1 cells. *J Bone Miner Res* **7:**235-246.

Franz-Odendaal, T,A., Hall, B.K. and Witten, P.E. (2005). Buried alive: How osteoblasts become osteocytes. *Dev Dyn* **235:**176-190.

Fujisawa, T., Kato, Y., Nagase, H., Atsuta, J., Terada, A., Iguchi, K., Kamiya, H., Morita, Y., Kitaura, M., Kawasaki, H., Yoshie, O. and Hirai, K. (2000). Chemokines induce eosinophil degranulation through CCR-3. *J Allergy Clin Immunol* **106:**507-513.

Fujiwara, M., Tagashira, S., Harada, H., Ogawa, S., Katsumata, T., Nakatsuka, M., Komori, T. and Takada, H. (1999). Isolation and characterization of the distal promoter region of mouse Cbfa1. *Biochim Biophys Acta* **1446**: 265-272.

Fuks, F. (2005). DNA methylation and histone modifications: teaming up to silence genes. *Curr Opin Genet Dev* **15:**490-495.

Garcia-Giralt, N., Nogues, X., Enjuanes, A., Puig, J., Mellibovsky, L., Bay-Jensen, A., Carreras, R., Balcells, S., Diez-Perez, A. and Grinberg, D. (2002). Two new single-nucleotide polymorphisms in the COL1A1 upstream regulatory region and their relationship to bone mineral density. *J Bone Miner Res* **17:**384-393.

Garcia-Zepeda, E.A., Rothenberg, M.E., Ownbey, R.T., Celestin, J., Leder, P. and Luster, A.D. (1996). Human eotaxin is a specific chemoattractant for eosinophil cells and provides a new mechanism to explain tissue eosinophilia. *Nat Med* **2:**449-456.

Garnero, P., Munoz, F., Borel, O., Sornay-Rendu, E. and Delmas P.D. (2005). Vitamin D receptor gene polymorphisms are associated with the risk of fractures in postmenopausal women, independently of bone mineral density. *J Clin Endocrinol Metab* **90:**4829-4835.

Gatchel, J.R. and Zoghbi, Y.Z. (2005) Diseases of unstable repeat expansion: mechanisms and common principles. *Nat Rev Genet* **6**:743-755.

Gaur, T., Lengner, C.J., Hovhannisyan, H., Bhat, R.A., Bodine, P.V., Komm, B.S., Javed, A., van Wijnen, A.J., Stein, J.L., Stein, G.S. and Lian, J.B. (2005). Canonical WNT signaling promotes osteogenesis by directly stimulating Runx2 gene expression. *J Biol Chem* **280:**33132-33140.

Geoffroy, V., Corral, D.A., Zhou, L., Lee, B., and Karsenty, G. (1998). Genomic organization, expression of the human CBFA1 gene, and evidence for an alternative splicing event affecting protein function. *Mamm Genome* **9**:54-57.

Geoffroy. V., Ducy, P. and Karsenty, G. (1995). A PEBP2 alpha/AML-1-related factor increases osteocalcin promoter activity through its binding to an osteoblast-specific cis-acting element. *J Biol Chem* **270**:30973-30979.

Gilbert, L., He, X., Farmer, P., Rubin, J., Drissi, H., van Wijnen, A.J., Lian, J.B., Stein, G.S. and Nanes, M.S. (2002). Expression of the osteoblast differentiation factor RUNX2 (Cbfa1/AML3/Pebp2alpha A) is inhibited by tumor necrosis factor-alpha. *J Biol Chem* **277**: 2695-2701.

Grant, S.F., Reid, D.M., Blake, G., Herd, R., Fogelman, I. and Ralston SH. (1996). Reduced bone density and osteoporosis associated with a polymorphic Sp1 binding site in the collagen type I alpha 1 gene. *Nat Genet* **14:**203-205.

Gronowicz, G.A., McCarthy, M.B., Zhang, H. and Zhang, W. (2004). Insulin-like growth factor II induces apoptosis in osteoblasts. *Bone* **35:**621-628.

Hanai, J., Chen, L.F., Kanno, T., Ohtani-Fujita, N., Kim, W.Y., Guo, W.H,. Imamura, T., Ishidou, Y., Fukuchi, M., Shi, M.J., Stavnezer, J., Kawabata, M., Miyazono, K. and Ito, Y. (1999). Interaction and functional cooperation of PEBP2/CBF with Smads. Synergistic induction of the immunoglobulin germline Calpha promoter. *J Biol Chem* **274:**31577-31582.

Harada, S., Matsumoto, T. and Ogata, E. (1991). Role of ascorbic acid in the regulation of proliferation in osteoblast-like MC3T3-E1 cells. *J Bone Miner Res* **6:**903-908.

Harada, H., Tagashira, S., Fujiwara, M., Ogawa, S., Katsumata, T., Yamaguchi, A., Komori, T., and Nakatsuka, M. (1999). Cbfa1 isoforms exert functional differences in osteoblast differentiation. *J Biol Chem* **274**:6972-6978.

Hayden, J.M., Mohan, S. and Baylink, D.J. (1995). The insulin-like growth factor system and the coupling of formation to resorption. *Bone* **17:**93S-98S.

Henry, M.J., Pasco, J.A., Seeman, E., Nicholson, G.C., Sanders, K.M. and Kotowicz, M.A. (2002). Fracture thresholds revisited. Geelong Osteoporosis Study. *J Clin Epidemiol* **55:**642-646.

Hess, J., Porte, D., Munz, C. and Angel, P. (2001). AP-1 and Cbfa/runt physically interact and regulate parathyroid hormone-dependent MMP13 expression in osteoblasts through a new osteoblast-specific element 2/AP-1 composite element. *J Biol Chem* **276:**20029-20038.

Hill, P.A., Reynolds, J.J. and Meikle, M.C. (1995). Osteoblasts mediate insulin-like growth factor-I and -II stimulation of osteoclast formation and function. *Endocrinology* **136:**124-131.

Hodge, J.M., Kirkland, M.A., Aitken, C.J., Waugh, C.M., Myers, D.E., Lopez, C.M., Adams, B.E. and Nicholson, G.C. (2004). Osteoclastic potential of human CFU-GM: biphasic effect of GM-CSF. *J Bone Miner Res* **19:**190-199.

Hurlin, P.J. (2005). N-myc functions in transcription and development. *Birth Defects Res C Embryo Today* **75:**340-352.

Inada, M., Wang, Y., Byrne, M.H., Rahman, M.U., Miyaura, C., Lopez-Otin, C. and Krane, S.M. (2004). Critical roles for collagenase-3 (Mmp13) in development of

growth plate cartilage and in endochondral ossification. *Proc Natl Acad Sci U S A* **101:**17192-17197.

Jackson, M., Baird, J.W., Cambray, N., Ansell, J.D., Forrester, L.M. and Graham, G.J. (2002). Cloning and characterization of Ehox, a novel homeobox gene essential for embryonic stem cell differentiation. *J Biol Chem* **277:**38683-38692.

Jackson, M., Baird, J.W., Nichols, J., Wilkie, R., Ansell, J.D., Graham, G. and Forrester, L.M. (2003). Expression of a novel homeobox gene Ehox in trophoblast stem cells and pharyngeal pouch endoderm. *Dev Dyn* **228:**740-744.

Javed, A., Guo, B., Hiebert, S., Choi, J.Y., Green, J., Zhao, S.C., Osborne, M.A., Stifani, S., Stein, J.L., Lian, J.B., van Wijnen, A.J. and Stein, G.S. (2000). Groucho/TLE/R-esp proteins associate with the nuclear matrix and repress RUNX (CBF(alpha)/AML/PEBP2(alpha)) dependent activation of tissue-specific gene transcription. *J Cell Sci* **113**:2221-2231.

Jilka, R.L. (2003). Biology of the basic multicellular unit and the pathophysiology of osteoporosis. *Med Pediatr Oncol* **41**:182-185.

Jimenez, M.J., Balbin, M., Lopez, J.M., Alvarez, J., Komori, T. and Lopez-Otin, C. (1999). Collagenase 3 is a target of Cbfa1, a transcription factor of the runt gene family involved in bone formation. *Mol Cell Biol* **19:**4431-4442.

Johansson, N., Saarialho-Kere, U., Airola, K., Herva, R., Nissinen, L., Westermarck, J., Vuorio, E., Heino, J. and Kahari, V.M. (1997). Collagenase-3 (MMP-13) is expressed by hypertrophic chondrocytes, periosteal cells, and osteoblasts during human fetal bone development. *Dev Dyn* **208:**387-397.

Kammerer, C.M., Schneider, J.L., Cole, S.A., Hixson, J.E., Samollow, P.B., O'Connell, J.R., Perez, R., Dyer, T.D., Almasy, L., Blangero, J., Bauer, R.L. and Mitchell, B.D. (2003). Quantitative trait loci on chromosomes 2p, 4p, and 13q influence bone mineral density of the forearm and hip in Mexican Americans. *J Bone Miner Res* **18:**2245-2252.

Kanis, J.A. (2002). Diagnosis of osteoporosis and assessment of fracture risk. *Lancet* **359:**1929-1936.

Kanis, J.A., Melton, L.J. 3rd., Christiansen, C., Johnston, C.C. and Khaltaev, N. (1994). The diagnosis of osteoporosis. *J Bone Miner Res* **9:**1137-1141.

Karasik, D., Myers, R.H., Cupples, L.A., Hannan, M.T., Gagnon, D.R., Herbert, A. and Kiel, D.P. (2002). Genome screen for quantitative trait loci contributing to normal variation in bone mineral density: the Framingham Study. *J Bone Miner Res* **17:**1718-1727.

Karsenty, G. (1999). The genetic transformation of bone biology. *Genes Dev* **13**:3037-3051.

Karsenty, G. (2001). Minireview: transcriptional control of osteoblast differentiation. *Endocrinology* **142**:2731-2733.

Katagiri, T., Yamaguchi, A., Komaki, M., Abe, E., Takahashi, N., Ikeda, T., Rosen, V., Wozney, J.M., Fujisawa-Sehara, A. and Suda, T. (1994). Bone morphogenetic protein-2 converts the differentiation pathway of C2C12 myoblasts into the osteoblast lineage. *J Cell Biol* **127:**1755-1766.

Kawano, Y. and Kypta, R. (2003). Secreted antagonists of the Wnt signalling pathway. *J Cell Sci* **116:**2627-2634.

Khan, S.N. and Lane, J.M. (2004). The use of recombinant human bone morphogenetic protein-2 (rhBMP-2) in orthopaedic applications. *Expert Opin Biol Ther* **4:**741-748.

Khandwala, H.M., McCutcheon, I.E., Flyvbjerg, A. and Friend, K.E. (2000). The effects of insulin-like growth factors on tumorigenesis and neoplastic growth. *Endocr Rev* **21:**215-244.

Kim, H.J., Nam, S.H., Kim, H.J., Park, H.S., Ryoo, H.M., Kim. S.Y., Cho, T.J., Kim, S.G., Bae, S.C., Kim, I.S., Stein, J.L., van Wijnen, A.J., Stein, G.S., Lian, J.B. and Choi, J.Y. (2005). Four novel RUNX2 mutations including a splice donor site result in the cleidocranial dysplasia phenotype. *J Cell Physiol* **207:**114-122.

Kim, I.S., Otto, F., Zabel, B. and Mundlos, S. (1999) Regulation of chondrocyte differentiation by Cbfa1. *Mech Dev* **80**:159-170.

Kim, M.S., Day, C.J. and Morrison, N.A. (2005). MCP-1 is induced by receptor activator of nuclear factor-{kappa}B ligand, promotes human osteoclast fusion, and rescues granulocyte macrophage colony-stimulating factor suppression of osteoclast formation. *J Biol Chem* **280:**16163-16169.

Kim, M.S., Day, C.J., Selinger, C.I., Magno, C.L., Stephens, S.R. and Morrison, N.A. (2006). MCP-1-induced human osteoclast-like cells are tartrate-resistant acid phosphatase, NFATc1, and calcitonin receptor-positive but require receptor activator of NFkappaB ligand for bone resorption. *J Biol Chem* **281:**1274-1285.

Knothe Tate, M.L., Adamson, J.R., Tami, A.E. and Bauer, T.W. (2004). The osteocyte. *Int J Biochem Cell Biol* **36**:1-8.

Koay, M.A., Woon, P.Y., Zhang, Y., Miles, L.J., Duncan, E.L., Ralston, S.H., Compston, J.E., Cooper, C., Keen, R., Langdahl, B.L., MacLelland, A., O'Riordan, J., Pols, H.A., Reid, D.M., Uitterlinden, A.G., Wass, J.A. and Brown, M.A. (2004). Influence of LRP5 polymorphisms on normal variation in BMD. *J Bone Miner Res* **19:**1619-1627.

Kobayashi, T. and Kronenberg, H. (2005). Minireview: transcriptional regulation in development of bone. *Endocrinology* **146**:1012-1017.

Koller, D.L., Econs, M.J., Morin, P.A., Christian, J.C., Hui, S.L., Parry, P., Curran, M.E., Rodriguez, L.A., Conneally, P.M., Joslyn, G., Peacock, M., Johnston, C.C. and Foroud, T. (2000) Genome screen for QTLs contributing to normal variation in bone mineral density and osteoporosis. *J Clin Endocrinol Metab* **85:**3116-3120

Komori, T., Yagi, H., Nomura, S., Yamaguchi, A., Sasaki, K., Deguchi, K., Shimizu, Y., Bronson, R.T., Gao, Y.H., Inada ,M., Sato, M., Okamoto, R., Kitamura, Y., Yoshiki, S. and Kishimoto, T. (1997). Targeted disruption of Cbfa1 results in a complete lack of bone formation owing to maturational arrest of osteoblasts. *Cell* **89**:755-764.

Lamkhioued, B., Abdelilah, S.G., Hamid, Q., Mansour, N., Delespesse, G. and Renzi, P.M. (2003). The CCR3 receptor is involved in eosinophil differentiation and is up-regulated by Th2 cytokines in CD34+ progenitor cells. *J Immunol* **170:**537-547.

Langdahl, B.L., Carstens, M., Stenkjaer, L. and Eriksen, E.F. (2002). Polymorphisms in the osteoprotegerin gene are associated with osteoporotic fractures. *J Bone Miner Res* **17:**1245-1255.

Langdahl, B.L., Kassem, M., Moller, M.K. and Eriksen, E.F. (1998). The effects of IGF-I and IGF-II on proliferation and differentiation of human osteoblasts and interactions with growth hormone. *Eur J Clin Invest* **28:**176-183.

Lean, J.M., Murphy, C., Fuller, K. and Chambers, T.J. (2002). CCL9/MIP-1gamma and its receptor CCR1 are the major chemokine ligand/receptor species expressed by osteoclasts. *J Cell Biochem* **87:**386-393.

Lee, B., Thirunavukkarasu, K., Zhou, L., Pastore, L., Baldini, A., Hecht, J., Geoffroy, V., Ducy, P. and Karsenty, G. (1997). Missense mutations abolishing DNA binding of the osteoblast-specific transcription factor OSF2/CBFA1 in cleidocranial dysplasia. *Nat Genet* **16**:307-310.

Lee, K.S., Kim, H.J., Li, Q.L., Chi, X.Z., Ueta, C., Komori, T., Wozney, J.M., Kim, E.G., Choi, J.Y., Ryoo, H.M. and Bae, S.C. (2000). Runx2 is a common target of transforming growth factor beta1 and bone morphogenetic protein 2, and cooperation between Runx2 and Smad5 induces osteoblast-specific gene expression in the pluripotent mesenchymal precursor cell line C2C12. *Mol Cell Biol* **20:**8783-8792.

Lee, M.H., Javed, A., Kim, H.J., Shin, H.I., Gutierrez, S., Choi, J.Y., Rosen, V., Stein, J.L., van Wijnen, A.J., Stein, G.S., Lian, J.B. and Ryoo, H.M. (1999). Transient upregulation of CBFA1 in response to bone morphogenetic protein-2 and transforming growth factor beta1 in C2C12 myogenic cells coincides with suppression of the myogenic phenotype but is not sufficient for osteoblast differentiation. *J Cell Biochem* **73**: 114-125.

Lee, M.H., Kim, Y.J., Kim, H.J., Park, H.D., Kang, A.R., Kyung, H.M., Sung, J.H., Wozney, J.M., Kim, H.J. and Ryoo, H.M. (2003). BMP-2-induced Runx2 expression is mediated by Dlx5, and TGF-beta 1 opposes the BMP-2-induced osteoblast differentiation by suppression of Dlx5 expression. *J Biol Chem* **278:**34387-34394.

Lefebvre, V. and Smits, P. (2005). Transcriptional control of chondrocyte fate and differentiation. *Birth Defects Res* **75**:200-212.

Lian, J.B. and Stein, G.S. (2003). Runx2/Cbfa1: a multifunctional regulator of bone formation. *Curr Pharm Des* **9:**2677-2685.

Liu, H., Holm, M., Xie, X.Q., Wolf-Watz, M. and Grundstrom, T. (2004). AML1/Runx1 recruits calcineurin to regulate granulocyte macrophage colony-stimulating factor by Ets1 activation. J Biol Chem **279:**29398-29408.

Livak, K.J. and Schmittgen, T.D. (2001). Analysis of relative gene expression data using real-time quantitative PCR and the 2(-Delta Delta C(T)) Method. *Methods* **25:**402-408.

MacDonald, H. M., McGuigan, F. A., New, S. A., Campbell, M. K., Golden, M. H., Ralston, S. H. and Reid, D. M. (2001) COL1A1 Sp1 polymorphism predicts perimenopausal and early postmenopausal spinal bone loss. *J Bone Miner Res* **16** : 1634-1641.

Mackie, E.J. (2003). Osteoblasts: novel roles in orchestration of skeletal architecture. *Int J Biochem Cell Biol* **35**:1301-1305.

Makovey, J., Naganathan, V. and Sambrook, P. (2005) Gender differences in relationships between body composition components, their distribution and bone mineral density: a cross-sectional opposite sex twin study. *Osteoporos Int* **16:**1495-1505.

Manolagas, S.C. (2000). Birth and death of bone cells: basic regulatory mechanisms and implications for the pathogenesis and treatment of osteoporosis. *Endocr Rev* **21**:115-137.

Martini, F. (1998). Fundamentals of Anatomy and Physiology, 4th edition. Prentice Hall, Inc. USA.

Massague, J., Seoane, J. and Wotton, D. (2005). Smad transcription factors. *Genes Dev* **19:**2783-2810.

Maurer, M. and von Stebut, E. (2004). Macrophage inflammatory protein-1. *Int J Biochem Cell Biol* **36:**1882-1886.

McLarren, K.W., Lo. R., Grbavec, D., Thirunavukkarasu, K., Karsenty, G. and Stifani, S. (2000). The mammalian basic helix loop helix protein HES-1 binds to and modulates the transactivating function of the runt-related factor Cbfa1. *J Biol Chem* **275**:530-538.

Mitsiadis, T.A., Salmivirta, M., Muramatsu, T., Muramatsu, H., Rauvala, H., Lehtonen, E., Jalkanen, M. and Thesleff, I. (1995). Expression of the heparin-binding cytokines, midkine (MK) and HB-GAM (pleiotrophin) is associated with epithelial-mesenchymal interactions during fetal development and organogenesis. *Development* **121:**37-51.

Miyamoto, T. and Suda, T. (2002). Differentiation and function of osteoclasts. *Keio J Med* **52**:1–7.

Miyamoto, T., Ohneda, O., Arai, F., Iwamoto, K., Okada, S., Takagi, K., Anderson, D.M. and Suda, T. (2001). Bifurcation of osteoclasts and dendritic cells from common progenitors. *Blood* **98:**2544-2554.

Modrowski, D., Lomri, A. and Marie, P.J. (1997). Endogenous GM-CSF is involved as an autocrine growth factor for human osteoblastic cells. *J Cell Physiol* **170:**35-46.

Mohan, S. (1993). Insulin-like growth factor binding proteins in bone cell regulation. *Growth Regul* **3:**67-70.

Morava, E., Karteszi, J., Weisenbach, J., Caliebe, A., Mundlos, S. and Mehes, K. (Cleidocranial dysplasia with decreased bone density and biochemical findings of hypophosphatasia. *Eur J Pediatr* **161**:619-622.

Morrison, N.A., Qi, J.C., Tokita, A., Kelly, P.J., Crofts, L., Nguyen, T.V., Sambrook, P.N. and Eisman, J.A. (1994). Prediction of bone density from vitamin D receptor alleles. *Nature* **367:**284-287.

Mundlos, S., Otto, F., Mundlos, C., Mulliken, J.B., Aylsworth, A.S., Albright, S., Lindhout ,D., Cole, W.G., Henn, W., Knoll, J.H., Owen, M.J., Mertelsmann, R., Zabel, B.U. and Olsen, B.R. (1997). Mutations involving the transcription factor CBFA1 cause cleidocranial dysplasia. *Cell* **89**:773-779.

Nakamura, H., Sato, G., Hirata, A. and Yamamoto, T. (2004). Immunolocalization of matrix metalloproteinase-13 on bone surface under osteoclasts in rat tibia. *Bone* **34:**48-56.

Nakashima, K., Zhou, X., Kunkel, G., Zhang, Z., Deng, J.M., Behringer, R.R. and de Crombrugghe, B. (2002). The novel zinc finger-containing transcription factor osterix is required for osteoblast differentiation and bone formation. *Cell* **108**:17-29.

Napierala, D., Garcia-Rojas, X., Sam, K., Wakui, K., Chen, C., Mendoza-Londono, R., Zhou, G., Zheng, Q. and Lee, B. (2005). Mutations and promoter SNPs in RUNX2, a transcriptional regulator of bone formation. *Mol Genet Metab* **86**:257-268.

Ogawa, E., Inuzuka, M., Maruyama, M., Satake, M., Naito-Fujimoto, M., Ito, Y. and Shigesada, K. (1993). Molecular cloning and characterization of PEBP2 beta, the heterodimeric partner of a novel Drosophila runt-related DNA binding protein PEBP2 alpha. *Virology*. **194**:314-331.

Okamatsu, Y., Kim, D., Battaglino, R., Sasaki, H., Spate, U. and Stashenko, P. (2004). MIP-1 gamma promotes receptor-activator-of-NF-kappa-B-ligand-induced osteoclast formation and survival. *J Immunol* **173:**2084-2090.

Olney, R.C., Wang, J., Sylvester, J.E. and Mougey, E.B. (2004). Growth factor regulation of human growth plate chondrocyte proliferation in vitro. *Biochem Biophys Res Commun* **317:**1171-1182.

Olsen, B.R., Reginato, A.M. and Wang, W. (2000). Bone development. *Annu Rev Cell Dev Biol* **16**:191-220.

Otto, F., Lubbert, M. and Stock, M. (2003). Upstream and downstream targets of RUNX proteins. *J Cell Biochem* **89:**9-18.

Otto, F., Thornell, A.P., Crompton ,T., Denzel, A., Gilmour, K.C., Rosewell, I.R., Stamp, G.W., Beddington, R.S., Mundlos, S., Olsen, B.R., Selby, P.B. and Owen, M.J. (1997). Cbfa1, a candidate gene for cleidocranial dysplasia syndrome, is essential for osteoblast differentiation and bone development. *Cell* **89**:765-771.

Paredes, R., Arriagada, G., Cruzat, F., Villagra, A., Olate, J., Zaidi, K., van Wijnen, A., Lian, J.B., Stein, G.S., Stein, J.L. and Montecino, M. (2004). Bone-specific transcription factor Runx2 interacts with the 1alpha,25-dihydroxyvitamin D3 receptor to up-regulate rat osteocalcin gene expression in osteoblastic cells. *Mol Cell Biol* **24:**8847-8861.

Park, M.H., Shin, H.I., Choi, J.Y., Nam, S.H., Kim, Y.J., Kim, H.J., and Ryoo, H.M. (2001). Differential expression patterns of Runx2 isoforms in cranial suture morphogenesis. *J Bone Miner Res* **16:**885-892.

Pelletier, N., Champagne, N., Stifani, S. and Yang, X.J. (2002). MOZ and MORF histone acetyltransferases interact with the Runt-domain transcription factor Runx2. *Oncogene* **21:**2729-2740.

Phimphilai, M., Zhao, Z., Boules, H., Roca, H. and Franceschi, R.T. (2006). BMP signaling is required for RUNX2-dependent induction of the osteoblast phenotype. J *Bone Miner Res* **21:**637-646.

Pocock, N.A., Eisman, J.A., Hopper, J.L., Yeates, M.G., Sambrook, P.N. and Eberl, S. (1987). Genetic determinants of bone mass in adults. A twin study. *J Clin Invest* **80:**706-710.

Pogoda, P., Priemel, M., Rueger, J.M. and Amling, M. (2005). Bone remodeling: new aspects of a key process that controls skeletal maintenance and repair. *Osteoporos Int* **Suppl 2:**S18-24.

Pope, S.M., Zimmermann, N., Stringer, K.F., Karow, M.L. and Rothenberg, M.E. (2005). The eotaxin chemokines and CCR3 are fundamental regulators of allergen-induced pulmonary eosinophilia. *J Immunol* **175:**5341-5350.

Provot, S. and Schipani, E. (2005). Molecular mechanisms of endochondral bone development. *Biochem Biophys Res Commun* **328**:658-665.

Quack, I., Vonderstrass, B., Stock, M., Aylsworth, A.S., Becker, A., Brueton, L., Lee, P.J., Majewski, F., Mulliken, J.B., Suri, M., Zenker, M., Mundlos, S. and Otto, F. (1999). Mutation analysis of core binding factor A1 in patients with cleidocranial dysplasia. *Am J Hum Genet* **65**:1268-1278.

Quarles, L.D., Yohay, D.A., Lever, L.W., Caton, R. and Wenstrup, R.J. (1992). Distinct proliferative and differentiated stages of murine MC3T3-E1 cells in culture: an in vitro model of osteoblast development. *J Bone Miner Res* **7:**683-692.

Ralston, S.H. (2003). Genetic determinants of susceptibility to osteoporosis. *Curr Opin Pharmacol* **3:**286-290.

Ralston, S.H. (2005). Genetic determinants of osteoporosis. *Curr Opin Rheumatol* **17:**475-479.

Ralston, S.H., Uitterlinden, A.G., Brandi, M.L., Balcells, S., Langdahl, B.L., Lips, P., Lorenc, R., Obermayer-Pietsch, B., Scollen, S., Bustamante, M., Husted, L.B., Carey, A.H., Diez-Perez, A., Dunning, A.M., Falchetti, A., Karczmarewicz, E., Kruk, M., van Leeuwen, J.P., van Meurs, J.B., Mangion, J., McGuigan, F.E., Mellibovsky, L., del Monte, F., Pols, H.A., Reeve, J., Reid, D.M., Renner, W., Rivadeneira, F., van Schoor, N.M., Sherlock, R.E. and Ioannidis, J.P.; GENOMOS Investigators. (2006). Large-scale evidence for the effect of the COLIA1 Sp1 polymorphism on osteoporosis outcomes: the GENOMOS study. *PLoS Med* **3:**e90.

Reginster, J.Y. and Burlet, N. (2006). Osteoporosis: A still increasing prevalence. *Bone* **38:**4-9.

Riley, E.H., Lane, J.M., Urist, M.R., Lyons, K.M. and Lieberman, J.R. (1996). Bone morphogenetic protein-2: biology and applications. *Clin Orthop Relat Res* **324:**39-46.

Rydziel, S., Delany, A.M. and Canalis, E. (1997). Insulin-like growth factor I inhibits the transcription of collagenase 3 in osteoblast cultures. *J Cell Biochem* **67:**176-183.

Sanders, K. M., Pasco, J. A., Ugoni, A. M., Nicholson, G. C., Seeman, E., Martin, T. J., Skoric, B., Panahi, S. and Kotowicz, M.A. (1998) The exclusion of high trauma fractures may underestimate the prevalence of bone fragility fractures in the community: the Geelong Osteoporosis Study. *J Bone Miner Res* **13**: 1337-1342.

Schroeder, T.M., Kahler, R.A., Li, X. and Westendorf, J.J. (2004). Histone deacetylase 3 interacts with runx2 to repress the osteocalcin promoter and regulate osteoblast differentiation. *J Biol Chem* **279:**41998-42007.

Schroeder, T.M., Jensen, E.D. and Westendorf, J.J. (2005). Runx2: a master organizer of gene transcription in developing and maturing osteoblasts. *Birth Defects Res C Embryo Today* **75:**213-225.

Selvamurugan, N., Kwok, S. and Partridge, N.C. (2004). Smad3 interacts with JunB and Cbfa1/Runx2 for transforming growth factor-beta1-stimulated collagenase-3 expression in human breast cancer cells. *J Biol Chem* **279:**27764-27773.

Shen, Q. and Christakos, S. (2005). The vitamin D receptor, Runx2, and the Notch signaling pathway cooperate in the transcriptional regulation of osteopontin. *J Biol Chem* **280:**40589-40598.

Sherwood, L. (1997). Human Physiology, from cells to systems, 3rd edition. Wadsworth Publishing Company. USA.

Sierra, J., Villagra, A., Paredes, R., Cruzat, F., Gutierrez, S., Javed, A., Arriagada, G., Olate, J., Imschenetzky, M., Van Wijnen, A.J., Lian, J.B., Stein, G.S., Stein, J.L. and Montecino, M. (2003). Regulation of the bone-specific osteocalcin gene by p300 requires Runx2/Cbfa1 and the vitamin D3 receptor but not p300 intrinsic histone acetyltransferase activity. *Mol Cell Biol* **23:**3339-3351.

Stanton, L.A., Underhill, T.M. and Beier, F. (2003). MAP kinases in chondrocyte differentiation. *Dev Biol* **263**:165-175.

Stein, G.S., Lian, J.B., van Wijnen, A.J., Stein, J.L., Montecino, M., Javed, A., Zaidi, S.K., Young, D.W., Choi, J.Y. and Pockwinse, S.M. (2004). Runx2 control of organization, assembly and activity of the regulatory machinery for skeletal gene expression. *Oncogene* **23:**4315-4329.

Stock, M. and Otto, F. (2005). Control of RUNX2 isoform expression: the role of promoters and enhancers. *J Cell Biochem* **95**:506-17.

Styrkarsdottir, U., Cazier, J.B., Kong, A., Rolfsson, O., Larsen, H., Bjarnadottir, E., Johannsdottir, V.D., Sigurdardottir, M.S., Bagger, Y., Christiansen, C., Reynisdottir, I., Grant, S.F., Jonasson, K., Frigge, M.L., Gulcher, J.R., Sigurdsson, G. and Stefansson, K. (2003). Linkage of osteoporosis to chromosome 20p12 and association to BMP2. *PLoS Biol* **1:**E69.

Suda, T., Takahashi, N., Udagawa, N., Jimi, E., Gillespie, M.T. and Martin, T.J. (1999). Modulation of osteoclast differentiation and function by the new members of the tumor necrosis factor receptor and ligand families. *Endocr Rev* **20**:345-357.

Sudhakar, S., Katz, M.S., and Elango, N. (2001). Analysis of type-I and type-II RUNX2 protein expression in osteoblasts. *Biochem Biophys Res Commun* **286**:74-79.

Takuwa, Y., Ohse, C., Wang, E.A., Wozney, J.M. and Yamashita, K. (1991). Bone morphogenetic protein-2 stimulates alkaline phosphatase activity and collagen synthesis in cultured osteoblastic cells, MC3T3-E1. *Biochem Biophys Res Commun* **174:**96-101.

Tare, R.S., Oreffo, R.O., Clarke, N.M. and Roach, H.I. (2002). Pleiotrophin/Osteoblast-stimulating factor 1: dissecting its diverse functions in bone formation. *J Bone Miner Res* **17:**2009-2020.

Thakkinstian, A., D'Este, C., Eisman, J., Nguyen, T. and Attia, J. (2004). Meta-Analysis of Molecular Association Studies: Vitamin D Receptor Gene Polymorphisms and BMD as a Case Study. *J Bone Miner Res* **19:** 419-428.

Thies, R.S., Bauduy, M., Ashton, B.A., Kurtzberg, L., Wozney, J.M. and Rosen, V. (1992). Recombinant human bone morphogenetic protein-2 induces osteoblastic differentiation in W-20-17 stromal cells. *Endocrinology* **130:**1318-1324.

Thirunavukkarasu, K., Mahajan, M., McLarren, K.W., Stifani, S. and Karsenty, G. (1998). Two domains unique to osteoblast-specific transcription factor Osf2/Cbfa1 contribute to its transactivation function and its inability to heterodimerize with Cbfbeta. *Mol Cell Biol* **18**:4197-4208.

Togari, A., Arai, M., Nakagawa, S., Banno, A., Aoki, M. and Matsumoto, S. (1995). Alteration of bone status with ascorbic acid deficiency in ODS (osteogenic disorder Shionogi) rats. *Jpn J Pharmacol* **68:**255-261.

Tsuji, K., Ito, Y. and Noda M. (1998). Expression of the PEBP2alphaA/AML3/CBFA1 gene is regulated by BMP4/7 heterodimer and its overexpression suppresses type I collagen and osteocalcin gene expression in osteoblastic and nonosteoblastic mesenchymal cells. *Bone* **22**: 87-92.

Uitterlinden, A.G., Arp, P.P., Paeper, B.W., Charmley, P., Proll, S., Rivadeneira, F., Fang, Y., van Meurs, J.B., Britschgi, T.B., Latham, J.A., Schatzman, R.C., Pols, H.A. and Brunkow, M.E. (2004). Polymorphisms in the sclerosteosis/van Buchem disease gene (SOST) region are associated with bone-mineral density in elderly whites. *Am J Hum Genet* **75:**1032-1045.

Uitterlinden, A.G., Burger, H., Huang, Q., Yue, F., McGuigan, F.E., Grant, S.F., Hofman, A., van Leeuwen, J.P., Pols, H.A. and Ralston, S.H. (1998). Relation of alleles of the collagen type Ialpha1 gene to bone density and the risk of osteoporotic fractures in postmenopausal women. *N Engl J Med* **338**:1016-1021.

Varghese, S., Rydziel, S. and Canalis, E. (2005). Bone morphogenetic protein-2 suppresses collagenase-3 promoter activity in osteoblasts through a runt domain factor 2 binding site. *J Cell Physiol* **202:**391-399.

Vaughan, T., Pasco, J.A., Kotowicz, M.A., Nicholson, G.C. and Morrison, N.A. (2002). Alleles of RUNX2/CBFA1 gene are associated with differences in bone mineral density and risk of fracture. *J Bone Miner Res* **17:**1527-1534.

Vaughan, T., Reid, D.M., Morrison, N.A. and Ralston, S.H. (2004). RUNX2 alleles associated with BMD in Scottish women; interaction of RUNX2 alleles with menopausal status and body mass index. Bone **34:**1029-1036.

Vega, R.B., Matsuda, K., Oh, J., Barbosa, A.C., Yang, X., Meadows, E., McAnally, J., Pomajzl, C., Shelton, J.M., Richardson, J.A., Karsenty, G. and Olson, E.N. (2004). Histone deacetylase 4 controls chondrocyte hypertrophy during skeletogenesis. *Cell* **119:**555-566.

Wang, E.A., Rosen, V., D'Alessandro, J.S., Bauduy, M., Cordes, P., Harada, T., Israel, D.I., Hewick, R.M., Kerns, K.M., LaPan, P., Luxenberg, D.P., McQuaid, D., Moutsatsos, I.K., Nove, J. and Wozney, J.M. (1990). Recombinant human bone morphogenetic protein induces bone formation. *Proc Natl Acad Sci U S A* **87:**2220-2224.

Wang, Q., Stacy, T., Miller, J.D., Lewis, A.F., Gu, T.L., Huang, X., Bushweller, J.H., Bories, J.C., Alt, F.W., Ryan, G., Liu, P.P., Wynshaw-Boris, A., Binder, M., Marin-Padilla, M., Sharpe, A.H. and Speck, N.A. (1996). The CBFbeta subunit is essential for CBFalpha2 (AML1) function in vivo. *Cell* **87:**697-708.

Wang, W., Wang, Y.G., Reginato, A.M., Glotzer, D.J., Fukai, N., Plotkina, S., Karsenty, G. and Olsen, B.R. (2004). Groucho homologue Grg5 interacts with the transcription factor Runx2-Cbfa1 and modulates its activity during postnatal growth in mice. *Dev Biol* **270:**364-681.

Westendorf, J.J., Zaidi, S.K., Cascino, J.E., Kahler, R., van Wijnen, A.J., Lian, .JB., Yoshida, M., Stein, .GS. and Li, X. (2002). Runx2 (Cbfa1, AML-3) interacts with histone deacetylase 6 and represses the p21(CIP1/WAF1) promoter. *Mol Cell Biol* **22:**7982-7792.

Westendorf, J.J., Kahler, R.A. and Schroeder, T.M. (2004). Wnt signaling in osteoblasts and bone diseases. Gene **341:**19-39.

Westendorf, J.J. (2006). Transcriptional co-repressors of Runx2. *J Cell Biochem* **98:**54-64

Xiao, Z.S., Hinson, T.K., and Quarles, L.D. (1999). Cbfa1 isoform overexpression upregulates osteocalcin gene expression in non-osteoblastic and pre-osteoblastic cells. *J Cell Biochem* **74**:596-605.

Xiao, Z.S., Hjelmeland, A.B. and Quarles, L.D. (2004). Selective deficiency of the "bone-related" Runx2-II unexpectedly preserves osteoblast-mediated skeletogenesis. *J Biol Chem* **279**:20307-20313.

Xiao, Z.S., Liu, S.G., Hinson, T.K. and Quarles, L.D. (2001). Characterization of the upstream mouse Cbfa1/Runx2 promoter. *J Cell Biochem* **82**: 647-659.

Xiao, Z.S., Thomas, R., Hinson, T.K. and Quarles, L.D. (1998). Genomic structure and isoform expression of the mouse, rat and human Cbfa1/Osf2 transcription factor. *Gene* **214**:187-197.

Yamada, Y., Miyauchi, A., Goto, J., Takagi, Y., Okuizumi, H., Kanematsu, M., Hase, M., Takai, H., Harada, A. and Ikeda, K. (1998). Association of a polymorphism of the transforming growth factor-beta1 gene with genetic susceptibility to osteoporosis in postmenopausal Japanese women. *J Bone Miner Res* **13:**1569-1576.

Yamagiwa, H., Tokunaga, K., Hayami, T., Hatano, H., Uchida, M., Endo, N. and Takahashi, H.E. (1999). Expression of metalloproteinase-13 (Collagenase-3) is induced during fracture healing in mice. *Bone* **25:**197-203.

Yang, X., Tare, R.S., Partridge, K.A., Roach, H.I., Clarke, N.M., Howdle, S.M., Shakesheff, K.M. and Oreffo, R.O. (2003). Induction of human osteoprogenitor chemotaxis, proliferation, differentiation, and bone formation by osteoblast stimulating factor-1/pleiotrophin: osteoconductive biomimetic scaffolds for tissue engineering. *J Bone Miner Res* **18:**47-57.

Yasuda, H., Shima, N., Nakagawa, N., Yamaguchi, K., Kinosaki, M., Mochizuki, S., Tomoyasu, A., Yano, K., Goto, M., Murakami, A., Tsuda, E., Morinaga, T., Higashio, K., Udagawa, N., Takahashi, N. and Suda, T. (1998). Osteoclast differentiation factor is a ligand for osteoprotegerin/osteoclastogenesis-inhibitory factor and is identical to TRANCE/RANKL. *Proc Natl Acad Sci* USA **95**:3597-3602.

Ying, S., Robinson, D.S., Meng, Q., Rottman, J., Kennedy, R., Ringler, D.J., Mackay, C.R., Daugherty, B.L., Springer, M.S., Durham, S.R., Williams, T.J. and Kay, A.B. (1997). Enhanced expression of eotaxin and CCR3 mRNA and protein in atopic asthma. Association with airway hyperresponsiveness and predominant co-localization of eotaxin mRNA to bronchial epithelial and endothelial cells. *Eur J Immunol* **27:**3507-3516.

Yoshida, T., Kanegane, H., Osato, M., Yanagida, M., Miyawaki, T., Ito, Y. and Shigesada, K. (2003). Functional analysis of RUNX2 mutations in cleidocranial dysplasia: novel insights into genotype-phenotype correlations. *Blood Cells Mol Dis* **30**:184-193.

Zaidi, S.K., Javed, A., Choi, J.Y., van Wijnen ,A.J, Stein, J.L., Lian, J.B. and Stein, G.S. (2001). A specific targeting signal directs Runx2/Cbfa1 to subnuclear domains and contributes to transactivation of the osteocalcin gene. *J Cell Sci* **114**:3093-3102.

Zambotti, A., Makhluf, H., Shen, J. and Ducy P. (2002). Characterization of an osteoblast-specific enhancer element in the CBFA1 gene. *J Biol Chem* **277**: 41497-41506.

Zeng, C., McNeil, S., Pockwinse, S., Nickerson, J., Shopland, L., Lawrence, J.B., Penman, S., Hiebert, S., Lian, J.B., van Wijnen, A.J., Stein, J.L. and Stein, G.S. (1998). Intranuclear targeting of AML/CBFalpha regulatory factors to nuclear matrix-associated transcriptional domains. *Proc Natl Acad Sci* U S A **95**:1585-1589.

Zeng, C., van Wijnen, A.J., Stein, J.L., Meyers, S., Sun, W., Shopland, L., Lawrence, J.B., Penman, S., Lian, J.B., Stein, G.S. and Hiebert, S.W. (1997). Identification of a nuclear matrix targeting signal in the leukemia and bone-related AML/CBF-alpha transcription factors. *Proc Natl Acad Sci* U S A **94**:6746-6751.

Zhang, M., Xuan, S., Bouxsein, M.L., von Stechow, D., Akeno, N., Faugere, M.C., Malluche, H., Zhao, G., Rosen, C.J., Efstratiadis, A. and Clemens, T.L. (2002). Osteoblast-specific knockout of the insulin-like growth factor (IGF) receptor gene reveals an essential role of IGF signaling in bone matrix mineralization. *J Biol Chem* **277:**44005-44012.

Zhang, Y.W., Yasui, N., Kakazu, N., Abe, T., Takada, K., Imai, S., Sato, M., Nomura, S., Ochi, T., Okuzumi, S., Nogami, H., Nagai, T., Ohashi, H. and Ito, Y. (2000a). PEBP2alphaA/CBFA1 mutations in Japanese cleidocranial dysplasia patients. *Gene* **244**:21-28.

Zhang, Y.W., Yasui, N., Ito, K., Huang, G., Fujii, M., Hanai, J., Nogami, H., Ochi, T., Miyazono, K. and Ito, Y. (2000b). A RUNX2/PEBP2alphaA/CBFA1 mutation displaying impaired transactivation and Smad interaction in cleidocranial dysplasia. *Proc Natl Acad Sci* U S A **97**:10549-10554.

Zhang, Y.Y., Liu, P.Y., Lu, Y., Xiao, P., Liu, Y.J., Long, J.R., Shen, H., Zhao, L.J., Elze, L., Recker, R.R. and Deng, H.W. (2006). Tests of linkage and association of PTH/PTHrP receptor type 1 gene with bone mineral density and height in Caucasians. *J Bone Miner Metab* **24:**36-41.

Zheng, Q., Sebald, E., Zhou, G., Chen, Y., Wilcox, W., Lee, B. and Krakow, D. (2005). Dysregulation of chondrogenesis in human cleidocranial dysplasia. *Am J Hum Genet* **77**:305-312.

Zhou, G., Chen, Y., Zhou, L., Thirunavukkarasu, K., Hecht, J., Chitayat, D., Gelb, B.D., Pirinen, S., Berry, S.A., Greenberg, C.R., Karsenty, G., and Lee, B. (1999). CBFA1 mutation analysis and functional correlation with phenotypic variability in cleidocranial dysplasia. *Hum Mol Genet* **8**:2311-2316.

Zimmermann, N., Hershey, G.K., Foster, P.S. and Rothenberg, M.E. (2003). Chemokines in asthma: cooperative interaction between chemokines and IL-13. *J Allergy Clin Immunol* **111:**227-242